

VOLUME XLI

SPRING 2005

GEMS & GEMOLOGY



*Treated-Color Red Diamonds ... Chameleon Diamonds
Coated Pink Diamond ... Tucson Report*

THE QUARTERLY JOURNAL OF THE GEMOLOGICAL INSTITUTE OF AMERICA



pg. 7




pg. 21

EDITORIAL _____

- 1 **In Memory of Dr. Edward J. Gübelin**
Alice S. Keller
- 2 **The Dr. Edward J. Gübelin Most Valuable Article Award**

4 LETTERS _____

FEATURE ARTICLES _____

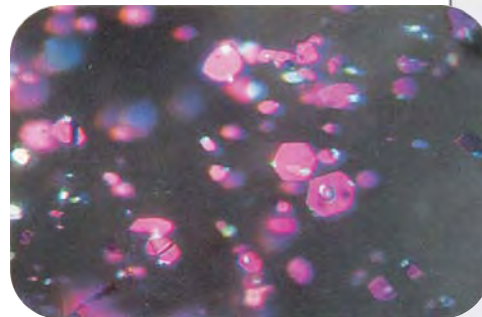
- 6 **Treated-Color Pink-to-Red Diamonds from Lucent Diamonds Inc.**
 *Wuyi Wang, Christopher P. Smith, Matthew S. Hall, Christopher M. Breeding, and Thomas M. Moses*
A report on the gemological properties and identifying characteristics of the new treated-color natural diamonds from Lucent Diamonds.
- 20 **A Gemological Study of a Collection of Chameleon Diamonds**
Thomas Hainschwang, Dusan Simic, Emmanuel Fritsch, Branko Deljanin, Sharrie Woodring, and Nicholas DelRe
Examines a collection of 39 chameleon diamonds and summarizes gemological and spectroscopic means for their identification.

NOTES AND NEW TECHNIQUES _____

- 36 **Coated Pink Diamond—A Cautionary Tale**
David J. F. Evans, David Fisher, and Christopher J. Kelly
Case study of a diamond that was stated to have been HPHT treated, but in fact had been *coated* to change its color to an intense purple-pink.

REGULAR FEATURES _____

- 42 **Lab Notes**
Diamond with color possibly affected by the 3H defect • HPHT-treated type IIa yellow diamond • Inhomogeneous cape diamond • Irradiated and fracture-filled diamond • A coated “night glowing pearl” • “Pink fire” quartz • Quartz with unusual surface texture • Spinel cabochon with an unusual natural surface
- 52 **Gem News International**
Lapidary art at AGTA Design Center, Tucson • Amethyst from Georgia • Amethyst and citrine from Namibia • Aquamarine from Colorado • Saturated blue aquamarine from Nigeria • Chalcedony chain • Emerald from Xinjiang, China • Gold-in-quartz from Mariposa County, California • Iolite from northeastern Brazil • Kyanite widely available in Tucson • “Moonstone” from Morogoro, Tanzania • Faceted pezzottaite from Afghanistan • Tanzanite marketing initiatives • Manufactured gold/silver-in-quartz • 10.53 ct diamond from Saskatchewan, Canada • Spiral in aquamarine • “Bamboo” moonstone • Pezzottaite in quartz • Treated-color topaz from Pakistan • Conference reports • Faceted Burmese rubies outside import ban
- 74 **2005 Gems & Gemology Challenge**
- 76 **Book Reviews**
- 78 **Gemological Abstracts**
- 86 **The Last Page: Fast Facts About Synthetic Diamonds**



pg. 48



pg. 52

In Memory of DR. EDWARD J. GÜBELIN

Gems & Gemology mourns the loss of Dr. Edward J. Gübelin, who died March 15, one day shy of his 92nd birthday. One of the most influential gemologists of the 20th century, Dr. Gübelin's work inspired the contemporary study of inclusions and established their significance in gem identification.

Edward Gübelin was born in 1913 in Lucerne, Switzerland, to a well-known family of watchmakers. Dr. Gübelin found his calling early on, when his father provided a gemological laboratory for his use. He studied mineralogy at the universities of Zurich and Vienna, earning a Ph.D. in 1938. His studies continued at the fledgling GIA in Los Angeles, where he graduated as a Certified Gemologist (then the precursor to the Graduate Gemologist degree) in 1939.

After returning to Switzerland, Dr. Gübelin began his famous work on inclusions, painstakingly documenting how internal features can be used to help pinpoint a gem's identity and origin. This research was the basis for several *G&G* articles he wrote during the 1940s, and GIA founder Robert M. Shipley encouraged the young mineralogist to expand his work into a book. The result was the groundbreaking *Inclusions as a Means of Gemstone Identification* (1953), which presented the first systematic classification of inclusions.

Numerous books, more than 150 research papers, and even a film (on the rubies of Mogok, Burma) followed, all in a style that was both scholarly and eloquent. He collaborated with John Koivula to write the classic *Photoatlas of Inclusions in Gemstones* (1986), which contains more than 1,400 photomicrographs and is widely considered the authoritative book on the subject.

Through the last two decades, at an age when most would be content to savor a lifetime of distinguished achievements, Dr. Gübelin never stopped producing. He continued writing, lecturing, and traveling to gem localities all over the world. His last book (with co-author John Koivula) is the totally new *Photoatlas of Inclusions in Gemstones, Vol. 2*, scheduled to be released this year.

Dr. Gübelin's influence on this journal alone was extraordinary. He contributed as author or reviewer for seven consecutive decades, beginning in the 1940s. One article, a memorable update on peridot from the Red Sea island of Zabargad, was the lead paper of my first issue as editor, the beginning of our 25 years of collaboration.

Two years ago, we dedicated our Spring 2003 issue to Dr. Gübelin in celebration of his 90th birthday. We commemorated the milestone with a profile of the great gemologist (pp. 1–2) and articles that mirrored his interest in new gem finds and photomicrography. This issue also included an article he co-authored on the rare gem poudretteite from Myanmar (formerly Burma), a land he knew better than any other Western gemologist. In a gracious letter written shortly after the issue appeared, Dr. Gübelin confided: "I may mention between the two of us that fame has never been my goal but enthusiasm and love for the science of gemstones have spurred me on."



Later in 2003, Dr. Gübelin established a fund to support *G&G*'s annual Most Valuable Article award, which had been named in his honor in 1997. The interest from this fund will be used in perpetuity to reward the winning authors. Writing from Lucerne, Dr. Gübelin said he created the award fund in connection with Easter—"not exactly for merely religious

reasons, but rather because Easter is the feast of hope. With this, though, I am truly combining the hope that *Gems & Gemology*...will last for many years to come."

It is with great sorrow that I say good-bye to Edward Gübelin, a good friend as well as a treasured colleague. Like so many others, I shall miss his beautiful letters, his depictions of exotic locales he had visited as exquisite as his description of dolomite in a Brazilian emerald "besieged by a swarm of chromite grains." Yet also like others, I feel every letter, every meal shared, every conversation was a gift that, like his impact on gemology, will truly last forever.

Dr. Gübelin is survived by five daughters, 12 grandchildren, and 11 great-grandchildren. In his honor, GIA has established the Edward J. Gübelin Research Fund, to perpetuate the science that he devoted his prodigious energy and intellect to establish.

Alice S. Keller
Editor-in-Chief

GIA will hold a tribute to Dr. Gübelin at 3:00 pm Saturday, May 21, at its world headquarters in Carlsbad, Calif. For more information or to RSVP, please e-mail tribute@gia.edu.

The
DR. EDWARD J. GÜBELIN
 MOST VALUABLE ARTICLE

Gems & Gemology is pleased to announce the winners of this year's Dr. Edward J. Gübelin Most Valuable Article Award, as voted by the journal's readers. We extend our sincerest thanks to all the subscribers who participated in the voting.

The first-place article was "A Foundation for Grading the Overall Cut Quality of Round Brilliant Cut Diamonds" (Fall 2004), which described the factors that are important in evaluating the quality of a diamond's cut and introduced the new GIA diamond cut grading system. Receiving second place was "The Creation of a Magnificent Suite of Peridot Jewelry: From the Himalayas to Fifth Avenue" (Winter 2004), which chronicled the making of a peridot jewelry suite, from the rough mined in Pakistan to the design and manufacture of the ensemble by Van Cleef & Arpels. Third place was awarded to "An Updated Chart on the Characteristics of HPHT-Grown Synthetic Diamonds" (Winter 2004), a summary of the features of synthetic diamonds that are grown at high-pressure and high-temperature (HPHT) conditions.

The authors of these three articles will share cash prizes of \$2,000, \$1,000, and \$500, respectively. Following are brief biographies of the winning authors.

Congratulations also to Dr. Casey Skvorc of Bethesda, Maryland, whose ballot was drawn from the many entries to win a five-year subscription to *Gems & Gemology*.



Left to right: John M. King, Ilene M. Reinitz, Thomas M. Moses



Left to right: Al M. Gilbertson, Kim Cino, James E. Shigley, Mary L. Johnson, Barak Green



Troy Blodgett



Ron H. Geurts



T. Scott Hemphill



Lisa Kornylak

First Place

A FOUNDATION FOR GRADING THE OVERALL CUT QUALITY OF ROUND BRILLIANT CUT DIAMONDS

Thomas M. Moses, Mary L. Johnson, Barak Green, Troy Blodgett, Kim Cino, Ron H. Geurts, Al M. Gilbertson, T. Scott Hemphill, John M. King, Lisa Kornylak, Ilene M. Reinitz, and James E. Shigley

Thomas M. Moses is vice president of Identification and Research at the GIA Gem Laboratory in New York. Mr. Moses, who attended Bowling Green University, is also an editor of *G&G's* Lab Notes section. **Mary L. Johnson** is manager of research and development for the GIA Gem Laboratory in Carlsbad, California. Dr. Johnson, a frequent contributor to the journal, received her Ph.D. in mineralogy and crystallography from Harvard University. **Barak Green** is manager of communications for the GIA Gem Laboratory. He has written several articles related to diamond cut for trade journals and the Institute website. Mr. Green holds a master's degree in anthropology from the University of California, San Diego. **Troy Blodgett** is a research scientist at GIA and joined the Carlsbad lab in 1998. Dr. Blodgett holds a bachelor's degree in geology-biology from Brown University, and a master's and doctorate in geology and remote sensing from Cornell University. **Kim Cino** is director of administration for the GIA Gem Laboratory, and project manager of the GIA Diamond Cut Grading

project. With more than a decade of experience at the Institute, Ms. Cino has led and managed other notable projects, such as the implementation of the Laboratory Operations and Management System (Horizon) in 1996 and the introduction of the GIA Diamond Dossier® in 1999. **Ron Geurts** is Research and Development manager at GIA Antwerp. Mr. Geurts was formerly technical director of the Certificates department of HRD, and for the last decade he has been deeply involved in efforts to implement new technology in the GIA diamond grading process. **Al Gilbertson** is a research associate with GIA Research in Carlsbad. A noted gemologist and appraiser, Mr. Gilbertson has published several articles on diamond cut and clarity. **T. Scott Hemphill**, a GIA research associate, has been programming computers for more than 30 years. Mr. Hemphill holds a bachelor's degree in engineering and a master's degree in computer science from the California Institute of Technology. **John M. King** is laboratory projects officer at the GIA Gem Laboratory in New York. Mr. King received his Master of Fine Arts degree from Hunter College, City University of New York. With over 20 years of laboratory experience, he frequently writes and lectures on colored diamonds and laboratory grading procedures. **Lisa Kornylak** received her G.G. in 1994 and has almost 20 years experience in the jewelry industry. Formerly with GIA Carlsbad, she worked in the Grading Laboratory and then in Research on the diamond cut project. **Ilene M. Reinitz** is manager of research and development at the GIA Gem Trade Laboratory in New York. Dr. Reinitz, who holds a Ph.D. in geochemistry from Yale University, has written numerous articles for *G&G* and other publications. **James E. Shigley** is director of GIA Research in Carlsbad. Prior to joining the Institute in 1982, Dr. Shigley received his doctorate in geology from Stanford University. He is the author of numerous articles on diamonds and other gemstones, and is the editor of the newly published *Gems & Gemology in Review: Synthetic Diamonds*.

Second Place

THE CREATION OF A MAGNIFICENT SUITE OF PERIDOT JEWELRY: FROM THE HIMALAYAS TO FIFTH AVENUE

Robert E. Kane

Robert E. Kane is president and CEO of Fine Gems International in Helena, Montana, and a member of the *G&G* Editorial Review Board since 1981. He is a former director of the Gübelin Gem Lab in Lucerne, Switzerland, and a former manager of gem identification at GIA's West Coast Gem Trade Laboratory. With more than 25 years of gemological experience, Mr. Kane is well known for his many articles on diamonds, gemstones, and gem identification.



Robert E. Kane

Third Place

AN UPDATED CHART ON THE CHARACTERISTICS OF HPHT-GROWN SYNTHETIC DIAMONDS

James E. Shigley, Christopher M. Breeding, and Andy Hsi-Tien Shen

James Shigley was profiled in the first-place entry. **Christopher M. Breeding** is a research scientist for the GIA Gem Laboratory in Carlsbad, where he investigates origin of color for diamonds and other gemstones. He holds a B.S. in geology from the College of William & Mary and a Ph.D. in geology from Yale University. **Andy Hsi-Tien Shen** is a research scientist at the GIA Gem Laboratory in Carlsbad. He holds a Ph.D. from Cornell University and has conducted research in mineral physics in the United States, Germany, and the United Kingdom for more than 15 years.



Christopher M.
Breeding



Andy Hsi-Tien Shen

TREATED-COLOR PINK-TO-RED DIAMONDS FROM LUCENT DIAMONDS INC.

Wuyi Wang, Christopher P. Smith, Matthew S. Hall,
Christopher M. Breeding, and Thomas M. Moses

Lucent Diamonds has developed a new treatment process for natural type Ia diamonds that produces colors ranging from pink-purple through red to orangy brown, using a multi-step process that involves HPHT annealing, irradiation, and low-pressure annealing at relatively lower temperatures. Those stones that achieve a predominant pink-to-red or purple color are marketed as "Imperial Red Diamonds." Gemological properties and characteristic spectra are presented for 41 diamonds, representing the range of colors produced thus far. These treated-color natural diamonds can be readily identified by internal graphitization and surface etching seen with magnification, distinctive color zoning, and reactions to long- and short-wave UV radiation. The color is caused primarily by the absorption of the (N-V)⁻ center, with further influence from the (N-V)⁰, H3, H4, and N3 centers. Other characteristic infrared and UV-visible absorption features include the H1a, H1b, H1c, 6170 cm⁻¹, and, frequently, 594 nm bands. This type of defect combination is not known in naturally colored diamonds.

Historically, diamonds in the pink-to-red color range have been among the most highly prized. In nature, most pink-to-red, brown, and purple colors (and combinations thereof) in diamond have been attributed to the development of defect centers caused by shear stress and plastic deformation. These defects, which gemologists describe as colored "graining," were formed after the growth of the gem was complete and either prior to or during the diamond's ascent to the earth's surface (see, e.g., Orlov, 1977; Collins, 1982; Fritsch, 1998; Moses et al., 2002). Many of the world's most famous diamonds owe their color to this mechanism, including such notable stones as the 0.95 ct Hancock Red, the 5.11 ct Moussaieff Red, the 59.60 ct Steinmetz Pink, and the 128.48 ct Star of the South.

As a result of the prestige and value associated with these colors, attempts have been made since antiquity to impart a pink-to-red coloration to diamonds. In the earliest times, topical coatings were used to achieve this goal; however, such coatings were not stable and could be readily removed. The

first treatment to induce a more stable hue in this range was introduced in the 1950s, when irradiation with high-energy electrons began to be applied experimentally to modify the color of natural diamonds. On rare occasions, a brownish pink to red hue would result when certain diamonds were irradiated in this manner and subsequently annealed (Crowningshield, 1959; Crowningshield and Reinitz, 1995). It was only significantly later, during the mid- to late 1980s, that scientists realized the stones that changed color in this manner were type Ib diamonds, which contain single substitutional nitrogen impurities (Fritsch, 1998; Shigley et al., 2004). More recently, high pressure/high temperature (HPHT) annealing of type IIa diamonds has been shown to change the color of some brown diamonds to hues in the purplish pink to brown-pink range (Hall and Moses, 2000).

See end of article for About the Authors and Acknowledgments.
GEMS & GEMOLOGY, Vol. 41, No. 1, pp. 6-19.
© 2005 Gemological Institute of America



Figure 1. Treated-color “Imperial Red Diamonds” are being produced by Lucent Diamonds of Denver, Colorado. Shown here are three loose stones (0.15–0.33 ct) and a selection of fine jewelry demonstrating the possibilities of these gems. The ring is set with a 1.25 ct diamond, while the bracelet and necklace feature 0.38 and 0.34 ct diamonds, respectively. The ring is courtesy of John Atencio Designer Jewelry, Denver; the bracelet and necklace are both courtesy of Avirom Associates, Boulder, Colorado. Photo © Harold & Erica Van Pelt.

The latest entrant into this specialized arena of treated-color diamonds is Lucent Diamonds Inc., a U.S. corporation based in Denver, Colorado. This company has specialized in the production of synthetic diamonds and the HPHT treatment of natural and synthetic diamonds since 1995. During the 2004 Tucson shows, Lucent Diamonds unveiled a new color series of treated-color natural diamonds, which they are marketing under the name “Imperial Red Diamonds” (figure 1). The treatment employs a complex, multiple-step procedure that is effective with only certain types of natural diamonds or HPHT-grown synthetic diamonds (A. Grizenko and V. Vins, pers. comms., 2004). Following the show, we contacted Lucent Diamonds to borrow samples in the full range of colors produced, so they could be examined and tested. From our study of several of these diamonds, we determined that a number of standard gemological and spectroscopic features will readily distinguish these stones as being diamonds of a natural origin (i.e., not synthetic) with treated color.

Lucent Diamonds first began applying this process to type Ib synthetic diamonds. Subsequently, they experimented with naturally grown diamonds. To date, more than 1,000 natural diamonds have

been treated in this manner, resulting in a dominant pink, red, purple, or brown color appearance. However, diamonds with a dominant brown appearance are excluded from the “Imperial Red Diamond” group, so only a small portion of the stones are sold under that trade name (A. Grizenko, pers. comm., 2005). Continued developments in the pre-screening of diamonds that can be treated successfully by this process have improved the percentage output of pink-to-red or purple stones, while they have confirmed the scarcity of appropriate natural-origin starting material. Mr. Grizenko projects that within a year, they will have achieved a stable production of 50 carats of “Imperial” diamonds per month. Given the rarity of natural-color intense pink-to-red diamonds, even such relatively small numbers may have a significant impact on the availability of diamonds in this color range (natural or treated) in the gemstone and jewelry market.

MATERIALS AND METHODS

A total of 41 diamonds (see, e.g., figure 2) were provided by Lucent Diamonds for this study. They ranged from 0.14 to 0.91 ct and are representative of



Figure 2. This group of 12 stones (0.14–0.65 ct) represents the range of colors Lucent Diamonds is marketing as “Imperial Red Diamonds.” These treated-color natural-origin diamonds have been produced by a new treatment method, which involves HPHT annealing, irradiation, and low-pressure annealing at relatively lower temperatures. Photo © Harold & Erica Van Pelt.

the color range that is currently being produced by this process (A. Grizenko, pers. comm., 2005).

Color grades were determined by experienced colored-diamond color graders using the standard conditions and methodology of GIA’s color grading system for colored diamonds (King et al., 1994). Internal features were observed with a standard binocular microscope using a variety of lighting techniques. Reactions to ultraviolet radiation were checked in a darkened room with a conventional four-watt combination long-wave (365 nm) and short-wave (254 nm) lamp. All of the stones were also examined using a Diamond Trading Company (DTC) DiamondView deep-ultraviolet (<230 nm) luminescence imaging system (Welbourn et al., 1996). A handheld spectroscope was used to view absorption features in the visible range, with the samples at both room temperature and low temperature.

All the samples were also analyzed using several other spectroscopic techniques. Absorption spectra in the ultraviolet to visible (UV-Vis) range were recorded with a Thermo-Spectronic Unicam UV500 spectrophotometer over the range 250–850 nm with

a sampling interval of 0.1 nm. The samples were mounted in a cryogenic cell and cooled using liquid nitrogen. Infrared absorption spectra were recorded in the mid-infrared (6000–400 cm^{-1} , 1 cm^{-1} resolution) and near-infrared (up to 11000 cm^{-1} , 4 cm^{-1} resolution) ranges at room temperature with a Thermo-Nicolet Nexus 670 Fourier-transform infrared (FTIR) spectrometer, equipped with KBr and quartz beam splitters. In collecting absorption spectra in the near-infrared range, the lower energy side was extended to 2700 cm^{-1} to cover the three-phonon region of diamond absorption, which—like the two-phonon region absorption in the middle-infrared region—can be employed to calibrate the absorption intensity of other defects. A 6 \times beam condenser focused the incident beam on the sample, and a total of 1,024 scans (per spectrum) were collected to improve the signal-to-noise ratio.

Low-temperature photoluminescence (PL) spectra were recorded using a Renishaw 1000 Raman microspectrometer with an Argon-ion laser at two different laser excitations: 488.0 nm (for the range 490–850 nm) and 514.5 nm (for the range 517–850 nm). PL spectra of 15 stones were also collected using a Diode laser (780 nm) for the range 782–1000 nm. The samples were cooled by direct immersion in liquid nitrogen. Up to three scans were accumulated in some cases to achieve a better signal-to-noise ratio.

RESULTS

Visual Appearance. All the samples had an obvious coloration that ranged from pink/red to purple and brown, as well as combinations thereof (again, see figure 2). In the face-up position, all samples appeared homogeneously colored; however, when viewed face-down, a few samples revealed subtle to more distinct uneven coloration (see below). When color graded, the majority of the samples fell within a relatively small area of color space. These are in the GIA hue ranges of purple-red to orangy red (figure 3), as well as in a rather confined area of tone and saturation.

Microscopic Characteristics. *Internal and Surface Features.* A broad range of internal characteristics were noted, including predominant octahedral growth sectors and color zoning, as well as a variety of natural mineral inclusions. Although these indicated that the diamonds had grown naturally (i.e., were not synthetic), they also showed evidence of strong alterations due to treatment in a laboratory.

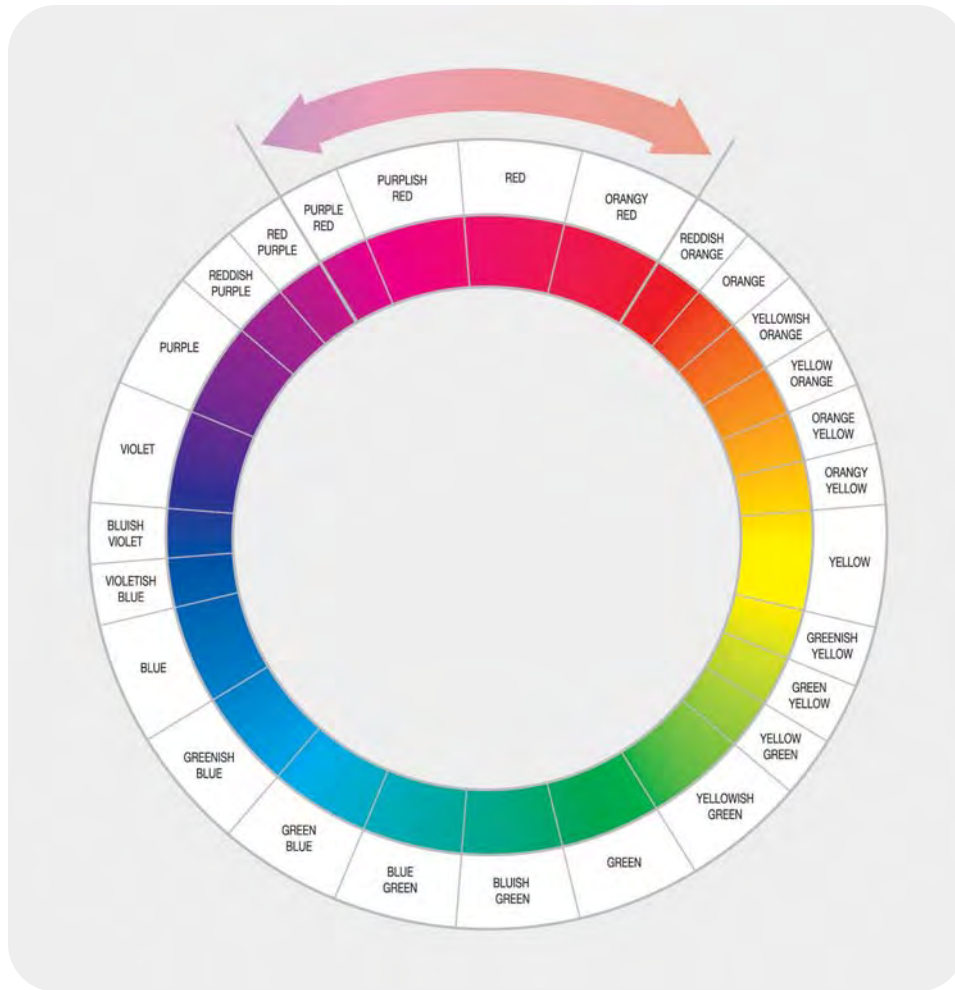


Figure 3. This color wheel illustrates the range of hues of most of the diamonds treated by the new method. The samples examined were given the following GIA color grades: Fancy Deep pink, brownish pink-purple, brown-pink, and pink-brown; Fancy purplish red, brownish purplish red, reddish brown, and brown-red; and Fancy Dark reddish brown, red-brown, and orangy brown. Brown colors, which depend on the degree of tone relative to the saturation of the hue, are not represented in this diagram.

In several of the samples, we observed precipitation of graphite at the interface between euhedral mineral inclusions and the host diamond, leading to the formation of large dark gray to black inclusions that had a very coarse surface texture (figure 4). The euhedral morphology of these inclusions was comparable to olivine or garnet, two very common inclusions in natural diamonds, and was distinctly different from that of metallic inclusions in synthetic diamonds. Although the identification of these inclusions was difficult due to the fact that they are covered entirely with graphite, their coarse texture and appearance was very distinctive. Some of the graphitized inclusions were also associated with stress fractures that had a similar texture and appearance (figure 5). Cleavages revealed inner surfaces that had been etched (figure 6), and a few stones displayed severely etched areas or facets on or adjacent to the girdle that had not been repolished (figure 7).

Strain. Most of the samples showed weak to moderately intense strain when they were viewed with

Figure 4. A very coarsely textured graphitization of the diamond surrounding naturally occurring mineral inclusions and along associated stress fractures was commonly seen in many of the Lucent samples. The graphitization was induced by the HPHT treatment conditions. The morphology of the mineral inclusions resembles that of olivine or garnet, which occur as inclusions only in natural diamonds; the metallic inclusions seen in many synthetic diamonds have a very different shape and appearance. Photomicrograph by C. P. Smith; magnified 62 \times .

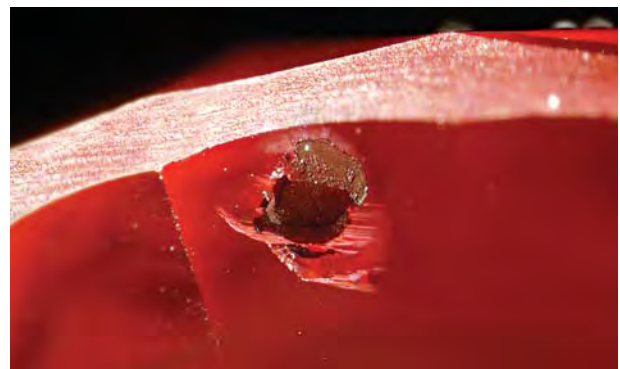




Figure 5. Graphitization was also evident along internal stress fractures. Typically, these stress fractures displayed a narrow, highly reflective fringe along the outermost extension of the fracture that was probably induced by the expansion pressure created when the walls of the stress fractures converted to graphite. Photomicrograph by C. P. Smith; magnified 58×.

the microscope between crossed polarizing filters. For the most part, the strain was in banded patterns that followed the octahedral growth zoning, exhibiting predominantly gray-to-blue interference colors (figure 8). A few samples, however, revealed higher levels of strain that were associated with mottled or “cellular” patterns (figure 9), similar to the patterns seen in natural-color type Ia pink-to-red or purple diamonds (see, e.g., figure 15 in King et al., 2002, p. 140).

Internal Growth Structures and Color Zoning.

Some of the most characteristic features of these

Figure 7. Small, severely etched areas were present on or near the girdles of several samples, indicating that the damage caused by certain phases of the treatment process had not been completely removed by repolishing. This kind of coarse etching is unlike what may be encountered when etching takes place in nature. Photomicrograph by C. P. Smith; magnified 50×.

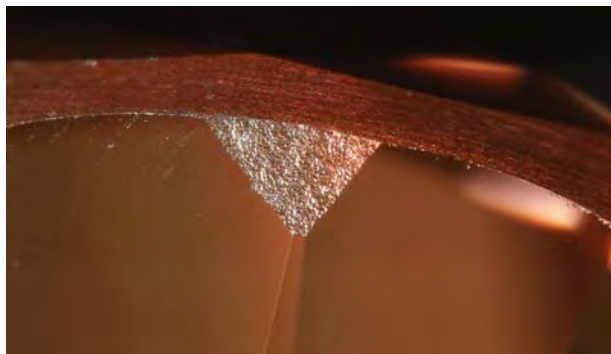


Figure 6. Cleavages that reached the surface exhibited distinct etching along their full extent. Such etching is also evidence of HPHT treatment. Photomicrograph by C. P. Smith; magnified 52×.

diamonds can be seen in their color zoning and its relation to the internal growth structures. In these stones, thick or extended regions of color were seen to conform to internal growth structures (i.e., various crystal faces). Visually, this resulted in various color concentrations that were a combination of straight and angular, including color zoning that appeared very irregular because of internal regions that had a more complex growth history. In addition, typically these color zones exhibited sharp,

Figure 8. Most of the samples exhibited relatively weak to moderately intense strain when viewed between crossed polarizing filters. The banded pattern shown here follows the octahedral growth planes. This type of strain is not seen in HPHT- or CVD-grown synthetic diamonds, providing additional confirmation that these Lucent diamonds are naturally grown. In addition, this type of strain is not typical of natural-color type Ia pink-to-red or purple diamonds. Photomicrograph by C. P. Smith; magnified 22×.

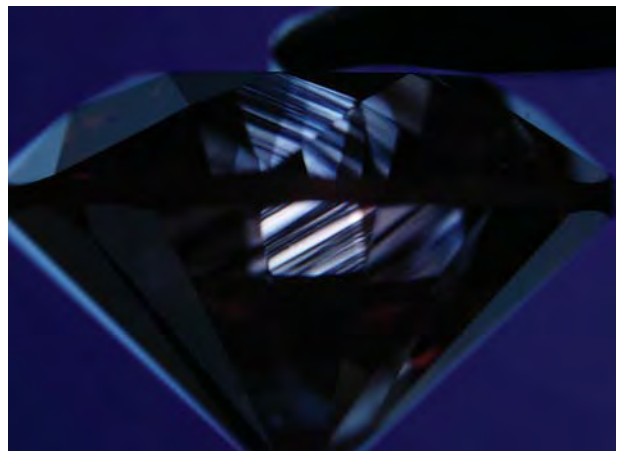




Figure 9. A few of the samples exhibited a higher degree of strain, in a mottled or “cellular” pattern, similar to that seen in natural-color natural diamonds in this color range (but not encountered in synthetic diamonds). Photomicrograph by C. P. Smith; magnified 32×.

clearly defined color boundaries. Such color zoning is very different from that encountered in natural-color pink-to-red diamonds, where localized color concentrations relate to colored “graining” that is caused by plastic deformation (see Discussion section below).

The color zoning of the Lucent samples typically ranged from pink to purple-pink and brown to

Figure 11. In this sample, the color zoning is more obvious, concentrated within complex, naturally occurring growth sectors. Here, saturated pink zones occur adjacent to paler pink to near-colorless growth sectors that for the most part follow octahedral crystal faces. Again, this form of pink-to-red color zoning is distinctly different from the linear pink-to-red graining that typically extends in only one direction in natural-color diamonds of this hue, Photomicrograph by C. P. Smith; magnified 48×.

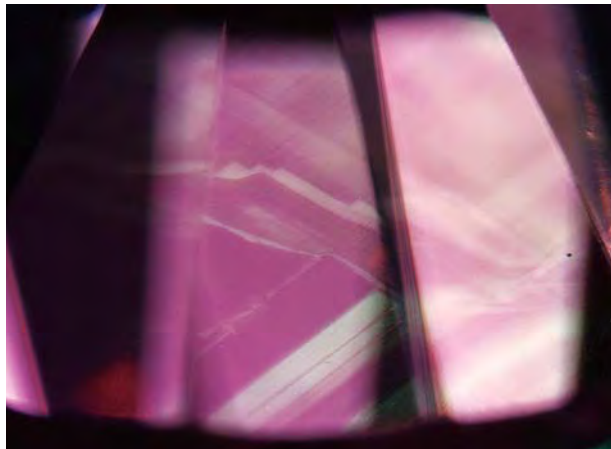


Figure 10. All the samples showed characteristic color zoning that was homogeneous or followed straight to angular growth sectors. In some samples, the zoning was subtle, occurring as highly saturated and less-saturated zones of the same hue. This is distinctly different from the colored graining evident in natural-color pink to red, purple, and brown diamonds, which is due to plastic deformation-related defects. Photomicrograph by C. P. Smith; magnified 40×.

purple-brown of varying saturation. In a few of the samples, this color zoning was rather subtle and typically consisted of more highly saturated pink zones bordered by less-saturated zones of the same hue (figure 10). In other samples, however, the color zoning was much more obvious, consisting of saturated zones of pink-to-red color bordered by growth sectors that were paler pink to near-colorless (figure 11). A few of the diamonds had all three types of color zoning: consisting of regions or

Figure 12. A few diamonds contained distinct pink-to-red zones in some areas, with brown and near-colorless zones in others. Photomicrograph by C. P. Smith; magnified 28×.



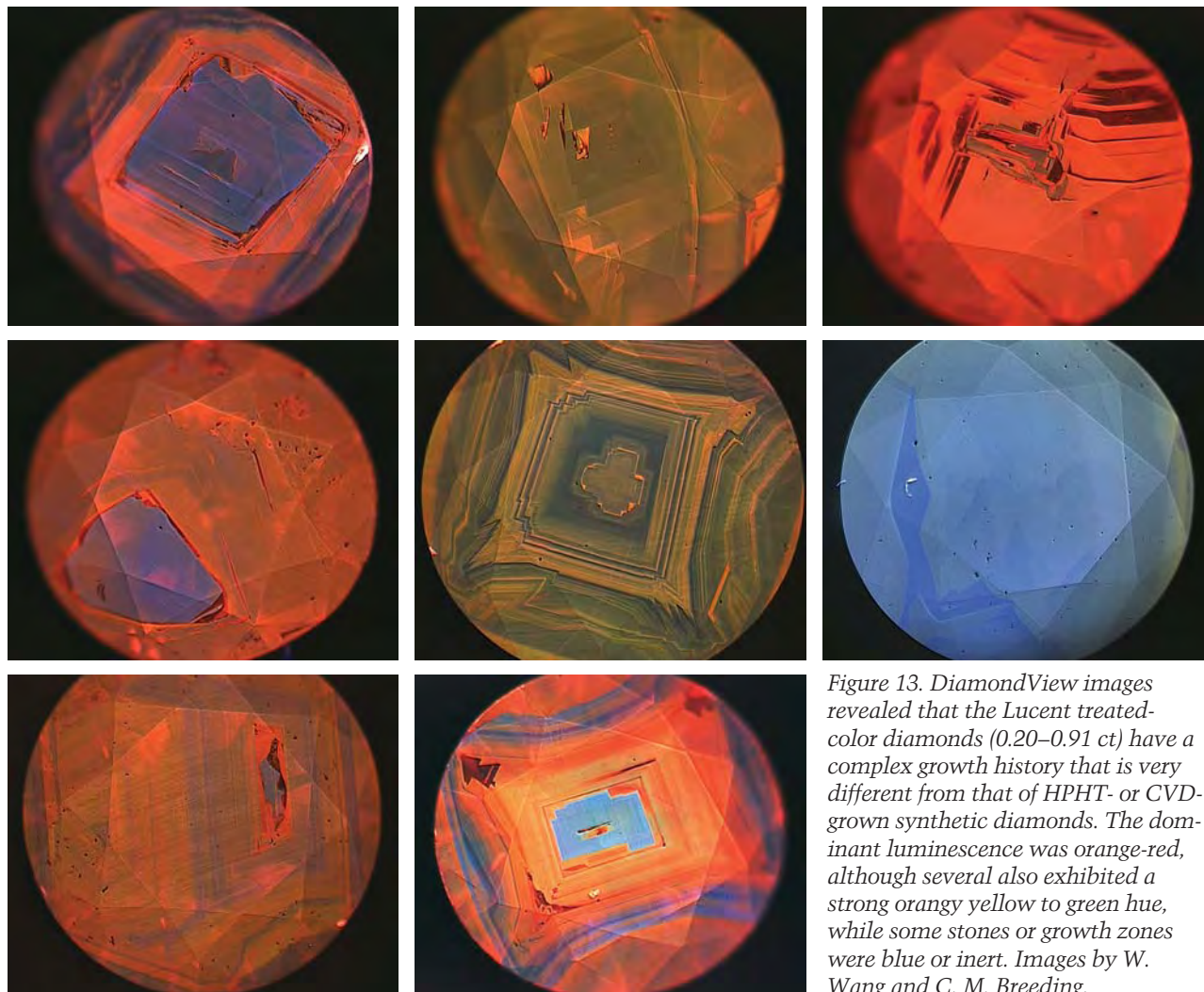


Figure 13. DiamondView images revealed that the Lucent treated-color diamonds (0.20–0.91 ct) have a complex growth history that is very different from that of HPHT- or CVD-grown synthetic diamonds. The dominant luminescence was orange-red, although several also exhibited a strong orangy yellow to green hue, while some stones or growth zones were blue or inert. Images by W. Wang and C. M. Breeding.

growth sectors that were saturated pink to purple-pink, brown to purple-brown, and pale pink to near-colorless (figure 12).

DiamondView Imaging. The luminescence images of the stones we examined revealed complex growth patterns (figure 13), as expected for natural diamonds. An orange-red fluorescence color dominated most growth sectors, while some other areas were orangy yellow to green, blue, or just dark in appearance. The confinement of the strong orange fluorescence to growth sectors was consistent with the color zoning observations described above. These patterns are a direct reflection of the large variation in the type and concentration of defects, as well as of the complex growth history, of most natural diamonds. Neither the fluorescence nor the growth features that are characteristic of synthetic diamonds (see, e.g., Wang et al., 2003; Shigley et al., 2004) were observed in these stones,

which confirmed their natural origin. The observed patterns are mostly attributed to octahedral {111} growth planes.

Visible Luminescence. There are certain defect centers in diamond that yield luminescence to visible light (refer to the UV-Vis-NIR Spectroscopy and Raman PL Spectroscopy sections below). When these centers are strong enough, distinctive luminescence may be seen in a microscope, a loupe, or even with the unaided eye if the stones are viewed with a strong light source. All the stones we examined exhibited a green luminescence to visible light that ranged from moderate to very strong; it was rather homogeneous in some samples, while heavily zoned in others (figure 14). This green luminescence is related to H3 emission centered at 503 nm. A strong orange-red luminescence was also seen in all samples. This luminescence relates to (N-V)⁻ emission centered at 637 nm and was variable in appearance,

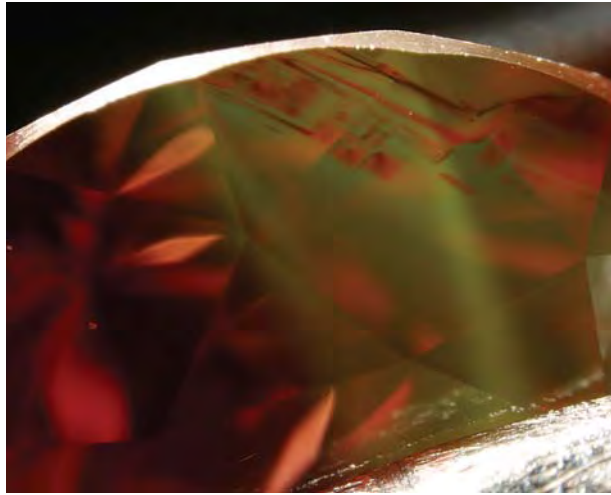


Figure 14. Green luminescence to visible light (related to the H3 center) was seen in all samples. In most samples, this luminescence followed the internal growth structures, as with the stepped octahedral zoning seen here. In some, however, the green luminescence was more evenly distributed throughout. Photomicrograph by C. P. Smith; magnified 35 \times .

ranging from homogeneous to an alignment with the internal growth structures. In addition, a few samples also displayed zones of yellow luminescence attributed to (N-V)⁰ emission centered at 575 nm. When all three luminescence colors were present in the same stone, they made for a very colorful image of the internal growth structures (figure 15), which we had not encountered previously.

Fluorescence. All the samples displayed a distinctive, moderate-to-strong, very chalky fluorescence reaction when exposed to either long- or short-wave UV radiation. In general, these diamonds revealed combinations of yellow, green, and orange fluorescence on exposure to long-wave UV, although a couple of samples also exhibited blue fluorescence. With close inspection, zoning (often subtle) could be seen between the different colors (figure 16). To short-wave UV, these diamonds displayed a rather consistent moderate-to-strong orange and yellow fluorescence. In most samples, the orange fluorescence dominated, and the yellow could be seen in only certain areas, such as near the culet (figure 17). No phosphorescence was evident in any of the samples following exposure to long- or short-wave UV.

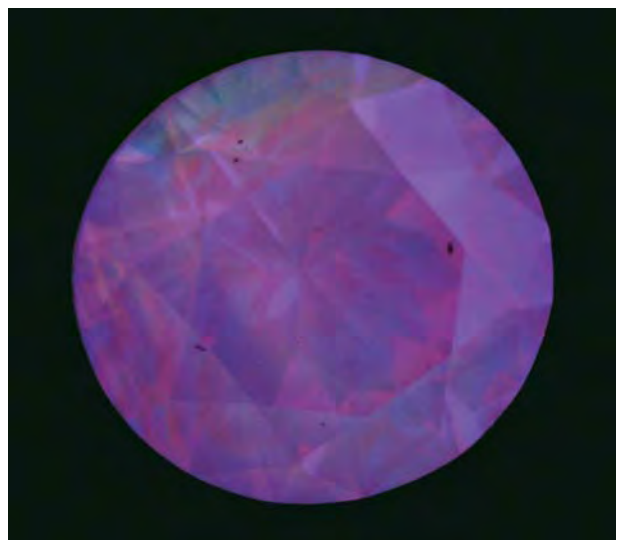
UV-Vis-NIR Spectroscopy. Overall, of the 41 stones included in this study, most revealed similar absorption features in the ultraviolet to visible and near-infrared regions of the spectrum,



Figure 15. Strikingly, when exposed to a strong light source, several of the samples exhibited all three luminescence colors—green, orange-red, and yellow—producing a combination of colors unlike any the authors had seen previously in a natural-color diamond. Photomicrograph by C. P. Smith; magnified 27 \times .

although certain variations were noted (figure 18). The most dominant series of bands included strong absorptions at 415 nm (N3), 503 nm (H3), 575 nm (N-V)⁰, and 637 nm (N-V)⁻, which were evident in all the samples. Of these, the absorption at 637 nm was consistently the most intense. A weak absorption at 496 nm (H4) was recorded

Figure 16. This image reveals the typical, chalky long-wave UV fluorescence of the “Imperial” treated-color diamonds, which results from a combination of orange, yellow, and green fluorescing zones. Such a reaction is not seen in natural-color pink-to-red and purple diamonds. Photomicrograph by C. P. Smith; magnified 10 \times .



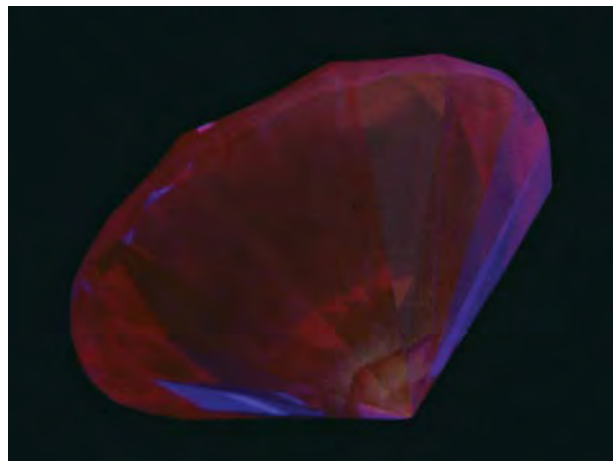


Figure 17. The reaction to short-wave UV of these diamonds is also highly indicative of the treatment, displaying a consistent moderate-to-strong orange and yellow fluorescence. In most samples, the orange fluorescence dominated; the yellow was seen only in certain areas, such as near the culet in this sample. Photomicrograph by C. P. Smith; magnified 10 \times .

in most samples (31 total); in only one of these was the H4 stronger than the H3. Half the samples had absorption at 594 nm that varied greatly in intensity from one sample to the next. In most cases, this band was weak to moderate, but it was extremely strong in three samples. In those samples where we detected the 594 nm absorption, we also typically recorded a weak 741 nm (GR1) absorption, as well as a weak 805 nm absorption. However, the 805 nm band also occurred in some stones that did not reveal either the 594 nm or GR1 features. Several of the samples that had both the 594 nm and GR1 also showed weak absorptions at 425 and 527 nm; five of these showed a very weak absorption at 394 nm (ND1).

When the samples were cooled and viewed with a standard handheld spectroscope, similar features were noted, consisting of strong, sharp lines at 415, 503, and 637 nm in all the samples, as well as sharp, weak-to-moderate lines at 575 and 594 nm in many of them.

IR Spectroscopy. All the diamonds we tested proved to be type Ia. The concentrations and relative aggregation states of nitrogen varied significantly between samples (figure 19). Absorption features at 1280 and 1215 cm^{-1} are attributed to nitrogen in the A-aggregate form (nitrogen atoms in pairs), and

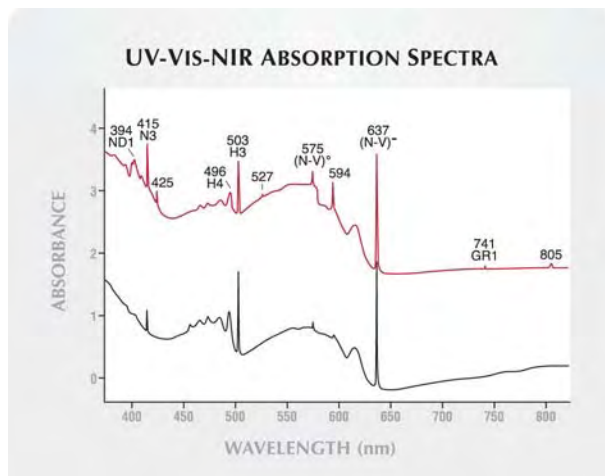


Figure 18. The absorption spectra through the ultraviolet, visible and near infrared regions show strong absorption features from several defect centers including the N3, H3, (N-V)⁰, and (N-V)⁻, which are typical of these treated-color diamonds. These absorption features combine to produce a transmission “window” in the red region, which is responsible for the pink/red coloration of these stones. In addition, absorptions with varying intensities at 394 (ND1), 425, 496 (H4), 527, 594, 741 (GR1), and 805 nm were also observed in several of the samples. The upper spectrum is from a 0.40 ct purplish pink diamond, and the lower spectrum is from a 0.41 ct brown-pink diamond. The spectra are offset vertically for clarity.

those at 1170 and 1010 cm^{-1} are attributed to nitrogen in the form of B-aggregates (four nitrogen atoms surrounding a common vacancy). In general, the concentration of A-aggregates was significantly higher than B-aggregates. This trend held true for all except seven of the samples, where the nitrogen was dominantly in the B-aggregate form. Using a spectral fitting calibration against the two-phonon absorption of diamond, we estimated the total nitrogen content to range from 23 to 322 ppm. In addition, most of the samples displayed weak-to-moderate absorption bands at 3107 and 1405 cm^{-1} , which are related to hydrogen impurities. Interestingly, the samples with nitrogen predominantly in the B-aggregate form also revealed significantly stronger hydrogen absorption.

A relatively strong absorption at 1450 cm^{-1} (H1a—an interstitial nitrogen atom; Woods, 1984) and a weak absorption at 1344 cm^{-1} related to isolated nitrogen impurities (type Ib component) were recorded in all samples. Again using spectral fitting

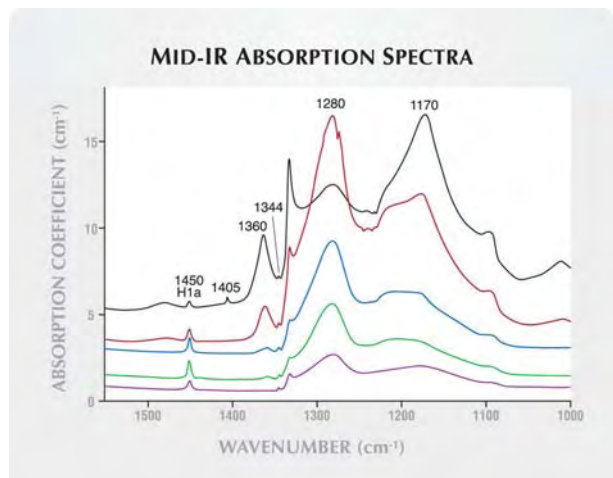


Figure 19. These representative absorption spectra in the mid-infrared range illustrate the large variation in nitrogen concentration of these treated-color diamonds. All of the stones in this study were classified as type Ia, and most are dominated by the A-aggregate form of nitrogen. However, a few samples (e.g., black line) contained more B-aggregates than A-aggregates. Also note the relatively strong H1a absorption at 1450 cm^{-1} , and the weak absorption at 1344 cm^{-1} , which is related to isolated nitrogen. Very weak absorptions at 1358 and 1355 cm^{-1} were also observed in those samples that had little or no platelet peak absorption at $\sim 1360 \text{ cm}^{-1}$. The spectra are offset vertically for clarity.

techniques, we calculated the intensity of the H1a absorption at around 0.2–1.2 cm^{-1} and estimated the concentration of isolated nitrogen at 3–28 ppm. Another common feature of varying intensity was the nitrogen platelet peak at $\sim 1360 \text{ cm}^{-1}$. In the samples in which this peak was absent or very weak, two very weak absorptions at 1358 cm^{-1} (intensity of 0.04 to 0.1 cm^{-1}) and 1355 cm^{-1} (0.04 to 0.1 cm^{-1}) were also evident.

In the near-infrared region (figure 20), the dominant features included strong absorptions at 5165 cm^{-1} (H1c) and/or 4935 cm^{-1} (H1b). The relative intensity of the H1b to H1c was determined to be proportional to the diamond's nitrogen aggregation state (see, e.g., Collins et al., 1986). In those diamonds that were dominated by A-aggregates, virtually no H1c was detected, whereas the diamond with B \gg A aggregations of nitrogen exhibited a much stronger H1c absorption than H1b. A moderate-to-strong H2 (negatively charged N-V-N center) absorption at $\sim 10125 \text{ cm}^{-1}$ (987.7 nm) was also seen

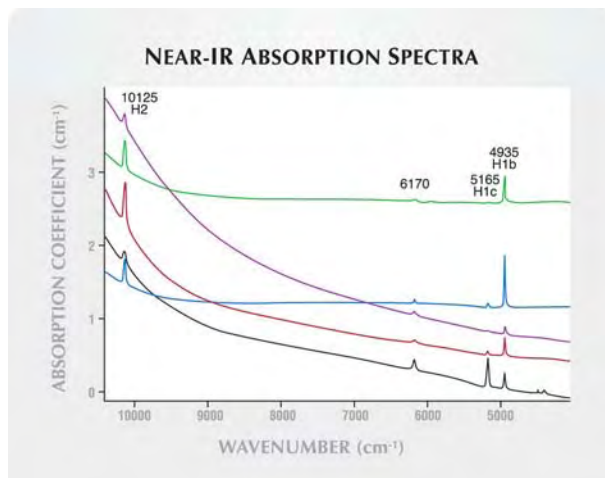


Figure 20. Strong H1c and/or H1b absorption lines, as well as a sharp peak at 6170 cm^{-1} , are features commonly seen in the near-infrared absorption spectra of these treated-color diamonds. A very strong H1c occurred in another sample, which was dominated by the B-aggregate form of nitrogen (black curve). A moderate-to-strong H2 absorption was observed in all samples. The spectra are offset vertically for clarity.

in all samples, with an intensity that varied from 0.05 to 0.6 cm^{-1} (majority $>0.2 \text{ cm}^{-1}$). The intensity of the H2 absorption had a direct correlation to the concentration of A-aggregates. In one sample, the intensity of the H2 was 0.5 cm^{-1} correlated to an A-aggregate concentration of 143 ppm. Another sample with an A-aggregate concentration of only 10 ppm had an H2 absorption intensity of only 0.1 cm^{-1} . Another sharp, relatively strong absorption was recorded at 6170 cm^{-1} in all the samples tested. The occurrence of this absorption in diamond was reported only very recently (see further comments below; De Weerd and Anthonis, 2004). To date, no correlation is evident between the 6170 cm^{-1} peak and the presence of H1a, H1b, or H1c.

Raman PL Spectroscopy. Low-temperature photoluminescence spectra revealed dominant PL bands of the same wavelength as the absorption bands recorded with the spectrophotometer. In addition to the strong emissions from the H3, (N-V) 0 , and (N-V) $^-$ centers, we also noted H4 emission at 496 nm of variable intensity in all the samples (figure 21). For those samples that were nearly pure type IaA, the H4 luminescence was the weakest. At 535 nm another weak intensity band was also commonly recorded. A weak but sharp emission at 588 nm was

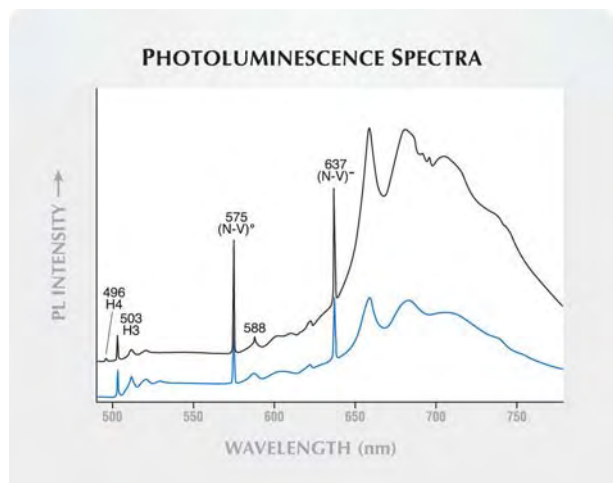


Figure 21. Photoluminescence spectra collected using an Ar-ion laser (488 nm excitation) exhibited strong emissions at 503, 575, and 637 nm. Weak luminescence peaks were also observed in some samples at 496, 535, and 588 nm. The spectra are offset vertically for clarity.

evident using both the 488 and 514 nm laser excitations. This independent 588 nm emission typically was superimposed onto the broad side band of 575 nm (N-V)⁰. The 588 nm emission was observed in 22 of the samples; the GR1 and 594 nm features were also detected in the absorption spectra of these same samples.

DISCUSSION

The Treatment Method. A recent patent by one of the Russian scientists associated with Lucent Diamonds describes the methods by which red color may be produced in diamonds in a laboratory (Vins, 2004). The technique consists of generating isolated nitrogen in natural type Ia diamond via HPHT conditions (6–7 GPa at over 2150°C), followed by irradiation using a high-energy electron beam and further annealing in a vacuum at a temperature no lower than 1100°C. Based on the results of our analyses, it is evident that the Lucent “Imperial” pink to red treated-color diamonds we have examined have been processed by a similar method. This is based on several standard gemological and spectroscopic features.

First, the severe graphitization and etching seen with magnification clearly indicate that these diamonds were exposed to HPHT conditions. In addition, the presence of isolated nitrogen in the infrared spectrum is consistent with the de-aggregation of nitrogen defects under similar conditions (see, e.g., Fisher and Spits, 2000), although the pres-

ence of isolated nitrogen alone is not proof of HPHT treatment. Further evidence of irradiation-induced defects is provided by the 594, 637, and 741 (GR1) absorptions in these type IaAB diamonds with a Ib component. The presence of the H1b and/or H1c bands in the near-infrared region is also consistent with annealing subsequent to irradiation. When a type Ia irradiated diamond is annealed at around 1000°C, the 594 nm center is removed, thus producing H1b and/or H1c lines (Collins, 1982). Also important is the presence of a much less stable defect in some of the samples, the ND1, which is removed at temperatures above 500°C (Zaitsev, 2001). When this band occurs in combination with the 594 nm band as well as H1b and H1c absorptions, it is indicative of a multi-step process involving HPHT annealing, irradiation, and relatively lower temperature, low pressure annealing.

In the patent, the overall nitrogen concentration is described as exceeding 800 ppm. However, during the course of our investigation, we determined that the total nitrogen concentration in the diamonds we tested was 23–322 ppm.

Characterization of the Samples. The majority of the diamonds were darker in tone and higher in saturation than the natural-color diamonds we have encountered in this hue range. However, there were two samples—a Fancy Deep pink and a Fancy Deep brown-pink—that closely resembled the appearance of natural-color diamonds.

The mineral inclusions we observed with magnification identified the diamonds as being naturally grown. However, the heavily graphitized and etched features also clearly indicated that these stones had been exposed to high pressure/high temperature (HPHT) processing. The larger, more massive, coarsely textured black to dark gray inclusions were foreign minerals that experienced severe graphitization of the diamond at the interface between the included crystal and the diamond host. The HPHT conditions were also responsible for the graphitization along internal fractures and the etching observed along surface-reaching cleavages and in those areas at the surface that were not repolished following treatment. It is important to note that graphitization may take place naturally in diamond; however, such natural inclusions are very different in appearance from these samples. It also should be noted that, depending on the specific HPHT conditions, there may be significantly less graphitization and etching in some treated samples.

In type Ia natural diamonds, naturally occurring pink-to-red and purple coloration is clearly associated with zones exhibiting plastic deformation. As a result, when such stones are viewed between crossed polarizing filters, they typically reveal very high levels of strain (see, e.g., figure 15 in King et al., 2002, p. 140). The strain visible in these treated-color samples was significantly weaker. In only a few of the Lucent samples did the strain levels approach what is typical for their natural-color counterparts.

The thick and extended regions of color zoning that were present in these samples occurred in a variety of straight, angular, and irregular patterns. Such color zoning is very different from that encountered in natural-color pink-to-red diamonds, which is visible as straight, parallel color zones that extend in only one direction and typically do not have sharp boundaries (see, e.g., Koivula, 2000, p. 92).

The DiamondView imaging accentuates the complex growth structure of these natural diamonds, which involves the development of primarily octahedral {111} growth planes. The large variation in fluorescence colors (red, orange, yellow, blue, and green) as well as the dark areas where no fluorescence was evident, is a direct reflection of the specific type and concentration of defects before treatment and the resultant reconfiguration of the defects by the treatment process. These features are markedly different from those of synthetic diamonds created by HPHT or CVD techniques, and they confirm the natural origin of these samples (Wang et al., 2003; Shigley et al., 2004).

When illuminated by a strong light source, green (H3) luminescence has been seen in many naturally colored, as well as artificially colored, diamonds (Fritsch, 1998; Reinitz et al., 2000). (It is often referred to as "transmission luminescence," though this is not strictly correct.) A weak orange-red luminescence due to N-V centers may be seen in some natural-color pink diamonds; however, it is more commonly associated with treated-color pink-to-red diamonds with moderate to high color saturation (see, e.g., Shigley et al., 2004). Nevertheless, we had not previously witnessed the combination of green (H3), orange-red (N-V)⁻, and yellow (N-V)⁰ visible luminescence seen in these treated-color diamonds. Nor have we encountered in natural-color pink-to-red diamonds the strong, chalky orange, green, and yellow fluorescence to long-wave UV that was evident in these treated stones.

The "Imperial" treated-color diamonds in this study owed their color to the absorption of N-V cen-

ters positioned at 575 and 637 nm, with some influence from other absorption features. The introduction of a relatively high concentration of H3/H4 defects, which absorb blue-green light, is essential to generate a pure red hue. If the H3/H4 absorptions are not strong enough, a distinct purple hue will be developed, as was observed in some of the stones we tested. High concentrations of the A/B form of nitrogen are necessary to generate H3/H4 defects during treatment. Additionally, if the absorption of the N-V centers is not strong enough relative to the absorption of the H3 and H4 centers, then brown colors develop.

In contrast, the vast majority of natural-color pink-to-red diamonds owe their hue to a broad absorption band centered at approximately 550 nm (e.g., Collins 1982; King et al., 2002; Moses et al., 2002). To date, we are not aware of any reports of the artificial introduction of the 550 nm band in type I natural diamonds. We have examined a small number of natural-color pink diamonds that owe their color to N-V centers. Typically, these diamonds are rather pale in color and are classified as type IIa. However, we have not observed strong H3 or N3 absorption in such diamonds.

The physics responsible for the 588 nm peak visible in the PL spectra of some samples is not fully understood (Zaitsev, 2001). On initial consideration, there seemed to be some correlation between the occurrence of this peak and the color saturation of the diamonds. After further investigation, however, we found that the 588 nm emission may also be observed in some natural green-yellow diamonds that have high concentrations of H3 centers.

The 6170 cm⁻¹ absorption in the infrared is another little-known defect. Its occurrence, reported in previous publications and the present study, is closely related to irradiation and annealing, either naturally or in the laboratory. De Weerd and Anthonis (2004) first reported a peak at 6172 cm⁻¹ in a treated diamond and, based on their experiments, suggested that it resulted from a complex treatment process. In addition, Hainschwang et al. (in preparation) have correlated a band at 6165 cm⁻¹ to the presence of H1c centers in irradiated and annealed diamonds. In this study of a large set of samples, we found no such correlation. However, those samples with the strongest 6170 cm⁻¹ band in general had very weak H1b/H1c bands and relatively stronger 594 nm absorption. In unpublished data from ongoing research at GIA, we have recorded the occurrence of this band (with position varying slightly from 6170 to 6168 cm⁻¹) in a few naturally

irradiated diamonds as well. A few of those natural-color stones displayed green radiation stains. All these observations indicate that the 6170 cm^{-1} absorption represents a defect that may be introduced via irradiation and annealing processes, either in the laboratory or in nature. Consequently, we do not consider the presence of this band as conclusive of color treatment on its own.

Although we did not perform stability testing per se, we concluded—based on the kinds of defects observed and their concentrations—that the colors produced by the multiple-step treatment process described here are both stable and permanent to normal conditions of wear and care. In addition, we did not detect any residual radioactivity.

IDENTIFYING CHARACTERISTICS

A number of standard gemological properties and advanced analytical features will readily identify that these stones are naturally grown and their color has been artificially induced. The fact that they were grown in nature can be confirmed by the presence of characteristic mineral inclusions and distinctive internal growth structures, as well as by the lack of the inclusion features and growth structures typical of HPHT- and CVD-grown synthetic diamonds. With standard gemological techniques, the artificial coloration can be identified by the strongly altered inclusion features in combination with the differences in appearance of the pink-to-purple or brown color zoning in these samples as compared to the colored graining in natural-color diamonds. In addition, with a standard handheld spectroscope, the distinctive combination of strong 415, 503, and 637 nm absorption lines, as well as weak-to-moderate 575 and 594 absorption lines, clearly identifies the treated origin of the color. Furthermore, the unique long- and short-wave UV fluorescence reactions are clear indicators that this material has been treated.

The more advanced analytical techniques also revealed some interesting identification criteria that

appear to be unique to this process. The occurrence of trace isolated nitrogen, together with H3 and H2 centers, are some of the common features related to HPHT treatment, whereas defects such as H1a, H1b, H1c, $(\text{N-V})^-$, 594 nm, $(\text{N-V})^0$, H3, and H4 commonly occur in diamonds that have been exposed to radiation. Although these defects may occur in natural-color diamonds, we have not seen a known natural-color diamond that has all of these features. The absorption at 6170 cm^{-1} , although not proof, may also suggest color treatment.

CONCLUSION

Naturally colored diamonds in the pink-to-red hue range are some of the most exotic and expensive gemstones. At auction, such diamonds have achieved as much as US\$895,000 per carat (Balfour, 2000). As a result, various forms of treatment have been applied in attempts to recreate these highly desirable colors. Previously, these ranged from simple topical coatings (e.g., Moses et al., 2004) to more advanced techniques such as irradiation of type Ib diamonds (Crowningshield, 1959; Crowningshield and Reinitz, 1995) and HPHT annealing of type IIa diamonds (e.g., De Beers Industrial Diamonds et al., 2001).

Most recently, Lucent Diamonds has introduced treated-color pink-to-red natural diamonds into the marketplace under the trade name “Imperial Red Diamonds.” The Lucent group began developing the technology to produce these stable colors on a commercial basis toward the end of 2003, and they first offered them for sale in the summer of 2004. Our investigations confirmed that a combination of treatment techniques, including HPHT annealing and irradiation, are applied to induce the coloration in these diamonds, consistent with the process described by Vins (2004). They can be readily identified by their distinctive inclusion features, color zoning, and long- and short-wave UV fluorescence, as well as by their unique combination of spectroscopic features.

ABOUT THE AUTHORS

Dr. Wang is research scientist, Mr. Smith is director of identification services, Mr. Hall is manager of analytical research services, and Mr. Moses is vice president of identification and research at the GIA Gem Laboratory in New York. Dr. Breeding is research scientist at the GIA Gem Laboratory in Carlsbad, California.

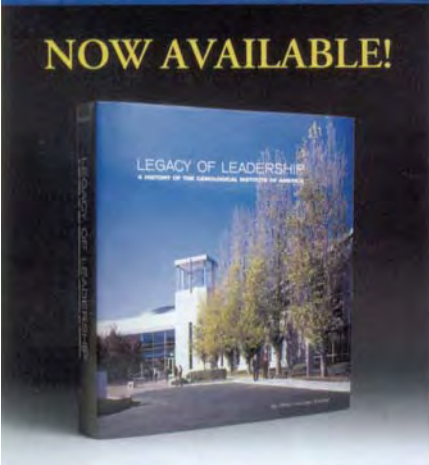
ACKNOWLEDGMENTS: The authors are grateful to Alex Grizenko, president of Lucent Diamonds Inc., for supplying specimens for this study, and to Dr. Victor Vins, research and development manager of New Diamonds of Siberia, Novosibirsk, Russia, for many helpful discussions. They also thank John King and Joshua Cohn, of the GIA Gem Laboratory in New York, for careful color grading observations and useful discussions.


REFERENCES

- Balfour I. (2000) *Famous Diamonds*. Christie, Manson & Woods, London.
- Collins A.T. (1982) Colour centres in diamond. *Journal of Gemmology*, Vol. 18, No. 1, pp. 37–75.
- Collins A.T., Davies G., Woods G.S. (1986) Spectroscopic studies of the H1b and H1c absorption lines in irradiated, annealed type-Ia diamonds. *Journal of Physics C: Solid State Physics*, Vol. 19, pp. 3933–3944.
- Crowningshield G.R. (1959) Highlights at the Gem Trade Lab in New York. *Gems & Gemology*, Vol. 9, No. 9, pp. 268–270.
- Crowningshield G.R., Reinitz I. (1995) Gem Trade Lab Notes: Treated-color pink diamond. *Gems & Gemology*, Vol. 31, No. 2, pp. 121–122.
- De Beers Industrial Diamonds, Spits R.A., Burns R., Fisher D. (2001) *High Temperature/Pressure Color Change of Diamond*. International (PCT) patent application WO 01/72404A1, filed April 2.
- De Weerd F., Anthonis A. (2004) A new defect observed in irradiated and heat treated type Ia diamonds. *The 55th Diamond Conference*, July 5–7, 2004, Warwick, England, p. 17.
- Fisher D., Spits R.A. (2000) Spectroscopic evidence of GE POL HPHT-treated natural type IIa diamonds. *Gems & Gemology*, Vol. 36, No. 1, pp. 42–49.
- Fritsch E. (1998) The color of diamond. In G. E. Harlow, Ed., *The Nature of Diamonds*, Cambridge University Press, Cambridge, U.K., pp. 23–47.
- Hainschwang T., Fritsch E., Notari F., Massi L. (in preparation) The properties of irradiated and annealed diamonds exhibiting an undescribed near-infrared absorption.
- Hall M., Moses T. (2000) Gem Trade Lab Notes: Diamond—blue and pink HPHT annealed. *Gems & Gemology*, Vol. 36, No. 3, pp. 254–255.
- King J.M., Moses T.M., Shigley J.E., Liu Y. (1994) Color grading of colored diamonds in the GIA Gem Trade Laboratory. *Gems & Gemology*, Vol. 30, No. 4, pp. 220–242.
- King J.M., Shigley J.E., Guhin S.S., Gelb T.H., Hall M. (2002) Characterization and grading of natural-color pink diamonds. *Gems & Gemology*, Vol. 38, No. 2, pp. 128–147.
- Koivula J.I. (2000) *The Microworld of Diamonds*. Gemworld International, Northbrook, IL.
- Moses T., King J.M., Wang W., Shigley J.E. (2002) A highly unusual 7.34 carat Fancy Vivid purple diamond. *Journal of Gemmology*, Vol. 28, No. 1, pp. 7–12.
- Moses T., Smith C., Wang W., Hall M. (2004) Topical coating on diamonds to improve their color: A long history. *Rapaport Diamond Report*, Vol. 27, No. 20, pp. 91–93.
- Orlov Yu. L. (1977) *The Mineralogy of Diamond*. Wiley Interscience, New York, pp. 128–131.
- Reinitz I.M., Buerki P.R., Shigley J.E., McClure S.F., Moses T.M. (2000) Identification of HPHT-treated yellow to green diamonds. *Gems & Gemology*, Vol. 36, No. 2, pp. 128–137.
- Shigley J.E., McClure S.F., Breeding C.M., Shen A.H., Muhlmeister S.M. (2004) Lab-grown colored diamonds from Chatham Created Gems. *Gems & Gemology*, Vol. 40, No. 2, pp. 128–145.
- Vins V.G. (2004) *The Technique of Production of Fancy Red Diamonds*. Russian Federation patent 2237113, filed June 26, 2003, issued Sept. 27, 2004. [in Russian]
- Wang W., Moses T., Linares R., Hall M., Shigley J.E., Butler, J. (2003) Gem-quality synthetic diamonds grown by a chemical vapor deposition (CVD) method. *Gems & Gemology*, Vol. 39, No. 4, pp. 268–283.
- Welbourn C.M., Cooper M., Spear P.M. (1996) De Beers natural versus synthetic diamond verification instruments. *Gems & Gemology*, Vol. 32, No. 3, pp. 156–169.
- Woods G.S. (1984) Infrared absorption studies of the annealing of irradiated diamonds. *Philosophical Magazine B*, Vol. 50, pp. 673–688.
- Zaitsev A.M. (2001) *Optical Properties of Diamond*. Springer-Verlag, Berlin, 502 pp.

LEADERSHIP LEGACY OF LEADERSHIP

NOW AVAILABLE!





LEGACY OF LEADERSHIP

A HISTORY OF THE GEMOLOGICAL INSTITUTE OF AMERICA

Prize-winning journalist William George Shuster of JCK magazine tells the story of GIA and the growth of the gemology movement worldwide. Features more than 200 archival images and interviews with dozens of the gem and jewelry industry's history makers.

Yours for only \$49.95

To order, visit www.gia.edu and click on **GIA Gem Instruments and Books**. Call 800-421-8161 within the U.S., or 760-603-4200.

LEADERSHIP LEGACY OF LEADERSHIP

A GEMOLOGICAL STUDY OF A COLLECTION OF CHAMELEON DIAMONDS

Thomas Hainschwang, Dusan Simic, Emmanuel Fritsch, Branko Deljanin, Sharrie Woodring, and Nicholas DelRe

Chameleon diamonds are among the rarest of gem diamonds. This article reports on a unique collection of 39 chameleon diamonds ranging from 0.29 to 1.93 ct, which exhibited temporary changes in color when heated to approximately 150°C and, for some, after prolonged storage in the dark (i.e., thermochromic and photochromic color changes, respectively). Most changed from “olive” green to brownish yellow or yellow, although some changed from light yellow to a more intense greenish yellow. The thermochromic and photochromic color change observed in the “olive” green chameleon diamonds is typical of “Classic” chameleons, whereas the solely thermochromic change shown by the light yellow group was the “Reverse” of that seen in Classic chameleon diamonds. The Classic and Reverse groups showed different spectroscopic and UV fluorescence characteristics, but all stones exhibited strong long-lasting phosphorescence after short-wave UV excitation. Hydrogen was identified in all samples by FTIR spectroscopy, and minor Ni-related emissions were detected by photoluminescence spectroscopy in most. Using this combination of reaction to UV radiation and spectroscopic properties, a gemologist can separate chameleon from other green diamonds without unnecessary exposure to heat.

The rarity of chameleon diamonds and their interest for the connoisseur are due to their unusual ability to change color temporarily when heated to about 150°C (“thermochromism”) or after prolonged storage in the dark (“photochromism”; see Fritsch et al., 1995). The stable color shown by chameleon diamonds is typically grayish yellowish green to grayish greenish yellow (“olive”), while the unstable hue is generally a more intense brownish or orangy yellow to yellow (figures 1 and 2). After heating, the color of a chameleon diamond quickly returns to its stable hue. The color change after storage in the dark is usually not as dramatic as that seen on heating. Some of these chameleons have a stable color reminiscent of “normal” green diamonds. While the green color of these diamonds is caused by exposure to radiation (either naturally or in the laboratory), the mechanism behind chameleon coloration is not yet well understood. Nevertheless,

chameleons are among the few green diamonds that can be conclusively identified as natural color, since this behavior cannot be created or enhanced in the laboratory.

Relatively little has been written about chameleon diamonds, and the precise definition of this behavior is not at all clear. For some members of the trade, a temporary photochromic color change must be present for a diamond to be referred to as “chameleon”; in contrast, many publications describe chameleon diamonds as having *either* a thermochromic (using rather low annealing temperatures) or photochromic temporary color change (Raal, 1969; *GIA Diamond Dictionary*, 1993; Fritsch et al., 1995).

See end of article for About the Authors and Acknowledgments.
GEMS & GEMOLOGY, Vol. 41, No. 1, pp. 20–35.
© 2005 Gemological Institute of America



Figure 1. One of the more spectacular chameleon diamonds examined for this study was this 1.01 ct marquise diamond, shown at room temperature (left) and at approximately 150°C (right). Photo by T. Hainschwang.

Chameleon diamonds were first documented in 1943 (*GIA Diamond Dictionary*, 1993), and since then they have been described in several brief reports (see, e.g., Chabert and Reinitz, 2000). Extensive research on a single large chameleon diamond was published by E. Fritsch and colleagues (1995). Most recently, Shigley et al. (2004) reported additional data on chameleon diamonds, including the presence of Ni-related emissions detected by

photoluminescence spectroscopy. We believe the present article is the first extensive study of a large number of chameleon diamond samples; it is part of ongoing research by EGL USA on colored diamonds in collaboration with other gemological laboratories and universities worldwide. Some preliminary observations on this collection of chameleon diamonds were published by Deljanin (2004).

Figure 2. These images show typical color changes seen in chameleon diamonds of the Classic (top, 0.83 ct) and Reverse (bottom, 1.09 ct) types. The left images show the stable color, while the unstable color is on the right. Photos by T. Hainschwang.



MATERIALS AND METHODS

Thirty-nine chameleon diamonds were included in this study (as described in table 1 and illustrated in figure 3). Unfortunately, the geographic origins of these diamonds are unknown. The stones were purchased between 1987 and 2004: 40% were obtained in India, 30% in Antwerp, and 30% in Tel Aviv. All the diamonds were accompanied by grading reports from either GIA or EGL, which stated that, under certain circumstances, they exhibited a change in color.

The stable color of the chameleon diamonds was graded by the above laboratories, while the unstable color was described by two of the authors (TH and DS). Luminescence to ultraviolet radiation and phosphorescence were observed with a 4-watt UVP UVGL-25 Mineralight Lamp using 254 nm (short-wave) and 365 nm (long-wave) excitation. Observations between crossed polarizers were made with a gemological microscope using Leica optics at 10–60× magnification. Color distribution was studied with each stone immersed in methy-

lene iodide. The change in color was observed using a 6500 K daylight-equivalent light and a hot plate (range of 40–325°C); the temperature during the heating process was monitored using a thermocouple connected to a digital multimeter. The samples were also cooled in liquid nitrogen to monitor possible color changes induced by low temperature.

We recorded infrared spectra in the range of 6000–400 cm⁻¹ on a Nicolet Nexus 670 FTIR spectrometer, using a diffuse reflectance (DRIFTS) accessory as a beam condenser to facilitate the analysis of small faceted stones, with an accumulation of 100 scans at a resolution of 2–4 cm⁻¹. We recorded pho-

toluminescence spectra with the diamonds immersed in liquid nitrogen ($T \approx -196^\circ\text{C}$), using an Adamas Advantage SAS2000 system equipped with a 532 nm semiconductor laser and an Ocean Optics SD2000 spectrometer (resolution 1.5 nm) with a 2048-element linear silicon CCD-array detector. Vis-NIR spectra in the range of 400–1000 nm were collected with the SAS2000 system, using the same spectrometer and detector as described above, with a resolution of 1.5 nm and 60–250 sample scans. The measurements were performed using an integrating sphere at liquid nitrogen temperature. Also, to monitor changes due to heating, we recorded

TABLE 1. The 39 chameleon diamonds in this study and their changes in color.

Stone no./ Grading lab ^a	Weight and shape	Classic or Reverse group	Stable color	Unstable color ^a	Magnitude of color change
1.1/GIA	0.39 ct round	Classic	Fancy Dark grayish greenish yellow	Fancy Intense orangy yellow	Strong
1.2/GIA	0.64 ct marquise	Classic	Fancy Dark brownish greenish yellow	Fancy Deep brownish orangy yellow	Strong
1.3/GIA	0.43 ct marquise	Classic	Fancy Dark grayish yellowish green	Fancy Deep brownish orangy yellow	Strong
1.4/EGL	0.63 ct marquise	Classic	Fancy Deep green yellow	Fancy Deep brownish greenish yellow	Weak
1.5/GIA	1.60 ct pear	Classic	Fancy Dark yellowish brown	Fancy Deep brownish orangy yellow	Strong
1.6/GIA	0.46 ct pear	Classic	Fancy Dark grayish yellowish green	Fancy Intense orangy yellow	Strong
1.7/EGL	0.83 ct heart	Classic	Fancy Deep grayish yellowish green	Fancy Intense orangy yellow	Strong
1.8/GIA	1.75 ct cushion	Classic	Fancy Dark grayish yellowish green	Fancy greenish yellow	Weak
1.9/GIA	0.67 ct oval	Classic	Fancy Dark grayish yellowish green	Fancy Intense yellow	Strong
2.1/GIA	1.93 ct marquise	Classic	Fancy Deep brownish greenish yellow	Fancy Deep brownish orangy yellow	Strong
2.2/GIA	0.72 ct marquise	Classic	Fancy brownish greenish yellow	Fancy Deep orangy brown yellow	Strong
2.3/GIA	0.58 ct marquise	Classic	Fancy grayish greenish brown yellow	Fancy Deep brownish orangy yellow	Strong
2.4/GIA	0.81 ct heart	Classic	Fancy Deep brownish greenish yellow	Fancy Deep brownish orangy yellow	Strong
2.5/GIA	0.48 ct marquise	Classic	Fancy brownish yellow	Fancy Intense yellowish orange	Strong
2.6/GIA	0.29 ct marquise	Classic	Fancy brownish greenish yellow	Fancy Intense orangy yellow	Strong
2.7/GIA	0.57 ct heart	Classic	Fancy grayish greenish yellow	Fancy brownish yellow	Strong
2.8/EGL	0.46 ct round	Classic	Fancy Deep brownish greenish yellow	Fancy Deep brownish orangy yellow	Strong
2.9/EGL	0.52 ct round	Reverse	Fancy Light brownish yellow	Fancy greenish yellow	Moderate

^aDescriptions of the unstable colors for all of the diamonds were determined by the authors. Note that, presently, GIA only recognizes the Classic type (and not the Reverse type) as a chameleon diamond.

spectra at room temperature as well as with some stones heated to approximately 325°C; the higher temperature was used to assure that the diamond was in its unstable color state during the accumulation of the spectrum.

In addition to the 39 diamonds included in the chameleon collection, one additional chameleon diamond was analyzed (box A); the sample, referenced as TH-A1, was first described by Hainschwang (2001). An FTIR spectrum of a hydrogen-rich chameleon diamond, which was not part of the collection, called "TH-cham1," is included to compare the strength of color change with hydrogen content.

RESULTS

Color Description. Two different stable-color groups were observed in the chameleon diamonds (see figure 3, top):

1. Green with a gray, brown, or yellow color component ("olive"); or yellow with green, brown, or gray modifying colors. These are referred to hereafter as "Classic."
2. Light yellow with typically a greenish, grayish, or brownish component. These are referred to as "Reverse."

Stone no./ Grading Lab	Weight and shape	Classic or Reverse group	Stable color	Unstable color	Magnitude of color change
3.2/GIA	1.52 ct oval	Classic	Fancy grayish yellowish green	Fancy Deep brownish yellow	Strong
3.3/GIA	0.47 ct marquise	Classic	Fancy grayish yellowish green	Fancy brownish yellow	Strong
3.4/GIA	0.58 ct marquise	Classic	Fancy Deep brownish yellow	Fancy Deep brownish yellow	Strong
3.5/GIA	1.01 ct marquise	Classic	Fancy grayish yellowish green	Fancy Intense yellow	Strong
3.6/GIA	1.54 ct marquise	Classic	Fancy gray yellowish green	Fancy grayish yellow	Moderate to strong
3.7/GIA	0.41 ct round	Classic	Fancy Dark greenish gray	Fancy Intense yellow	Strong
3.8/GIA	0.29 ct round	Classic	Fancy Dark greenish gray	Fancy Deep brownish yellow	Strong
3.9/GIA	0.47 ct round	Classic	Fancy Dark grayish yellowish green	Fancy Intense yellow	Strong
3.10/GIA	0.47 ct round	Classic	Fancy grayish yellowish green	Fancy Intense yellow	Strong
3.11/GIA	0.51 ct round	Classic	Fancy gray greenish yellow	Fancy greenish yellow	Moderate
3.12/GIA	0.39 ct round	Classic	Fancy yellowish-yellowish green	Fancy orangy yellow	Strong
4.2/GIA	0.47 ct round	Classic	Fancy Light yellow	Fancy greenish yellow	Weak
4.3/EGL	0.57 ct round	Reverse	Light grayish greenish yellow	Fancy yellow-green	Moderate
4.4/GIA	0.56 ct round	Classic	Fancy Light grayish greenish yellow	Fancy brownish yellow	Weak
4.5/EGL	0.59 ct round	Reverse	Very Light yellow	Fancy Light greenish yellow	Moderate to strong
4.7/EGL	0.51 ct marquise	Reverse	Very Light grayish yellow	Fancy yellow-green	Strong
4.8/EGL	0.46 ct marquise	Reverse	Light grayish greenish yellow	Fancy Light yellow-green	Moderate to strong
4.9/EGL	0.58 ct marquise	Reverse	Light brownish yellow	Fancy greenish yellow	Moderate to strong
4.10/EGL	0.47 ct marquise	Reverse	Light yellow (U-V)	Fancy Light greenish yellow	Moderate
4.11/GIA	0.80 ct marquise	Classic	Fancy brownish greenish yellow	Fancy Intense orangy yellow	Strong
4.12/EGL	0.36 ct marquise	Reverse	Light yellow (U-V)	Fancy Light greenish yellow	Moderate

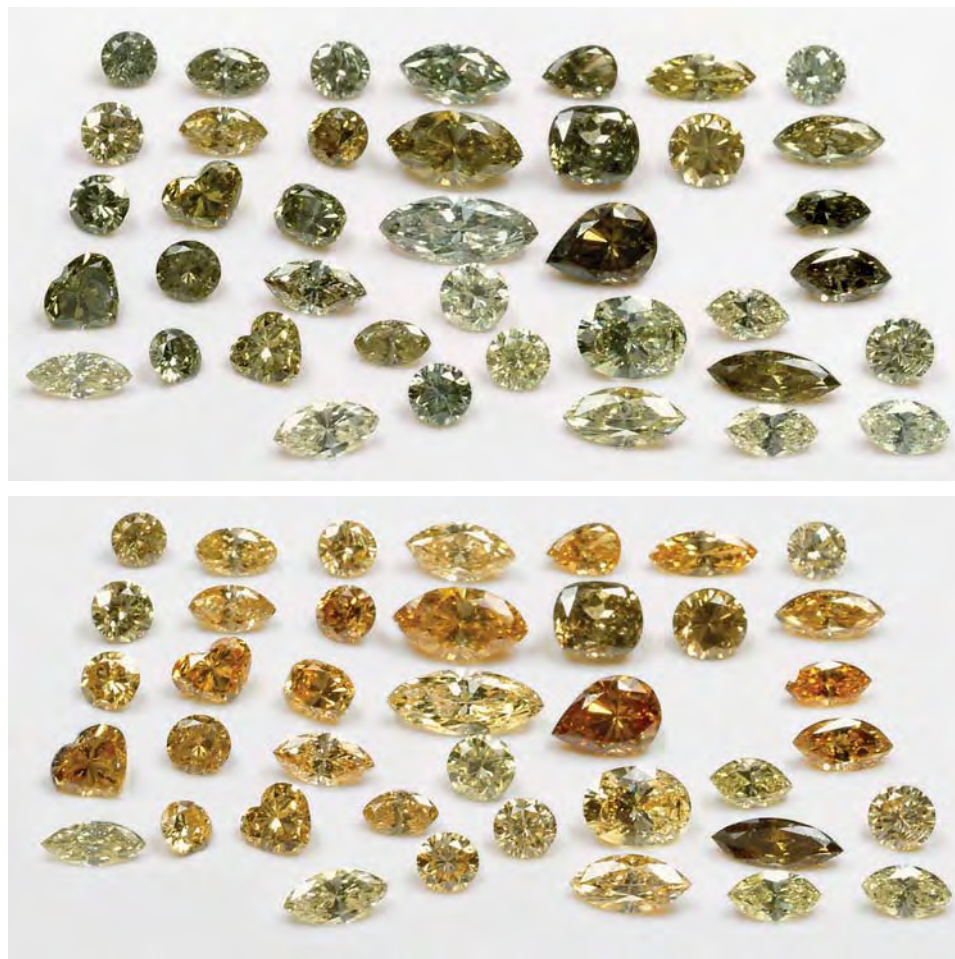


Figure 3. The collection of 39 chameleon diamonds (0.29 to 1.93 ct) is shown at room temperature (top) and when heated to 150°C (bottom). Photos by Julia Kagantsova, EGL.

The Classic group of chameleons (31 of the 39 diamonds) exhibited a distinct change in color when heated (figure 3, bottom). The unstable color varied from saturated brown-yellow to orange-yellow to yellow. The same change of color also was observed after prolonged storage in the dark for all except four stones, but it was not nearly as pronounced as the change induced by heating. Usually a couple of hours in darkness was sufficient to induce the color change. Cooling to liquid nitrogen temperature did not provoke a color change.

The Reverse group (8 of the 39 diamonds) differed from the first group in that heating induced only a weak-to-moderate change to a more saturated and greener color (again, see figure 3, bottom). Storage in the dark, even for days, did not provoke a change in color. As in the Classic chameleons, the color was not influenced by cooling to liquid nitrogen temperature (-196°C). We use the term *Reverse* for such chameleon diamonds, because their yellow-to-yellowish green color change is almost the opposite of the green-to-yellow change seen in typical chameleon diamonds.

The change in color due to heating began at approximately $100\text{--}120^{\circ}\text{C}$ in both groups. For the majority of the stones, the unstable color was most intense between 120 and 140°C . Although the diamonds were heated up to 300°C , no further changes in color were observed above about 140°C . At this temperature, a complete change in color could be induced within a few seconds.

Color Distribution. The color in most of the chameleon diamonds was evenly distributed; however, a few of the samples from the Classic group showed very slight patchy (irregular) color zoning. One diamond, also from the Classic group, exhibited very distinct yellow-brown banding (figure 4).

Anomalous Double Refraction. Between crossed polarizing filters, no characteristic pattern was seen. Some strain was observed in all samples, evident as interference colors of various intensity, and was mainly associated with inclusions. Deformation-related extinction patterns along octahedral slip planes (as typically seen in many brown to brownish

yellow-green diamonds) were observed in only a few samples, and were localized and very indistinct.

Reaction to UV Radiation. All samples exhibited characteristic long- and short-wave UV fluorescence. There were basically two types of responses:

1. *Classic group*: chalky white to chalky yellow to yellow, stronger to long-wave than to short-wave UV (figure 5)
2. *Reverse group*: chalky blue to blue to long-wave, and weaker chalky blue to yellow to short-wave UV (figure 6)

Most of the diamonds displayed moderate to strong luminescence to long-wave UV radiation, with a weak to moderate response to short-wave UV. The most interesting feature was that all stones exhibited persistent phosphorescence, more distinctly to short-wave than to long-wave UV. The phosphorescent color was yellow for all samples, but its strength and decay time varied considerably: Light yellow stones of the Reverse group that exhibited blue fluorescence had much weaker and shorter phosphorescence than the Classic-group diamonds that exhibited chalky white to yellow luminescence (again, see figures 5 and 6). Some of the diamonds of the Classic group emitted a faint, but still eye-vi-



Figure 4. This 1.93 ct chameleon diamond from the Classic group was the only sample that showed distinct color banding. Photo by T. Hainschwang.

ble, yellow glow over one hour later. In contrast, the phosphorescence of the Reverse group diamonds lasted just a few seconds to a few minutes. A Reverse-type diamond (TH-A1) analyzed prior to

BOX A: AN UNUSUAL REVERSE CHAMELEON DIAMOND

What is believed to be the first report of a “low-temperature” (i.e., below 200°C) thermochromic color change observed in a very high-nitrogen and high-hydrogen yellow diamond exhibiting Reverse chameleon behavior was published by Hainschwang (2001). The 1.09 ct marquise cut diamond, here referred to as TH-A1 (figure 2, bottom; figure 8, orange trace), exhibited a Vis-NIR spectrum with several hydrogen-related peaks—notably at 425, 440, 452, 462, 474, 545, and 563 nm—similar to the spectrum shown in figure 11 (green trace). The Reverse

chameleon diamonds included in the present article exhibit only a few of these absorptions, and they commonly show distinctly less IR-active hydrogen. Nevertheless, the color change shown by those diamonds is as strong, and in some stones stronger, than exhibited by sample TH-A1. An interesting characteristic of this diamond is that the luminescence and phosphorescence behavior change on heating (table A-1). Further research will be needed before the mechanism that produces these phenomena can be understood.

TABLE A-1. Variations in the emissions excited by UV radiation observed in sample TH-A1.

Luminescence	Long-wave UV		Short-wave UV	
	Room temperature	Hot (~200°C)	Room temperature	Hot (~200°C)
Fluorescence	Violetish blue	Zoned blue and yellow	Chalky bluish yellow	Blue with yellow zones
Phosphorescence	Weak yellow	Distinct blue	Distinct yellow	Weak blue

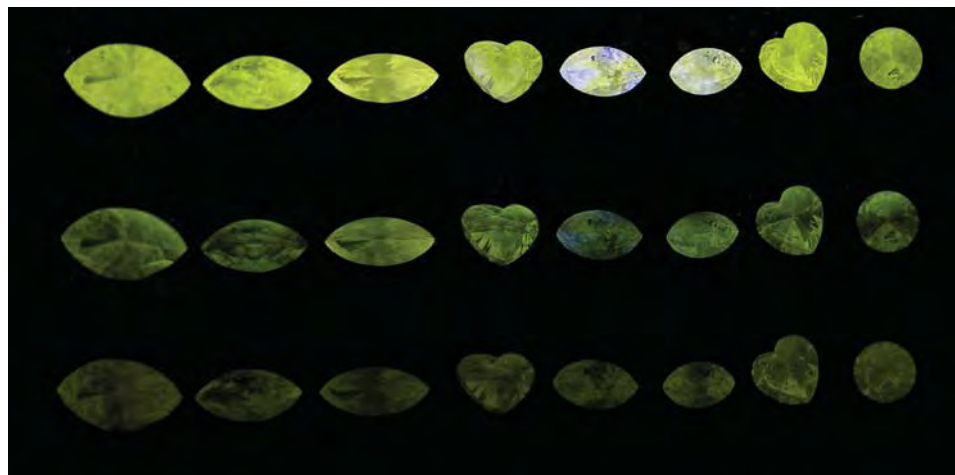


Figure 5. These samples (nos. 2.1–2.8, from left to right) demonstrate the appearance of Classic chameleon diamonds when exposed to long-wave UV (top row), short-wave UV (center row), and after the UV source was turned off (bottom row). Composite photo by T. Hainschwang.

this study exhibited a remarkable inversion of luminescence and phosphorescence behavior when heated (box A).

Infrared Spectroscopy. The infrared spectra also help distinguish the two groups of chameleon diamonds:

1. *Classic group:* low to moderate concentrations of nitrogen, mainly A aggregates (rarely A~B), and low-to-moderate hydrogen content (figure 7)
2. *Reverse group:* high to very high concentrations of nitrogen, mainly in the form of B aggregates (very rarely B<A), and low-to-high hydrogen content (figure 8)

Classic Group. The low-to-moderate nitrogen, type IaA chameleon spectra (Classic group) are characterized by hydrogen-related absorptions at 4496, 4167, 3235, 3186, 3181, 3160, 3143, 3138, 3107, 2786, and 1405 cm^{-1} (not all of these are visible in figure 7). A peak present in most Classic chameleons at 1434–1428 cm^{-1} (again, see figure 7) was relatively weak and broad (FWHM $\sim 25\text{--}35\text{ cm}^{-1}$). This absorption was in no way related to the intensity of a platelet peak at 1358–1380 cm^{-1} , as described by Woods (1986; see figure 9). Most of the stones showed a weak type Ib character, which was visible as some hydrogen-related peaks such as the 3143 cm^{-1} line (Woods and Collins, 1983), a shoulder at 1135 cm^{-1} , and in a few stones as very weak sharp peaks at 1344 cm^{-1} .

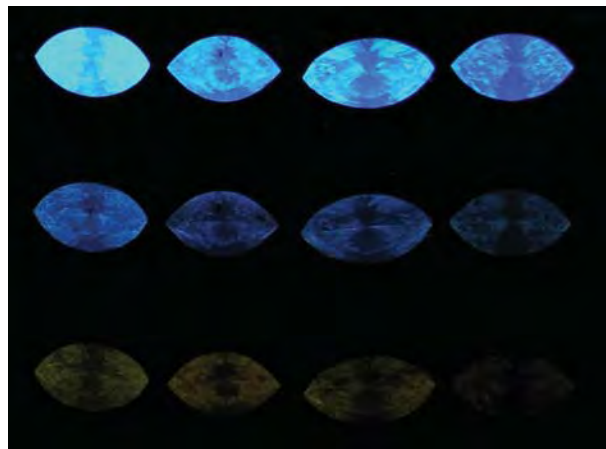
In addition to the hydrogen- and nitrogen-related features, the Classic chameleon diamonds exhibited absorptions at 1548–1544 cm^{-1} and 1590–1577 cm^{-1} , plus a weak peak at 1464 cm^{-1} .

Reverse Group. The high-nitrogen, mostly type IaB chameleon spectra (Reverse group) also exhibited

hydrogen-related features: sharp peaks at 4496, 4167, 3236, 3107, 3055, 2982, 2813 and 2786 cm^{-1} were observed (figure 8; peaks at 3055, 2982 and 2813 are too small to be seen at this scale). However, the Reverse chameleon diamonds lacked any features assigned to a type Ib character. The peak at 1430 cm^{-1} was found to be asymmetric and relatively strong and sharp (FWHM $\sim 8\text{--}9\text{ cm}^{-1}$), and it could be directly correlated with the intensity of the platelet peak (figure 9) as documented by Woods (1986).

The N-related absorptions in the one-phonon region were truncated in the Reverse chameleon spectra (see figure 8), so the strengths of the 1282 and 1175 cm^{-1} absorptions that indicate the relative amounts of A- and B-aggregates could not be compared. Consequently, to determine which aggre-

Figure 6. These samples (nos. 4.7–4.10, from left to right) demonstrate the appearance of Reverse chameleon diamonds when exposed to long-wave UV (top row), short-wave UV (center row), and after the UV was turned off (bottom row). Composite photo by T. Hainschwang.



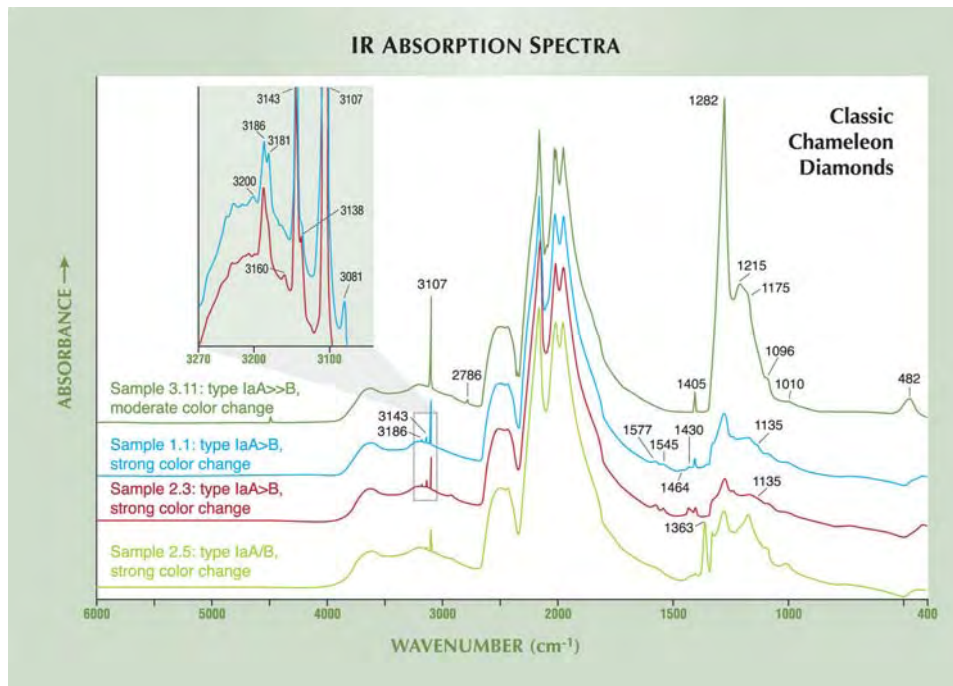


Figure 7. The infrared spectra of Classic chameleon diamonds show variable hydrogen and nitrogen contents. The spectrum of sample 2.5 is the exception, since strong B-aggregate absorption is very rare in such diamonds. The spectra show that the quantity of IR-active hydrogen does not correlate to the intensity of the color change. The hydrogen-related absorptions indicating a type Ib character are shown in the inset. The spectra have been shifted vertically for clarity.

gates were dominant, related peaks at 1010 cm^{-1} (B-aggregates) and 482 cm^{-1} (A-aggregates) were compared. In these stones, the 482 cm^{-1} peak was typically very weak or absent, whereas the 1010 cm^{-1} feature was always strong; it thus could be concluded that the Reverse chameleon diamonds are predominantly type IaB diamonds.

Several absorptions between 1577 and 1450

cm^{-1} were noted in spectra of certain Reverse group diamonds (i.e., at 1577, 1554, 1551, 1546, 1543, 1526, 1523, 1521, 1518, 1508, 1500, 1498, 1490, 1473, and 1450 cm^{-1}). None of the studied chameleon diamonds exhibited deformation-related amber center absorptions (i.e., with main features in the range of $4165\text{--}4065\text{ cm}^{-1}$; DuPreez, 1965 and Hainschwang, 2003).

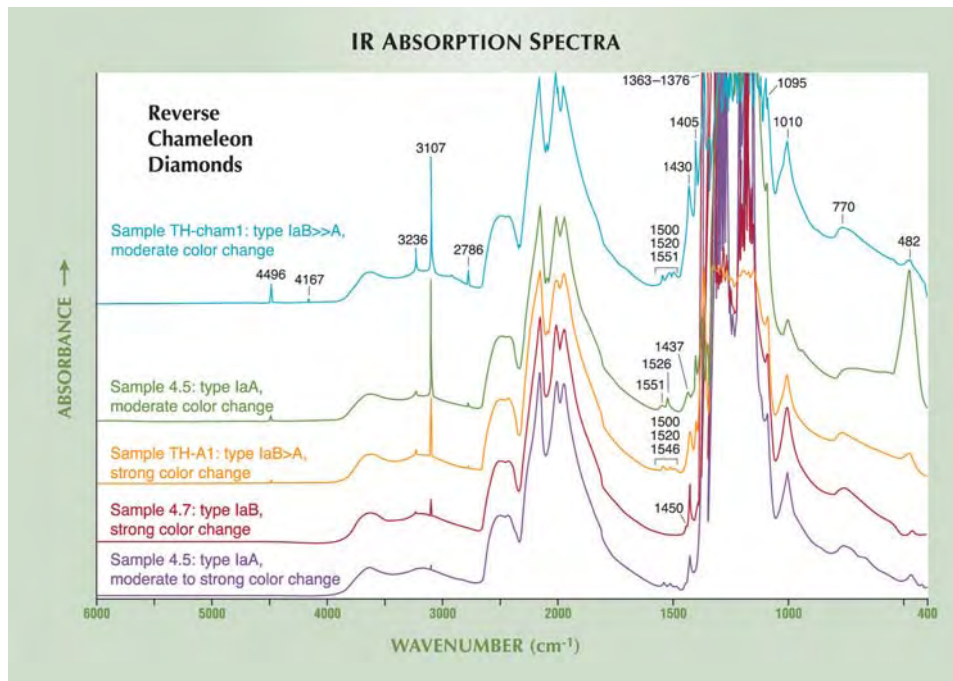


Figure 8. The infrared spectra of Reverse-chameleon diamonds show similar features, except for a more variable hydrogen content. The spectrum of sample 4.5 is the exception, since strong A-aggregate absorption is very rare in such diamonds. The spectra show that the quantity of IR-active hydrogen does not correlate to the intensity of the color change. The spectra have been shifted vertically for clarity.

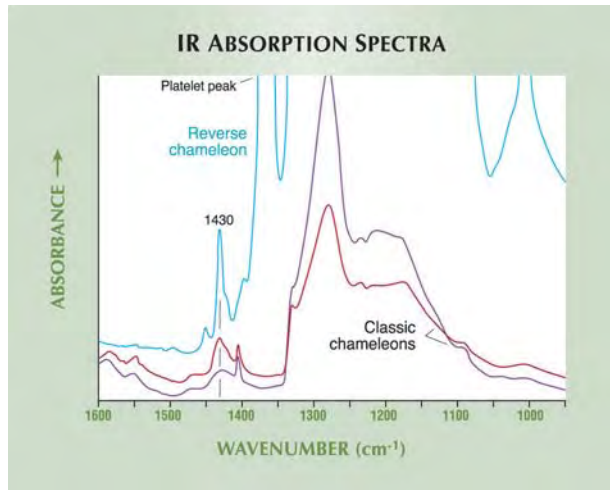


Figure 9. The 1430 cm^{-1} absorption is present in the IR spectra of both Classic and Reverse chameleon diamonds. However, the specific appearance of this absorption and absence of a platelet peak in the Classic chameleon diamonds indicates that the 1430 cm^{-1} peak in those diamonds has a different origin than the platelet-related 1430 cm^{-1} feature in the Reverse chameleons.

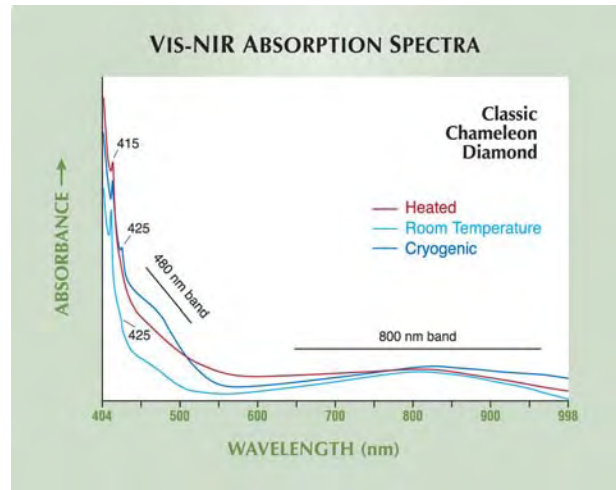


Figure 10. These Vis-NIR spectra were recorded for a Classic-group chameleon diamond at room temperature, when cooled with liquid nitrogen, and when heated. The characteristic 425 nm band and the broad features at 480 and 800 nm became less pronounced when the diamond was heated. The spectra have been shifted vertically for clarity.

Vis-NIR Spectroscopy. As was the case for standard gemological testing and FTIR spectroscopy, the two groups of chameleon diamonds also showed different absorption spectra in the visible to near-infrared range.

Classic Group. Diamonds from this group showed absent or usually weak absorption at 415 nm (N3), weak absorption at 425 nm, a weak to distinct broad band at 480 nm, and a very broad band centered at 775–825 nm (figure 10).

Figure 11. These Vis-NIR spectra compare the absorption features of a yellow-orange type Ib/aA diamond colored by the 480 nm band, a grayish yellow-green H-rich diamond, and a Classic chameleon diamond showing the 480 nm band and H-related features. The spectra have been shifted vertically for clarity.

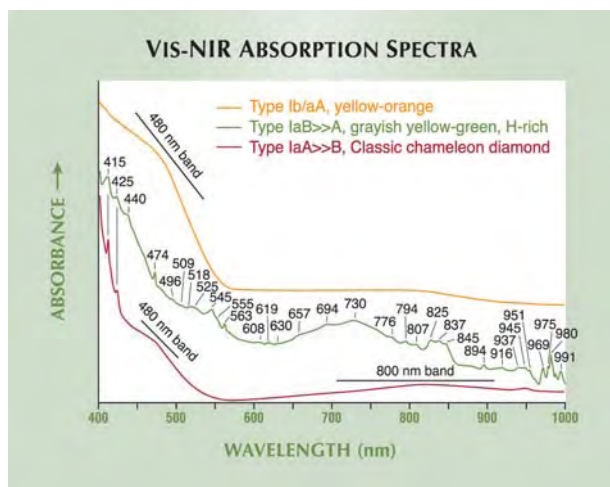
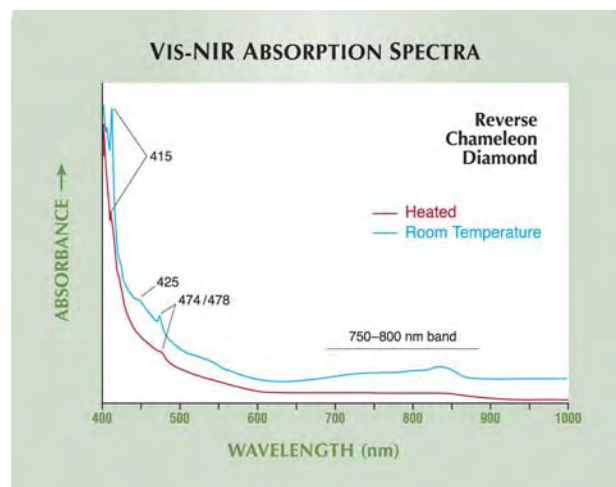


Figure 12. These Vis-NIR spectra of a Reverse-group chameleon diamond were recorded at room temperature and when heated. Heating weakened the characteristic peaks between 415 and 478 nm and the broad band centered at 750–800 nm. The spectra have been shifted vertically for clarity.



Spectra taken at temperatures of 150–350°C (i.e., with a stone exhibiting its unstable color) revealed a weakening of all the above-mentioned absorption features. There was also a general decrease in transmittance in the blue and, particularly, green regions of the spectrum (again, see figure 10). This behavior was reported previously by Fritsch et al. (1995).

In addition to the hydrogen-related features recorded in the infrared spectra (e.g., at 3107 and 1405 cm^{-1}), evidence of hydrogen was found in the visible range as the 425 nm absorption, which always occurred together with the 480 nm band. The 480 nm band is known from type Ib/aA diamonds of orange to orangy yellow color (Field, 1992; Zaitsev, 2001, p. 296). In the experience of the authors, hydrogen-related bands are known mainly from the spectra of grayish green to grayish yellow diamonds. A comparison of these spectra with that of a Classic chameleon diamond can be seen in figure 11.

Reverse Group. Diamonds from this group showed strong N3 and N2 centers, with absorptions between 415 and 478 nm (“cape lines”) and a broad asymmetric band in the 650–900 nm region that was centered at 750–800 nm (figure 12). The differences between the spectra of heated and ambient-temperature stones were not always very distinct. All of the absorption features commonly weakened on heating (again, see figure 12).

Photoluminescence Spectroscopy. Again, two different groups of spectra were obtained, corresponding to the Classic and Reverse groups (figures 13 and 14). While the spectra differed considerably between the two groups, they also had some peaks in common, such as a strong emission at 701 nm. The Classic group exhibited a total of 44 PL emissions between 554 and 949 nm, versus 20 emissions for the Reverse group.

Classic Group. The broadband emission of the Classic group chameleon diamonds occurred mainly as one band centered at 630–650 nm; a weak band centered at 730 nm also was usually visible, which is caused by the vibronic structure of the 701 nm center (Iakoubovskii and Adriaenssens, 2001). The color of this luminescence induced by the 532 nm laser is equivalent to reddish orange or orangy red. In the experience of the authors, this broadband emission is similar to the one exhibited by type IaA/Ib orange to orangy yellow diamonds that exhibit the 480 nm band (figure 15), which is consistent with the comparison seen in figure 11.

The chameleon diamonds of the Classic group (figure 13) were characterized mainly by usually strong emissions at 590 and 595 nm, sometimes a weak to strong peak at 701 nm with associated vibronic sidebands at 716 and 726 nm (Iakoubovskii and Adriaenssens, 2001), and several weaker but

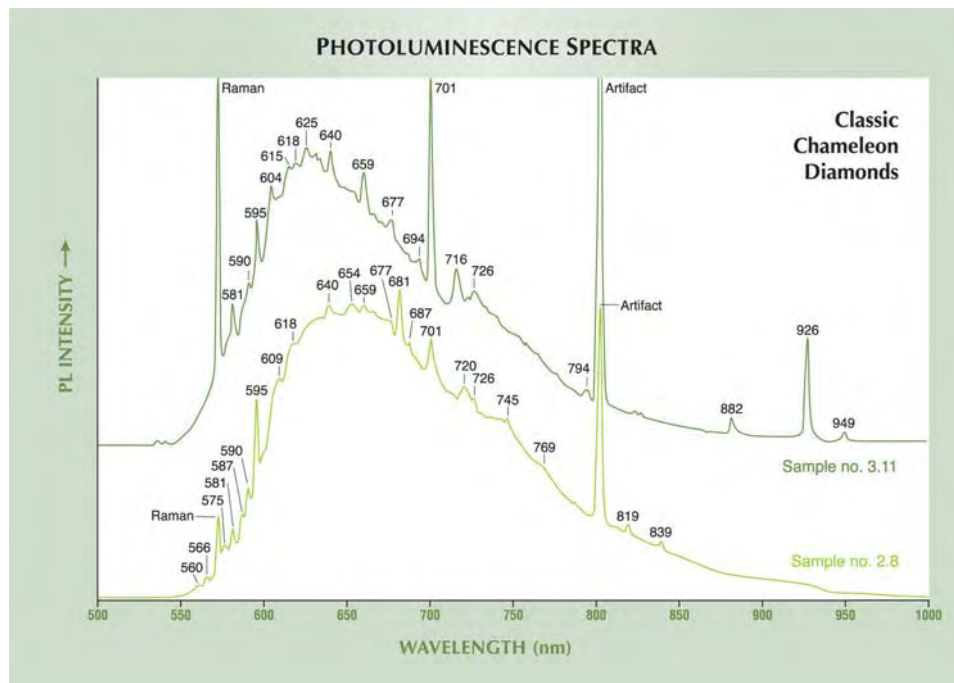


Figure 13. Typical PL spectra for Classic chameleon diamonds are shown here. The peaks in the NIR region between 700 and 950 nm are characteristic. The spectra have been shifted vertically for clarity.

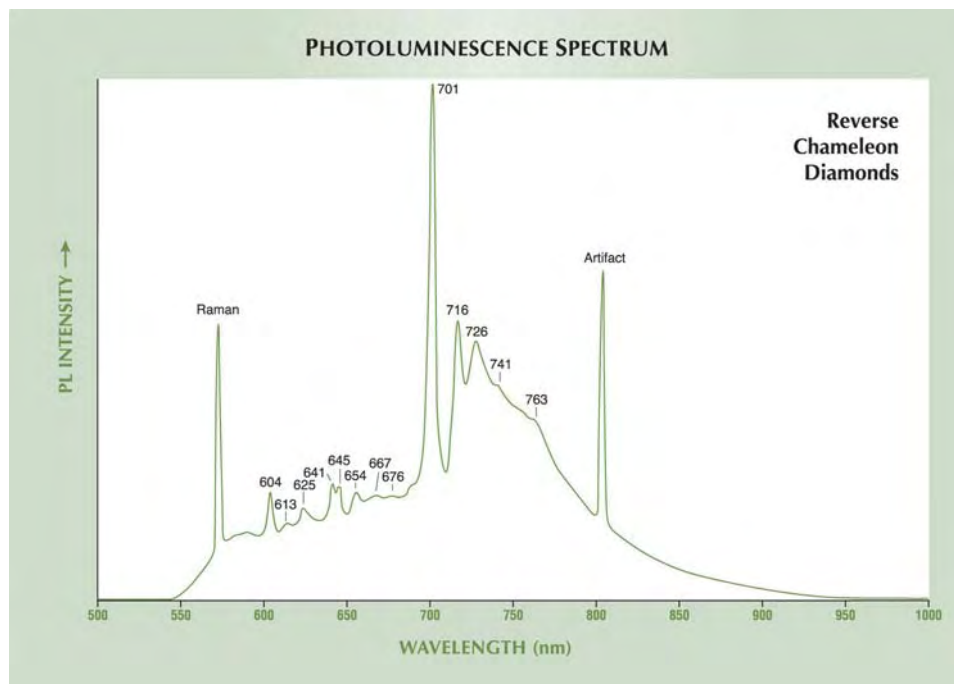


Figure 14. This PL spectrum is typical for a chameleon diamond of the Reverse group (sample 4.5) is shown here. Characteristic features include the peak at 604 nm, the dominant 701 nm center, the doublet at 641/645 nm, and the GR1 peak at 741 nm.

very characteristic peaks in the NIR region of the PL spectrum, at 769, 794, 800, 819, 839, 882, 926, and 949 nm.

Reverse Group. For the Reverse group, PL variations from stone to stone were minor (figure 14). These diamonds had luminescence spectra that basically consisted of one large, sloping plateau-like structure comprised of multiple bands between 580 and 800 nm. The luminescence excited by the 532 nm laser was equivalent to an orange yellow to orange emission.

The PL spectra of the Reverse group samples (figure 14) were characterized mainly by a peak at 604 nm, a doublet at 641 and 645 nm, and a strong to very strong emission at 701 nm with vibronic sidebands at 716 and 726 nm (Iakoubovskii and Adriaenssens, 2001). The PL peaks in the NIR region of the Classic samples were not present in the spectra of the Reverse chameleons, except for the 926 nm feature, which was detected in the spectra of two samples. Most of the Reverse group diamonds showed a very weak 741 nm GR1 peak and a weak feature at 763 nm.

DISCUSSION

Analysis of the Vis-NIR absorption spectra of the chameleon diamonds confirms that the transmission window between the two broad bands at 480 and 800 nm is responsible for the green color of the Classic group (Fritsch et al., 1995). On heating, the

480 nm absorption is slightly reduced and the 800 nm band practically disappears, which explains the change in color (Fritsch et al., 1995). The 800 nm band is very broad and ranges all the way from about 575 to 1000 nm; thus, it absorbs from the red all the way to the yellow region. Therefore, there is a transmission window centered at about 560 nm, which is shifted toward the red and yellow regions on heating. The 480 nm band absorbs slightly in the blue and accentuates the transmission window at 560 nm in the green. Unfortunately, UV-Vis absorption spectroscopy at room and elevated temperatures did not record any features consistent with a change to a greener color in the Reverse group. Further work is needed to establish the cause of this color modification. The reduction of the bands centered at 750–800 nm would only explain a yellower color, but not a greener hue. A luminescence effect can be excluded, since no green transmission luminescence was observed in the Reverse chameleon diamonds, regardless of temperature.

The long-lasting phosphorescence is a very characteristic feature of chameleon diamonds. Conversely, the authors have noted a lack of phosphorescence in samples of yellow to “olive” hydrogen-containing diamonds with spectral properties similar to chameleons, but lacking any chameleon behavior.

The Reverse chameleons contain more nitrogen and hydrogen than the stones from the Classic group. There is a known correlation in diamond between the presence of hydrogen and relatively

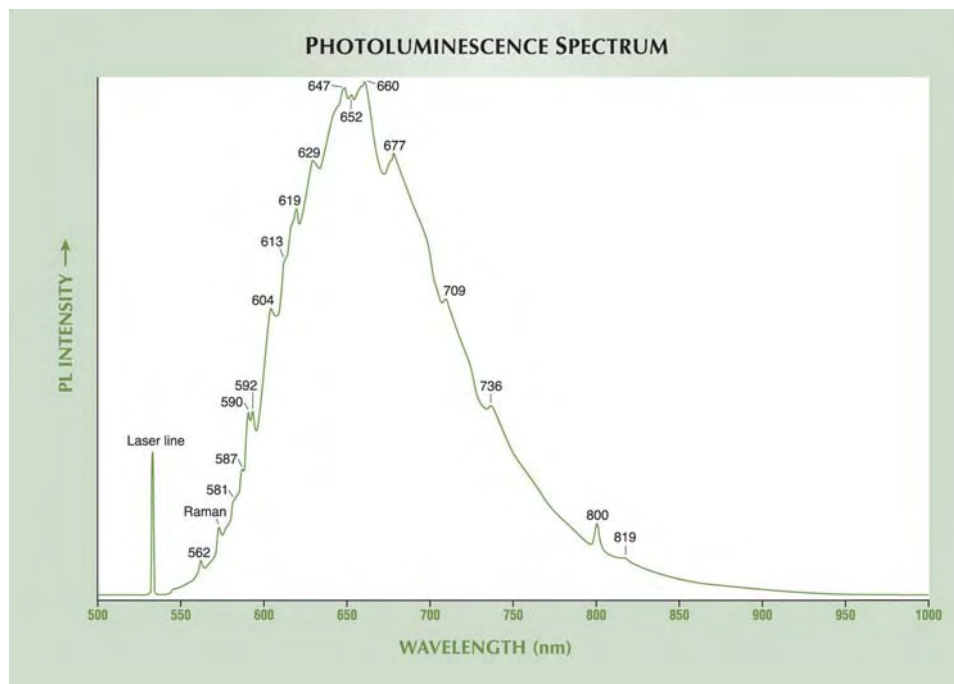


Figure 15. In this PL spectrum of a natural yellow-orange diamond colored by the 480 nm band, the broadband emission is very similar to the one observed in the Classic chameleon diamonds.

large amounts of nitrogen (Iakoubovskii and Adriaenssens, 2001; Rondeau et al., 2004); therefore, any H-rich diamond will be N-rich as well. As expected, Reverse chameleons show more distinct absorptions related to their hydrogen-rich character, in particular in the visible range, with bands of the “yellow-gray to violet to brown family,” for example, at 563 and 474 nm (Fritsch et al., 1991). Although no definite proof exists that these absorptions are due to a defect containing hydrogen, the authors can confirm that all these absorptions are exclusively present in hydrogen-rich diamonds and are therefore hydrogen-related. The absorption complex between approximately 600 and 900 nm, with apparent maxima in the range of 820–860 nm (not seen in Classic chameleons) is also probably H-related (see figure 11). Therefore, the change in color seen in the Reverse chameleon diamonds, mostly explained by the reduction in these bands at around 140°C and above, is clearly related to the presence of hydrogen. The exact atomic-scale nature of these defects is unknown at present.

In the infrared range, the C-H related absorptions in H-rich diamonds have been described by Fritsch et al. (1991), as well as by Woods and Collins (1983), and have been recently reviewed by DeWeerd et al. (2003) and Rondeau et al. (2004). In the chameleon diamonds studied here, no correlation was found between the strength of the color change and the amount of the IR-active hydrogen. On the contrary, yellow to “olive” diamonds with very high hydrogen content usually exhibit no chameleon behavior

(Hainschwang, 2004). “Olive” diamonds colored by plastic deformation do not show a chameleon behavior, either. However, such stones do clearly show different color distribution in the form of colored graining along octahedral slip planes (Hainschwang, 2003). The infrared spectra of such “olive” type IaA and Ib stones exhibit amber center absorptions (Du Preez, 1965), typically with the main feature being a double peak at 4165 and 4065 cm^{-1} (Hainschwang, 2003; Massi, 2003). Previous work has demonstrated that in strongly zoned Classic chameleons, the more intensely colored zones are richer in hydrogen; thus, at least the intensity of color appears to be hydrogen-related (F. Notari, pers. comm., 2004).

The presence of the 1495 cm^{-1} absorption seems to imply that Reverse chameleons have undergone irradiation and annealing (Zaitsev, 2001, p. 44) in nature, unlike the Classic ones. This natural irradiation is confirmed by the presence of a weak GR1 emission at 741 nm in the PL spectra of most Reverse chameleons.

The 1430 cm^{-1} absorptions seen in both groups appear to be different: In the Classic chameleons, the observed range of positions between 1434 and 1428 cm^{-1} , the band width of 25 to 35 cm^{-1} , and the missing correlation with the platelet peak indicate that this absorption is not the same as the 1430 cm^{-1} absorption described by Woods (1986). This is in fact the first report of this feature. In contrast, the sharp 1430 cm^{-1} absorption in the Reverse chameleons correlates well with the

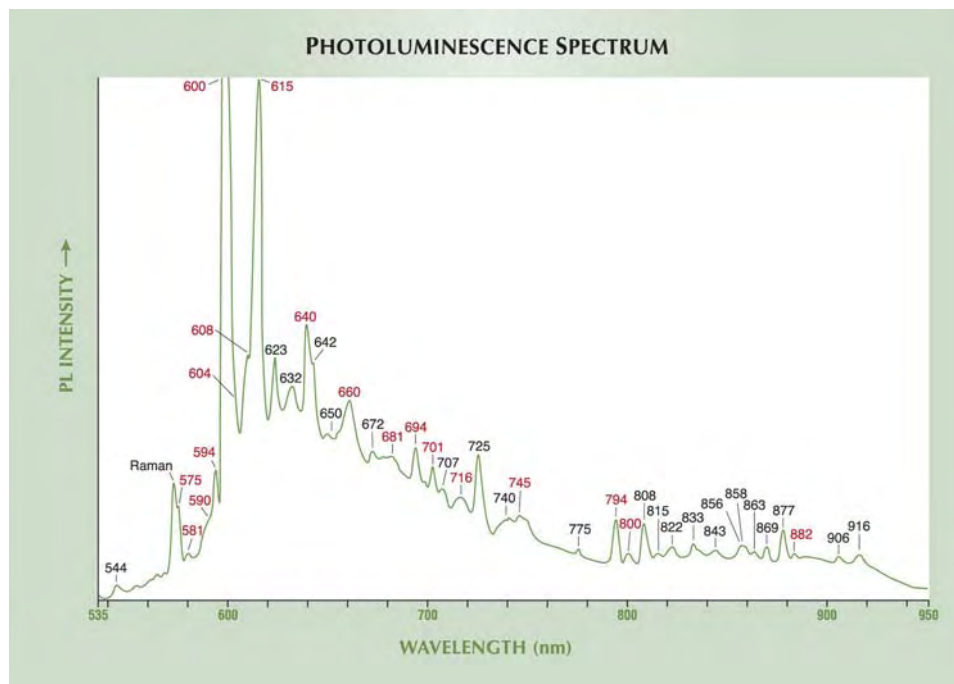


Figure 16. In this PL spectrum of a Ni-rich HPHT-treated synthetic diamond, the emissions in the NIR region are typical for Ni-related defects. There are many similarities to the features seen in Classic chameleon diamonds; identical peak positions are marked in red.

platelet peak and thus clearly points toward the feature published by Woods (1986).

The Classic chameleon category shows two absorptions (at 1590–1577 and 1548–1544 cm^{-1}) that may correspond to those reported at 1580 and 1544 cm^{-1} by Collins and Mohammed (1982) in natural brown diamonds. Interestingly, the somewhat broad 1434–1428 cm^{-1} feature was only present together with the 1548–1544 cm^{-1} and 1590–1577 cm^{-1} absorptions; none of them occurred as isolated features. Even though these absorptions were found only in the Classic chameleon diamonds, which were richer in hydrogen, a direct correlation between them and the hydrogen content could not be established with certainty. Nevertheless, our observations indicate that these absorptions may tentatively be assigned to a hydrogen-related defect. The features at 1546, 1543, 1518, and 1500 cm^{-1} seen in the Reverse chameleons have been described by Iakoubovskii and Adriaenssens (2001) and Hainschwang (2004) in hydrogen-rich diamonds. The absorptions at 1577 and 1546 cm^{-1} seem to be the same as those seen in the Classic chameleons.

Emissions at 581 and 596 nm detectable by PL spectroscopy have been reported previously, for diamonds with yellow luminescence (Zaitsev, 2001, pp. 212, 216) to long-wave UV. They are absent in Reverse chameleons, which primarily luminesce blue to long-wave UV. The vibronic structure of the 701 nm center (with its sidebands at 716 and 726 nm) was identified by Iakoubovskii and Adriaenssens (2001) as probably nickel-related. The 794 nm emis-

sion seen in the PL spectra of many Classic chameleon diamonds is interpreted as a nickel-nitrogen defect that has been documented in synthetic and certain natural diamonds (Lawson and Kanda, 1993). A distinct doublet at 883 and 884 nm found in synthetic diamonds grown by the temperature-gradient method with a Ni catalyst was assigned to a nickel defect (Lawson and Kanda, 1993); in certain samples, a single peak at 882 nm was found instead (figure 16). The peak observed in the Classic chameleon diamonds at 882 nm can most probably be assigned to the same or a similar Ni-related defect.

The 926 nm PL peak in the Classic (and rarely also the Reverse) chameleon diamonds has been recorded by one of us (TH) in some hydrogen-rich violet-blue-gray and “straw” yellow diamonds, as well as in one HPHT-treated yellow diamond that was originally olive-brown. In this diamond, the 926 nm peak (absent before treatment) was created during the HPHT process (2000°C at 65 kbar for 10 minutes). Interestingly, it was produced together with a vibronic system, yielding peaks at 701, 716, and 726 nm (Hainschwang et al., 2005). The tentative assignment of the 701 nm center to a Ni-related defect by Iakoubovskii and Adriaenssens (2001) leads to the possible attribution of these apparently related features to a nickel-nitrogen defect. This is due to the fact that a defect created by the annealing of a “normal” type Ia diamond most probably involves nitrogen. Assuming that this is a nickel defect as proposed by the above authors, its creation by annealing indicates a nickel-

nitrogen complex for the defects at 701 and 926 nm.

Most of the other sharp bands in the PL spectra of Classic chameleon diamonds also have been observed in natural brown diamonds (Smith et al., 2000; Zaitsev, 2001; Hainschwang, 2003), and the ones seen in the Reverse chameleons are seen in hydrogen-rich diamonds from the Argyle mine (Iakoubovskii and Adriaenssens, 2001). The defects responsible for most of these emissions are unknown. Many of the PL emissions shown by Classic chameleons are reminiscent of those seen in synthetic diamonds grown with a Ni catalyst; such stones characteristically show multiple emissions in the NIR range (figure 16).

The presence of Ni in the Classic and the Reverse chameleons as indicated by PL spectroscopy was recently confirmed by one of us (TH) using EDXRF chemical analysis: two Reverse and two Classic chameleons were analyzed and all of them exhibited rather distinct Ni peaks.

The observation of a color change solely induced by relatively low heat in the Reverse chameleons indicates that a thermochromic color change can be caused by a hydrogen-related defect. The photochromic color change induced by storage in the dark is unique to the Classic chameleon diamonds. Three factors may be involved in the combined thermochromic and photochromic chameleon behavior of the Classic group: the implied weak type Ib character, a specific (although unknown) hydrogen-related defect, and possibly the presence of Ni.

The Classic and Reverse groups are related to some degree and do have significant properties in common. However, the fact that the Reverse group lacks a photochromic color change and exhibits only a weak-to-distinct thermochromic color change raises the question as to whether such solely thermochromic diamonds should be called chameleon diamonds, or whether this name should be reserved for diamonds exhibiting both thermochromic and photochromic color change. Presently, the GIA Gem Laboratory only recognizes diamonds in the latter, "Classic" group as chameleons.

CONCLUSIONS

This study has differentiated two sample groups from a collection of 39 chameleon diamonds: those showing only thermochromic color change and those that exhibit both thermochromic and photochromic behavior. Each group exhibited distinctive hue changes. We propose the term *Classic* for

those that show the green-to-yellow behavior with heating or after prolonged storage in the dark; this color change is commonly associated with chameleon diamonds. Those that lack a photochromic color change—that is, they become slightly greener and more saturated only when heated—are here called *Reverse* chameleons.

The presence of the 480 nm band and hydrogen-related features such as the 425 nm absorption suggests that Classic chameleon diamonds fall between very hydrogen-rich diamonds and type IaA/Ib diamonds that exhibit the 480 nm absorption band (figure 11). This is also strongly indicated by the fact that some truly hydrogen-rich diamonds such as the Reverse chameleons exhibit this "low temperature" (i.e., below 200°C) thermochromic color change. This is further confirmed by comparison of the PL spectra of Classic chameleons and those of type Ib/aA orange diamonds that exhibit the 480 nm band (again, see figures 13 and 15). Hydrogen-rich diamonds very frequently exhibit PL spectra reminiscent of those of the Reverse chameleons (Hainschwang, 2001; Iakoubovskii and Adriaenssens, 2001). The influence and role of single nitrogen and the 480 nm band in the color change of the Classic chameleon diamonds will be the subject of future research by the authors.

We have shown that the easiest way to identify chameleon diamonds is by heating them to moderate temperature and observing the change in color. However, this study proved that the Classic chameleon diamonds also could be identified by a combination of their spectroscopic properties and their reaction to UV radiation. This is preferable to heating, to avoid modifying the color of green diamonds that are not chameleons; their radiation-caused coloration is rather sensitive to heat and in some cases absorptions in the visible range are known to be modified at temperatures as low as 275°C (see, e.g., Collins et al., 1988). All of the chameleon diamonds exhibited yellow phosphorescence after exposure to short-wave UV. The absence of this yellow afterglow in any hydrogen-containing yellow to "olive" diamond indicates that no chameleon effect will be present. Also, in the experience of the authors, stones that lack traces of hydrogen in their IR spectra and stones that show amber-center absorption were never found to exhibit this unusual change in color (see e.g., Hainschwang, 2003). The Reverse chameleon diamonds cannot always be identified without heating, but since yellow diamonds are not permanently modified by

simple heating at relatively low temperature, the heating test is not problematic for such samples.

The presence of hydrogen and nickel in these diamonds has been demonstrated by various spectroscopic methods; emissions assigned to Ni impurities were identified particularly in the Classic group by PL spectroscopy.

At present, we can only speculate about the cause of the color change in Classic chameleon diamonds.

The results presented here point toward a defect involving hydrogen combined with the 480nm band, which is related to isolated single nitrogen atoms. This combination seems to cause the thermochromic and photochromic change in color; whether Ni plays a role in this color change remains to be seen. In the diamonds exhibiting only a thermochromic color change, such as the Reverse chameleons, the defects appear to be solely hydrogen-related.

ABOUT THE AUTHORS

Mr. Hainschwang (thomas.hainschwang@gia.edu) is research gemologist at GIA's GemTechLab in Geneva, Switzerland; he performed the research for this article prior to joining GIA, while he was director of Gemlab Gemological Laboratory in Liechtenstein. Mr. Simic is a gemologist at EGL USA, New York. Dr. Fritsch is professor at the University of Nantes, Institut des Matériaux Jean Rouxel (IMN-CNRS), Nantes, France. Mr. Deljanin is director of research and director of Canadian operations for the EGL USA

group, Vancouver, British Columbia, Canada. Ms. Woodring is a gemologist and educational instructor, and Mr. DelRe is manager of Gemological Services, at EGL USA, New York.

ACKNOWLEDGMENTS: The authors are grateful to Nileshe Sheth of Nice Diamonds, New York, a subsidiary of Forever Collections Inc., for loaning the "Forever Chameleon Collection" for this research, and to Franck Notari, Director of GemTechLab, for fruitful discussions.

REFERENCES

- Collins A.T., Mohammed K. (1982) Optical studies of vibronic bands in yellow luminescing natural diamonds. *Journal of Physics C*, Vol. 15, No. 1, pp. 147–158.
- Collins A.T., Szechi J., Tavender S. (1988) Resonant excitation of the GR centre in diamond. *Journal of Physics C*, Vol. 21, No. 7, pp. L161–L164.
- Chabert V., Reinitz I. (2000) Gem Trade Lab Notes: Diamond—chameleon, with blue-to-violet "transmission" luminescence. *Gems & Gemology*, Vol. 36, No. 1, pp. 60–61.
- Deljanin B. (2004) Lab Notes: Chameleon diamonds. *Canadian Diamonds*, Summer, pp. 24–25.
- DeWeerd F., Pal'yanov Y.N., Collins A.T. (2003). Absorption spectra of hydrogen in ¹³C diamond produced by high-pressure, high-temperature synthesis. *Journal of Physics: Condensed Matter*, Vol. 15, No. 19, pp. 3163–3170.
- Du Preez L. (1965) Paramagnetic resonance and optical investigations of defect centres in diamond. Ph.D. dissertation, University of the Witwatersrand, Johannesburg, South Africa, pp. 83–84.
- Field J.E., Ed. (1992) *The Properties of Natural and Synthetic Diamond*. Academic Press, London.
- Fritsch E., Scarratt K., Collins A.T. (1991) Optical properties of diamonds with an unusually high hydrogen content. In R. Messier, J.T. Glass, J.E. Butler, R. Roy, Eds., *Materials Research Society International Conference Proceedings*, Second International Conference on New Diamond Science and Technology, Washington D.C., Sept. 23–27, Materials Research Society, Pittsburgh, PA, pp. 671–676.
- Fritsch E., Shigley J.E., Moses T., Rossman G.R., Zucker B., Balfour I. (1995) Examination of the twenty-two carat green chameleon diamond. In D.J. Content, Ed., *A Green Diamond: A Study of Chameleonism*, W. S. Maney & Son, Leeds, England, 42 pp.
- GIA Diamond Dictionary*, 3rd ed. (1993) Gemological Institute of America, Santa Monica, CA, p. 44.
- Hainschwang T. (2001) Characterization of hydrogen rich diamonds from Argyle/Australia with Vis/NIR—and photoluminescence—spectroscopy. http://www.gemlab.net/research1_1.htm [accessed 02/18/05].
- Hainschwang T. (2003) Classification and color origin of brown diamonds. Diplôme d'Université de Gemmologie, University of Nantes, France.
- Hainschwang T. (2004) Gem News International: A diamond exhibiting a spectacular phantom. *Gems & Gemology*, Vol. 40, No. 1, pp. 76–78.
- Hainschwang T., Katrusha A., Vollstaedt H. (2005) HPHT treatment of different classes of type I brown diamonds. *Journal of Gemmology*, Vol. 29 (in press).
- Iakubovskii K., Adriaenssens G.J. (2001) Optical characterization of natural Argyle diamonds. *Diamond and Related Materials*, Vol. 11, No. 1, pp. 125–131.
- Lawson S.C., Kanda H. (1993) An annealing study of nickel point defects in high-pressure synthetic diamond. *Journal of Applied Physics*, Vol. 73, No. 8, pp. 3967–3973.
- Massi L. (2003) Défauts responsables de la couleur brune dans les diamants. Mémoire de stage du Diplôme d'Études Approfondies, Sciences des Matériaux, University of Nantes, France.
- Rondeau B., Fritsch E., Guiraud M., Chalain J.P., Notari F. (2004) Three historical "asteriated" hydrogen-rich diamonds: Growth history and sector-dependent impurity incorporation. *Diamond and Related Materials*, Vol. 13, No. 9, pp. 1658–1673.
- Raal F.A. (1969) Mineralogical notes: A study of some gold mine diamonds. *American Mineralogist*, Vol. 54, Nos. 1–2, pp. 292–295.
- Shigley J., Wang W., Moses T., Hall M. (2004) Photoluminescence features of "chameleon" diamonds. *Proceedings of the 55th De Beers Diamond Conference*, Coventry, England, pp. 4.1–4.2.
- Smith C.P., Bosshart G., Ponahlo J., Hammer V.M.F., Klapper H., Schmetzer K. (2000) GE POL diamonds: Before and after. *Gems & Gemology*, Vol. 36, No. 3, pp. 192–215.
- Woods G.S., Collins A.T. (1983) Infrared absorption spectra of hydrogen complexes in type I diamonds. *Journal of Physics and Chemistry of Solids*, Vol. 44, No. 5, pp. 471–475.
- Woods G.S. (1986) Platelets and the infrared absorption of type I diamonds. *Proceedings of the Royal Society of London A*, Vol. 407, pp. 219–238.
- Zaitsev A.M. (2001) *Optical Properties of Diamond: A data Handbook*. Springer, Berlin, pp. 44, 45, 190–230, 212, 216, 296.

COATED PINK DIAMOND— A CAUTIONARY TALE

David J. F. Evans, David Fisher, and Christopher J. Kelly

The Diamond Trading Company (DTC) Research Centre had the opportunity to examine a diamond that, on submission to a commercial gem laboratory, was stated to have been HPHT treated. However, spectroscopic analysis yielded data inconsistent with this statement. After further testing, it was determined that this diamond, which originally was probably pale yellow, had been coated to change its color to the equivalent of Fancy Intense purple-pink. Careful examination with a microscope revealed evidence of a coating exclusively on the pavilion facets. Elemental analysis of the coating suggests it may be calcium fluoride with a gold impurity that was added either to generate the absorption responsible for the pink color or to assist as a nucleating agent for the calcium fluoride film.

The emergence of high pressure/high temperature (HPHT) color treatment of natural diamond has brought about a marked increase in the sophistication of the spectroscopic analysis used by grading laboratories when testing diamonds (see, e.g., Fisher and Spits, 2000; Smith et al., 2000). Care must be exercised, however, that the reliance on such advanced analytical techniques does not cause the gemologist to neglect the more “traditional” means of identifying simpler forms of treatment. The case described here serves to highlight the potential consequences of such

neglect, although the net result was the gathering of interesting analytical information on a diamond treated by an older technique.

A CASE STUDY

During September 2004, scientists at the DTC Research Centre in Berkshire, United Kingdom, had the opportunity to study the 0.85 ct round brilliant cut diamond shown in figure 1. The diamond had been graded Fancy Intense purple-pink by a gemological laboratory and was said to have been color enhanced by HPHT treatment. Although pink HPHT-treated diamonds with colors as strong as Fancy Deep have been reported (see, e.g., Hall and Moses, 2000), they are extremely rare. Therefore, this identification immediately raised our suspicions.

Spectroscopic Analysis. Because the diamond had been described as HPHT treated, testing began with the advanced analytical instrumentation that is typically used to determine when the color of a diamond has been modified by exposure to HPHT treatment conditions. This involved the use of several spectrometers, including those that analyze the absorption of light throughout the ultraviolet, visible, and near-infrared regions of the spectrum (a Perkin Elmer Lambda 19 UV-Vis-NIR spectrometer, with the diamond at room temperature as well as cooled to liquid nitrogen temperature using a

See end of article for About the Authors and Acknowledgments.
GEMS & GEMOLOGY, Vol. 41, No. 1, pp. 36–41.
© 2005 Gemological Institute of America

suitable cryostat) and the mid-infrared region (a Nicolet Magna IR 750 Fourier-transform infrared [FTIR] spectrometer, at room temperature only). The diamond's photoluminescence (PL) spectra were recorded under a range of different laser-excitation wavelengths: 325 and 633 nm excitation using a Jobin-Yvon Labram Infinity spectrometer; 488 and 514 nm excitation using a Spex 270M spectrometer. For the PL spectroscopy, the diamond was again cooled to liquid nitrogen temperature in a cryostat.

UV-Vis-NIR spectroscopy revealed that the pink color was caused by a broad absorption band centered at around 550 nm (figure 2). A similar absorption feature at this wavelength is responsible for the color in most natural-color pink diamonds, both (nitrogen containing) type I and (nitrogen free) type II stones (see, e.g., Collins, 1982; King et al., 2002). In natural-color pink diamonds, however, this 550 nm band typically is accompanied by a broad absorption band at 390 nm (again, see figure 2), which was not recorded in this sample. The diamond did show an absorption line at 415 nm (the N3 center), a nitrogen-related feature that is found in most type Ia diamonds.

Figure 2. The UV-Vis-NIR absorption spectra of the 0.85 ct diamond at room temperature and liquid nitrogen temperature show a broad 550 nm band and N3 absorption at 415 nm; the latter is present in most type Ia diamonds. A room-temperature absorption spectrum of a type IaAB natural-color pink diamond is provided for comparison. It shows the two broad absorption bands at 390 and 550 nm that are characteristic of such diamonds; careful examination allows the 390 nm band to be distinguished from the broad absorption associated with N3.

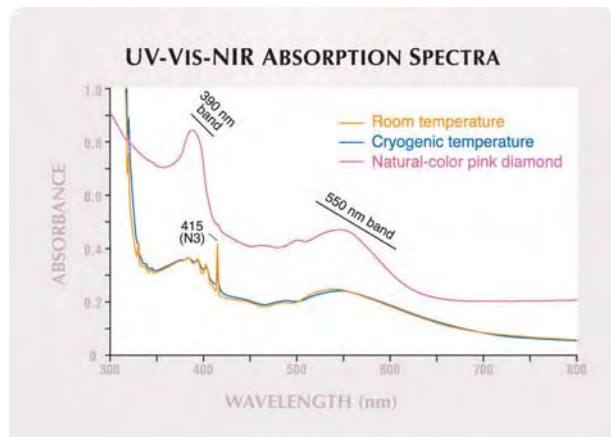
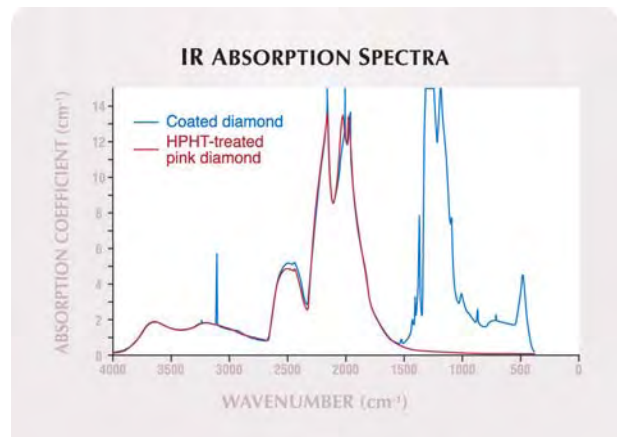


Figure 1. This 0.85 ct purple-pink diamond was examined at the DTC Research Centre to investigate the claim that it had been HPHT treated. Careful analysis and observation revealed that the color of the diamond was due to a topical coating that had been applied to the pavilion of the stone. Photo by Chris Kelly.

Using FTIR, we discovered that the diamond was a type IaAB, with the majority of the nitrogen in the A aggregate form (figure 3). (For a description of diamond types and how they relate to the various aggregation states of nitrogen impurities in diamond, refer, for example, to Fritsch and Scarratt, 1992.) Although the spectrum was saturated in the region

Figure 3. The infrared spectrum of the 0.85 ct diamond revealed that it was a type IaAB, whereas pink HPHT-treated diamonds are typically type IIa.



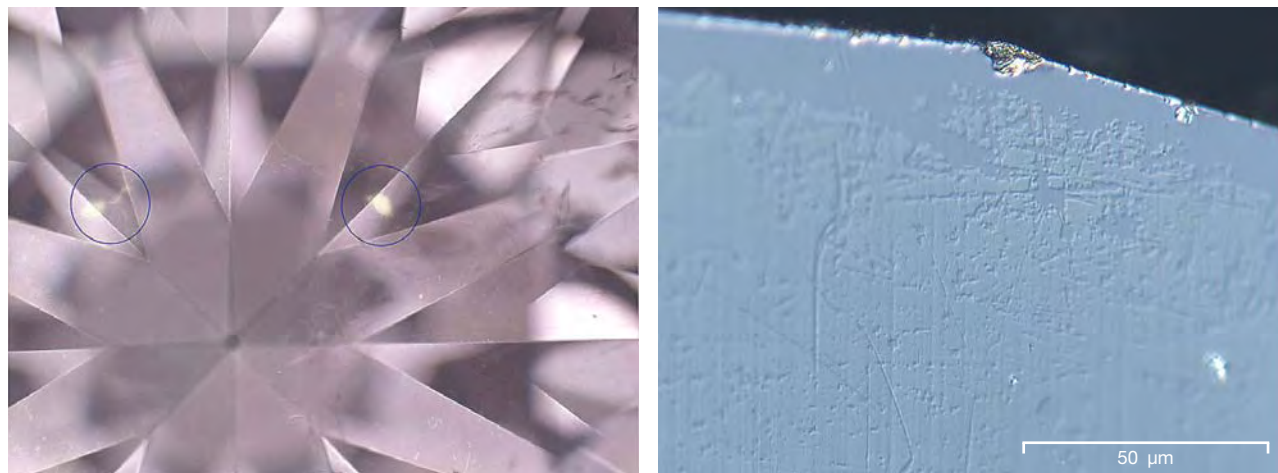


Figure 4. This photomicrograph of the 0.85 ct diamond in transmitted light (left) shows two pale yellow regions (circled) where the pink color is not visible (photomicrograph by Chris Kelly; magnified 35×). The Nomarski image (right) of the edge of one of the pavilion facets shows how the coating has worn away (photomicrograph by David Fisher).

associated with nitrogen-related absorption (approximately $1300\text{--}1100\text{ cm}^{-1}$), spectral fitting techniques developed at the DTC Research Centre provided nitrogen concentration estimates of 470 parts per million (ppm) of A-form nitrogen and 280 ppm of B-form nitrogen. Fairly strong hydrogen-related absorption also was detected in the form of the C-H stretch mode at 3107 cm^{-1} . These results contradict the stated origin of color: HPHT-treated pink diamonds are typically type IIa, and the absorption characteristics were not consistent with those one would expect to encounter in *any* type IaAB diamond that had undergone HPHT treatment at temperatures sufficiently high to generate a significant color change (Reinitz et al., 2000). Natural-color pink diamonds do show a range of nitrogen concentrations and aggregation states, but in our experience they typically do not show the very high levels measured in this case and their aggregation levels tend to be higher.

Low-temperature photoluminescence spectroscopy with 325 nm excitation revealed dominant N3 luminescence (main line at 415 nm), consistent with its observation in the absorption spectra. The spectrum taken with 488 nm excitation showed two lines at 503 nm separated by 0.2 nm. One was the frequently observed H3 center (from a nitrogen-vacancy-nitrogen impurity). The identity of the other line, at a slightly shorter wavelength, is not certain, but it may be the S1 center (for a description of luminescence centers, see Davies, 1977, and Field, 1992). Other strong luminescence features observed with 488, 514, and 633 nm excitation were lines at 701, 787, and 793 nm. All of these have been seen in natural “cape” yellow diamonds (Field,

1992), and it is the experience of the authors that they are generally encountered in untreated near-colorless to pale yellow diamonds with a nitrogen content of a few hundred parts per million and significant hydrogen-related absorption. No indication of HPHT treatment was found, and we have not seen the 701, 787, and 793 nm lines at the strength observed here in natural-color pink diamonds.

Although the diamond had been described as being HPHT treated, the data recorded using various advanced spectroscopic techniques did not support this assessment. However, they were not wholly consistent with natural-color pink diamonds either. Rather, in the experience of the authors, the spectroscopic features recorded were more consistent with those seen in natural-color near-colorless to pale yellow diamonds. It was therefore determined that additional testing was needed to resolve the cause of the pink coloration in this diamond.

Further Investigation. When viewed with a microscope, the diamond revealed a somewhat uneven color distribution. This is not necessarily unusual in natural-color pink diamonds, but in such stones the pink coloration tends to be concentrated along so-called slip planes where plastic deformation has taken place. Closer examination showed that the uneven color distribution in this sample was actually related to “patches” where the pink color was absent (figure 4, left), revealing pale yellow regions with transmitted light. This raised the possibility that the diamond had been coated in some way to produce the pink color. Examination of the pavilion facets showed clear evidence of a coating that had

worn away at facet junctions and in the centers of some facets. The coating was most easily viewed using the Nomarski differential interference contrast technique (Robinson and Bradbury, 1992), as illustrated in figure 4 (right). No coating was observed on the table and crown facets. Once we had established the location of the coating, we were able to find it with the microscope using reflected light; the coating appeared as slightly yellower regions with the set-up used. This yellow color is likely due to interference associated with the thin film coating, as such effects are relatively strong in reflected light. No fluorescence associated with the coating was detected, but careful imaging with the Diamond Trading Company DiamondView instrument showed that the luminescence intensity was slightly lower from the coated regions. We concluded that the coating was fairly durable, as it had not been removed by the several cycles of cooling to liquid nitrogen temperatures and re-warming to room temperature the diamond experienced during the spectroscopic testing.

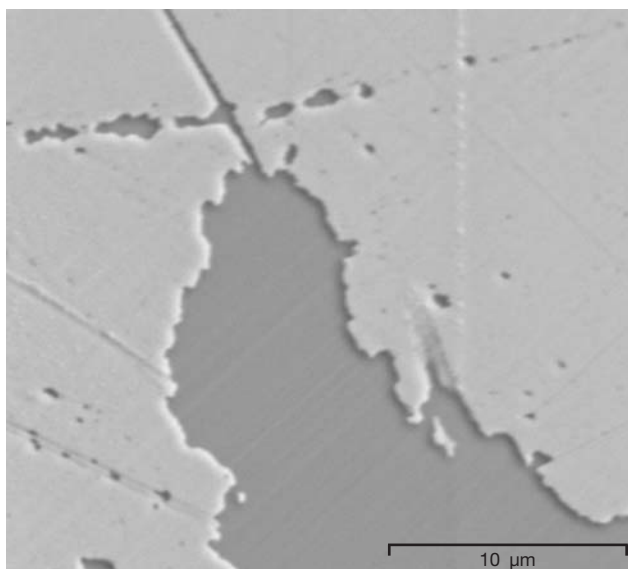
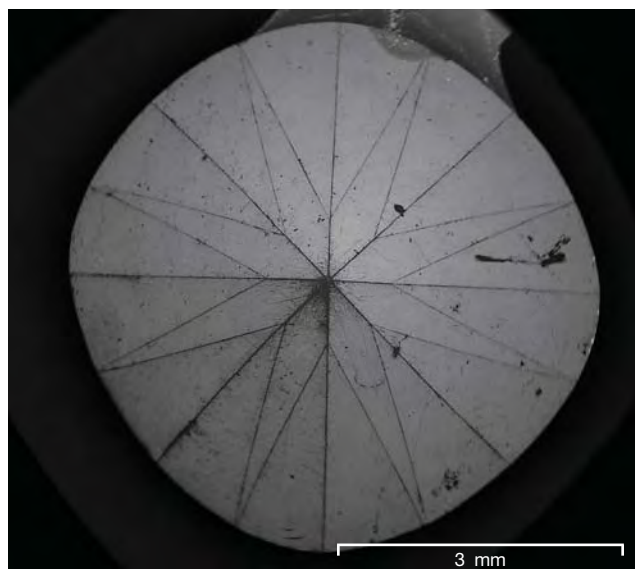
Following these observations, we conducted a detailed analysis to determine the composition of the coating. First, we examined the pavilion region with a Philips Quanta 200 low-vacuum scanning electron microscope (SEM). The microscope scans a beam of high-voltage electrons across the surface of the sample in a variable pressure chamber. As the

electrons impinge on the surface of the sample, they are scattered and X-rays of energies characteristic of the elements comprising the material are produced. The scattered electrons can be imaged to provide topographic information, and specific X-ray energies can be selected and mapped on the same scale to produce a distribution map of a particular element. The low-vacuum technique has benefit over a more conventional SEM analysis in that the sputtered metallic (usually gold) or carbon coating typically required for SEM work on nonconducting diamond was not necessary.

SEM imaging of the areas being analyzed clearly confirmed the presence of minor wear and removal of the coating (figure 5). Further analysis using energy-dispersive X-ray (EDX) mapping (figure 6) revealed that the coating was comprised of gold, calcium, and fluorine exclusively. Peaks associated with carbon from the underlying diamond and oxygen contaminant present equally in both the coating and the diamond also were observed. As the sample had not been conventionally prepared for SEM, the gold content was found to be a genuine component of the coating and not a specimen preparation artifact.

Discussion. Although the diamond had been presented as HPHT treated, spectral analyses and microscopic examination contradicted this conclusion and

Figure 5. These low-vacuum SEM backscattered electron images reveal damage and wear to the coating on the pavilion of the stone (left) and, at higher magnification, bright areas where the coating was intact and dark areas where it had worn away (right).



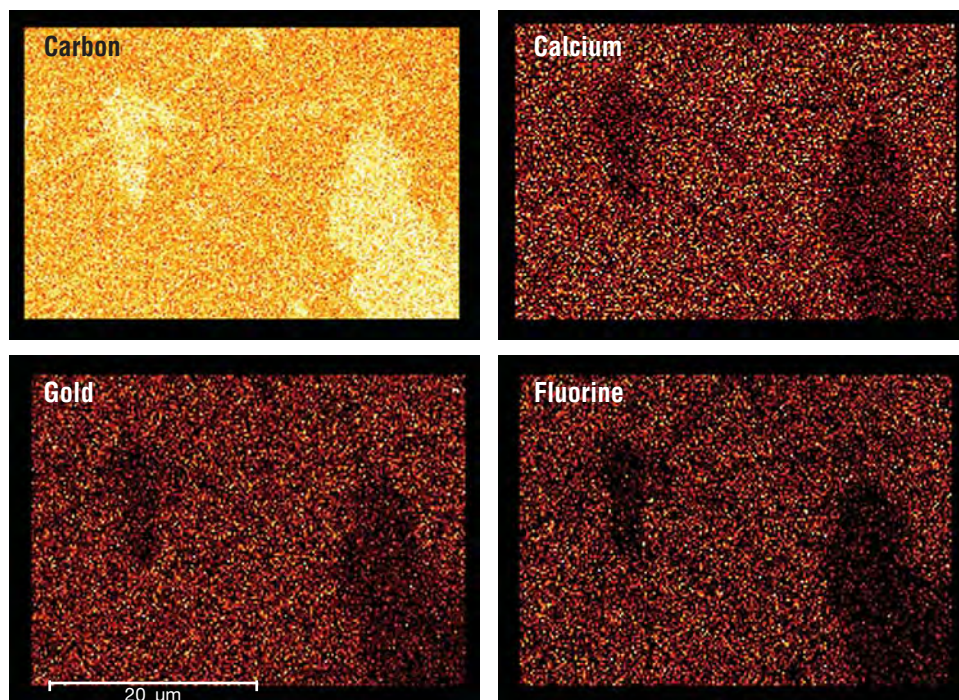


Figure 6. These energy-dispersive X-ray maps show the distributions of the main elements detected in the analysis: carbon, calcium, gold, and fluorine. Bright spots correspond to regions of high concentrations of the specific element. The feature to the lower right in each is the area where the coating was worn away in figure 5 (right). The carbon X-ray map shows a high signal where the coating has been removed (due to the underlying diamond). The calcium, gold, and fluorine signals are significantly stronger in the regions where the coating is intact.

established that the purple-pink color was the result of a topical coating.

The use of fluoride coatings on diamond has been reported previously as being “considered unsatisfactory by coaters, since they are easily detected by their purplish-blue iridescence” (Miles, 1962, p. 356). However, the present sample did not reveal such an iridescence effect. Calcium fluoride (CaF_2) is a material commonly used in optical components. Naturally occurring calcium fluoride (as the mineral fluorite) exists in a range of colors variously attributed to impurities or lattice defects due to irradiation (Deer et al., 1966), with the lattice defects having been associated with purple in some instances. There has been work on the implantation of calcium fluoride with gold to generate nanoparticles that can produce a broad absorption band at about 520 nm, similar to the broad absorption peak observed in this diamond (Henderson et al., 1997). While the gold may be responsible for the color in this case, it is also possible that it was used to promote the nucleation or adhesion of the coating. The exact form of the coating on this diamond is not known, but clearly it involves the deposition of calcium fluoride either as the color-producing layer or as a protective or host layer for gold particles, which themselves are responsible for the absorption feature resulting in the pink color.

CONCLUDING COMMENTS

Gemologists and gemological laboratories must contend with an ever-increasing number of sophisticated diamond treatments that can only be identified with advanced analytical techniques. Therefore, it is not surprising that the more traditional forms of color treatment may be overlooked when they are assessing whether a particular diamond’s color is natural or has been artificially induced. A recent *Gems & Gemology* lab note on coated diamonds (Sheby, 2003) emphasized the importance of keeping these earlier treatments in mind during a gemological examination.

For the diamond described in this report, the spectroscopic data conflicted with the stated HPHT origin of the pink color, whereas careful examination with the microscope revealed evidence of a coating. This coating produced a broad absorption band at around 550 nm, which imparted a pink color to an originally pale yellow stone. Analysis of the coating suggests that it is calcium fluoride with gold, but the data acquired do not allow for the determination of whether the gold or some other impurity doping the calcium fluoride is responsible for the color-causing absorption. This study serves to re-emphasize the importance of sound gemological observation when examining stones for the possibility of color treatments.

ABOUT THE AUTHORS

Mr. Evans is a senior research assistant, Dr. Fisher is a senior research scientist, and Mr. Kelly is a physics technician at the Diamond Trading Company (DTC) Research Centre in Maidenhead, Berkshire, United Kingdom.

ACKNOWLEDGMENTS: The authors would like to thank

Andy Taylor at the DTC Research Centre for assistance with the differential interference contrast microscopy and Mark Peers at Oxford Instruments, High Wycombe, U.K., for access to and assistance with the X-ray mapping. Members of the Consumer Confidence Technical Research team at the DTC Research Centre provided valuable input to discussions throughout this work.

REFERENCES

- Collins A.T. (1982) Colour centres in diamond. *Journal of Gemmology*, Vol. 18, No. 1, pp. 37–75.
- Davies G. (1977) The optical properties of diamond. In P.L. Walker and P.A. Thrower, Eds., *Chemistry and Physics of Carbon*, Vol. 13, Marcel Dekker, New York, pp. 1–143.
- Deer W.A., Howie R.A., Zussman J. (1966) *An Introduction to the Rock Forming Minerals*. Longmans, Green and Co., London, p. 512.
- Field J.E. (1992) *The Properties of Natural and Synthetic Diamond*. Academic Press, London, pp. 687–698.
- Fisher D., Spits R.A. (2000) Spectroscopic evidence of GE POL HPHT-treated natural type IIa diamonds. *Gems & Gemology*, Vol. 36, No. 1, pp. 42–49.
- Fritsch E., Scarratt K. (1992) Natural-color nonconductive gray-to-blue diamonds. *Gems & Gemology*, Vol. 28, No. 1, pp. 35–42.
- Hall M., Moses T. (2000) Gem Trade Lab Notes: Diamond—blue and pink HPHT annealed. *Gems & Gemology*, Vol. 36, No. 3, p. 255.
- Henderson D.O., Tung Y.S., Mu R., Ueda A., Chen J., Gu Z., White C.W., Zhu J.G., McKay M., Scott O. (1997) Gold implanted calcium fluoride single crystals: Optical properties of ion induced defects and metal nanocrystals. *Materials Science Forum*, Vol. 239–241, pp. 695–698.
- King J.M., Shigley J.E., Guhin S.S., Gelb T.H., Hall M. (2002) Characterization and grading of natural-color pink diamonds. *Gems & Gemology*, Vol. 38, No. 2, pp. 128–147.
- Miles E.R. (1962) Diamond-coating techniques and methods of detection. *Gems & Gemology*, Vol. 10, No. 12, pp. 355–383.
- Robinson P.C., Bradbury S. (1992) *Qualitative Polarized-Light Microscopy*. Oxford University Press, Oxford, pp. 94–108.
- Reinitz I.M., Buerki P.R., Shigley J.E., McClure S.F., Moses T.M. (2000) Identification of HPHT-treated yellow to green diamonds. *Gems & Gemology*, Vol. 36, No. 2, pp. 128–137.
- Sheby J. (2003) Lab Notes: Coated diamonds. *Gems & Gemology*, Vol. 39, No. 4, pp. 315–316.
- Smith C.P., Bosshart G., Ponahlo J., Hammer V.M.F., Klapper H., Schmetzer K. (2000) GE POL diamonds: Before and after. *Gems & Gemology*, Vol. 36, No. 3, pp. 192–215.

NOW AVAILABLE!

GEMS & GEMOLOGY®
IN REVIEW
SYNTHETIC DIAMONDS

The best of *Gems & Gemology* on the subject of synthetic diamonds: now available in one comprehensive research volume.

- More than 30 years of cutting-edge synthetic diamond research by leading gemological researchers and producers
- Editorial commentary by Dr. James Shigley of GIA Research
- Insights on the past, present, and future of synthetic diamonds, and their effects on the gem and jewelry industry
- 50 separate entries comprising more than 300 pages of material
- Includes two wall charts in a sturdy bound-in pouch: the Separation of Synthetic and Natural Diamonds (1995), and Characteristics of HPHT-Grown Synthetic Diamonds (2004)
- Softbound in an attractive slipcase

\$49.95
(plus shipping and handling)

To order your copy today, visit
GIA Gem Instruments & Books at
www.gia.edu

Some of the material in **SYNTHETIC DIAMONDS** is from *Gems & Gemology* issues that are long out of print. That means you won't find this information anywhere else.

2005

LAB NOTES

EDITORS

Thomas M. Moses and Shane F. McClure
GIA Gem Laboratory

CONTRIBUTING EDITORS

G. Robert Crowningshield
GIA Gem Laboratory, East Coast

Cheryl Y. Wentzell
GIA Gem Laboratory, West Coast

DIAMOND

With Bodycolor Possibly Affected by the 3H Defect

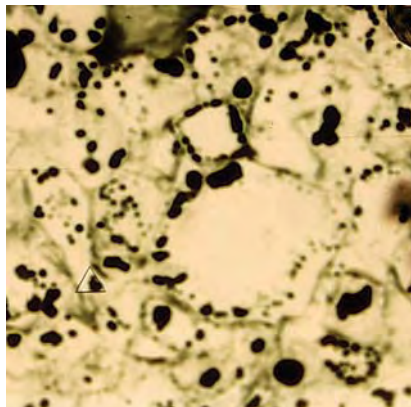
Irradiation is an important mechanism for diamond coloration. It occurs naturally to some diamonds over geologic time, and has been performed for over a century in the laboratory. Features such as radiation stains and color distribution are useful for differentiating these two processes. However, definitive identification of color origin is still a challenge. Understanding defect configurations in known natural and treated stones

is a helpful way to recognize some subtle differences between naturally and laboratory-irradiated diamonds. For example, H3 and 3H are two common radiation-related defects. The 3H defect consists of an interstitial carbon atom, while the H3 defect is formed by two nitrogen atoms and one vacancy. Because the 3H defect requires relatively little energy to relax into a normal diamond bond, it is much less stable than the H3 defect at high temperature. The zero phonon line—or principal absorption—of H3 is at 503.2 nm, and that of 3H is at 503.6 nm.

The East Coast laboratory recently examined a radiation “damaged” stone that showed some interesting features. The 8.08 ct diamond (12.67 × 10.60 × 6.74 mm) in figure 1 (left) was color graded as Fancy Deep grayish yellowish green; however, magnification revealed that the green color was concentrated in the diamond’s “skin” (figure 1, right). Over large areas of the pavilion and girdle, intense green stains remained on original crystal surfaces that had not been entirely removed in the polishing process. In contrast to the green skin, the diamond’s bodycolor was a distinct brownish yellow. This color “contrast” was different from that seen in many other naturally irradiated diamonds, which sometimes display a less saturated greenish or bluish coloration after the darker skin is removed in the manufacturing process.

Infrared absorption spectroscopy revealed that this was a type Ia diamond with a high concentration of nitrogen. A very weak absorption at 1450 cm⁻¹ due to the H1a defect was observed, but no H1b or H1c defects were detected. The color distribution,

Figure 1. This 8.08 ct diamond was graded Fancy Deep grayish yellowish green (left). However, with magnification it is apparent that the green color is concentrated in areas of the diamond’s “skin,” while the rest of the stone shows distinct brownish yellow coloration (right; width of image is 1.6 mm). Many intense green radiation stains were noted on original crystal surfaces that remained on large areas of the pavilion and girdle. These distinctive surface stains, readily seen with a combination of reflected and transmitted light, are believed to result from natural irradiation.



Editor's note: The initials at the end of each item identify the editor(s) or contributing editor(s) who provided that item. Full names are given for other GIA Gem Laboratory contributors.

GEMS & GEMOLOGY, Vol. 41, No. 1, pp. 42–50
© 2005 Gemological Institute of America

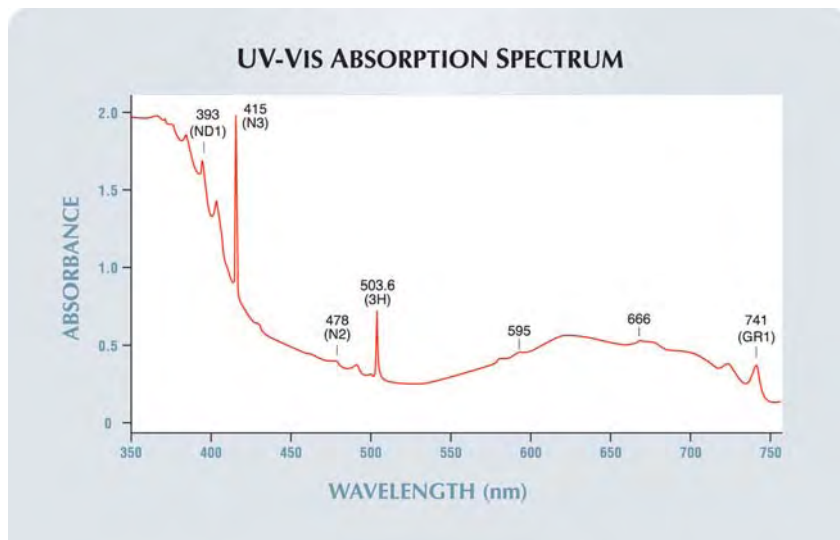


Figure 2. The UV-Vis absorption spectrum of the diamond in figure 1 shows a strong absorption at 503.6 nm from the 3H defect, in addition to other absorptions common in diamonds that have been exposed to radiation either naturally or in the laboratory (e.g., ND1, N2, N3, 595 nm, 666 nm, and GR1).

absence of H1b and H1c, and intense green radiation stains at the surface established that this diamond was untreated.

In addition to those absorptions common in this type of diamond (ND1, N2, N3, 595 nm, 666 nm, and GR1), the ultraviolet-visible absorption spectrum contained a strong 3H line (figure 2). The presence of the 3H defect throughout the whole stone was confirmed with Raman photoluminescence spectroscopy at 488 nm laser excitation. The intensity of the 3H absorption varied substantially in the different locations analyzed, but without any consistent trends. Only rarely has the 3H defect been observed in intensity as strong as that seen in this stone (approximately 0.43 cm^{-1} in absorption coefficient, assuming the path length of light is equal to the girdle diameter at the point of analysis). Although typically the 3H defect does not cause color, its intensity in this stone suggests that this defect could make a significant contribution to the diamond's yellow bodycolor.

However, as noted above, the 3H

defect is somewhat unstable. In N-rich diamond, its intensity can be enhanced by heating to about 300°C , but it can be annealed out at temperatures above 500°C (see, e.g., A. M. Zaitsev, *Optical Properties of Diamond*, Springer-Verlag, Berlin, 2001). Since the polishing process can easily produce these temperatures, it could

Figure 3. This 4.33 ct rectangular modified brilliant cut (left) proved to be a type IIa HPHT-treated diamond. In contrast to many other HPHT-treated type IIa diamonds, it shows a pure yellow color that is surprisingly similar to the 1.21 ct untreated type Ia cape stone on the right, which was also color graded as Fancy yellow.



either enhance or decrease the concentration of the 3H defect. (In contrast, much higher temperatures are required to affect the H3 defect.) We have noted in the past when examining diamonds before and after cutting that the 3H absorption is often removed during faceting. We do not know the manufacturing history of this specific stone, but slight color modification during cutting cannot be ruled out entirely. Slight color change by this process is not considered artificial treatment, but it obviously adds one more variable to the complexity of identification.

Wuyi Wang and Tom Moses

HPHT-Treated Type IIa Yellow Diamond

High pressure/high temperature (HPHT) annealing can be used to alter the bodycolor of type IIa diamonds. Depending on the properties of the starting material and the pressures and temperatures employed, most of these diamonds are colorless or near-colorless after treatment, with a small percentage resulting in a predominantly pink bodycolor. Recently, the East Coast laboratory examined a stone (figure 3) with a color very similar to that associated with natural-color type Ia yellow diamonds commonly re-

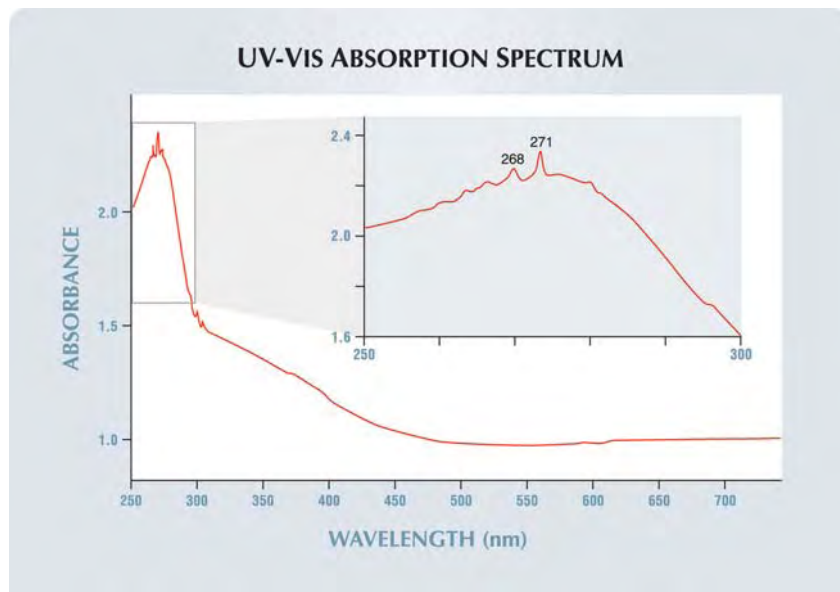


Figure 4. The moderately strong and broad absorption centered at 270 nm, together with the two sharp absorptions at 268 and 271 nm, in the UV-Vis absorption spectrum of the 4.33 ct yellow type IIa diamond confirmed the presence of isolated nitrogen. The gradual increase in absorption at energies above ~500 nm due to isolated nitrogen is the main cause of the yellow bodycolor.

ferred to as “cape” diamonds. However, its gemological properties and spectral analyses led to a very different identification.

The 4.33 ct cut-cornered rectangular modified brilliant cut ($9.84 \times 8.92 \times 5.50$ mm) was color graded Fancy yellow. It did not have any unusual internal characteristics, either inclusions or fractures. It displayed a very weak blue fluorescence to long-wave ultraviolet (UV) radiation and a very weak yellow fluorescence to short-wave UV, with no phosphorescence. However, in contrast to the overall turbid blue fluorescence that is very common in type Ia cape yellow diamonds, the long-wave reaction appeared much more transparent. This is very unusual for any diamond other than a type IIa. Observation with a handheld spectroscope revealed no absorption lines. It was clear that further spectroscopic analysis was necessary, as these results did not explain the cause of the pure yellow color.

The infrared absorption spectra showed features typical of a type IIa

diamond, with no detectable A-form or B-form nitrogen. However, there was a weak but clear absorption from isolated nitrogen. The absorption coefficient of the peak at 1344 cm^{-1} was approximately 0.02 cm^{-1} , corresponding to a nitrogen concentration of about 0.8 ppm. In the UV-Vis absorption spectrum (figure 4) taken at cryogenic temperature, a moderately strong and broad absorption centered at 270 nm, with two superimposed sharp absorptions at 268 and 271 nm, and the gradual increase in absorption at energies above ~500 nm confirmed both the presence of isolated nitrogen and that it was the main defect responsible for the yellow color. In addition, a very weak N3 absorption at 415 nm and several other weak absorptions (~300 nm) related to isolated nitrogen also were observed.

D. Fisher and R. A. Spits (“Spectroscopic evidence of GE POL HPHT-treated natural type IIa diamonds,” Spring 2000 *Gems & Gemology*, pp. 42–49) reported nine HPHT-treated type IIa stones in

which isolated nitrogen was detected, although their concentrations were lower. Since it is well known that natural type IIa diamonds may contain traces of highly aggregated nitrogen, the occurrence of isolated nitrogen in this 4.33 ct yellow diamond raised suspicions of HPHT treatment. This was confirmed by photoluminescence (PL) analysis. PL spectra collected using an Ar laser at 488 and 514 nm excitations exhibited strong emissions from N-V centers, with the peak at 637 nm being much stronger than that at 575 nm. Additional evidence included the presence of a strong H3 emission (but see the following Lab Note) and the absence of 3H and H4 emissions. Imaging with a Diamond Trading Company (DTC) DiamondView instrument showed a homogeneous distribution of greenish yellow luminescence, which is very different from what we have observed in natural-color type IIa or Ib diamonds, or in typical type IIa HPHT-treated diamonds.

The temperatures employed in HPHT treatment are much higher than the natural conditions of diamond formation. Conceivably, HPHT annealing not only could remove brown coloration possibly caused by plastic deformation, but it also could transform part of the highly aggregated nitrogen into isolated nitrogen. When the concentration of isolated nitrogen is high enough, the diamond will show a pure yellow color. The Fancy yellow bodycolor of this stone could be a combination of the relatively high concentration of isolated nitrogen with the stone’s relatively large size and its cut. The existence of this high-quality type IIa yellow diamond indicates that HPHT annealing is capable of producing a wider range of colors than previously believed.

This diamond is a reminder of the complexity of identifying HPHT-annealed diamonds. Although we have encountered a few diamonds like this in the past, we do not know if this was a “planned” result or an accidental outcome of the treatment.

Wuyi Wang and Thomas Gelb



Figure 5. This natural-color 1.03 ct cape diamond showed localized H3 absorption, a feature typically associated with treated-color yellow diamonds.

Inhomogeneous Cape Diamond

Yellow type Ia cape diamonds show a characteristic visible absorption spectrum, with primary peaks at 415.5 and 478.0 nm and weaker bands at 453.0 and 466.0 nm. Absence of H3 absorption is also typical. These are the most common colored diamonds in the market. Attractive yellow color in diamond can be artificially created by irradiation and annealing, as well as by HPHT treatment. These processes, particularly irradiation and annealing, create a strong absorption of H3, which selectively absorbs blue light. As a result, a distinct yellow hue is produced. Occurrence of a relatively strong H3 absorption in an otherwise typical cape diamond usually raises suspicions of treatment.

Recently, the East Coast laboratory had a chance to examine a very unusual 1.03 ct Fancy Intense yellow cushion modified brilliant diamond (figure 5). Although it had absorption features and other gemological properties that proved it was a natural-color cape stone, it displayed an unusual luminescence pattern when examined using the DTC DiamondView. In contrast to typical cape diamonds, which show homogeneous blue (and, to a lesser extent, brownish yellow) UV fluorescence in the DiamondView (figure 6, left), this stone displayed obvious zoning (figure

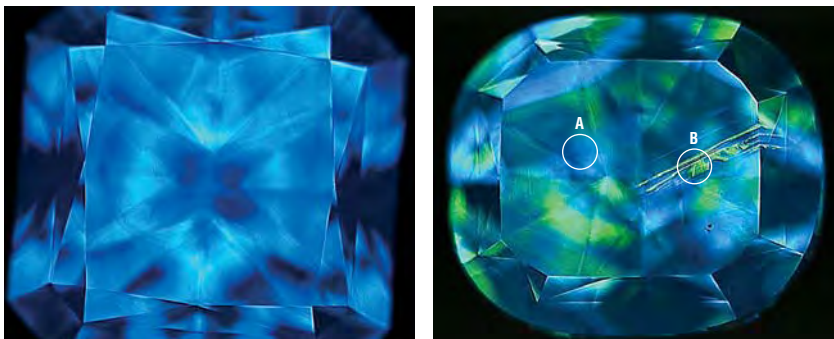


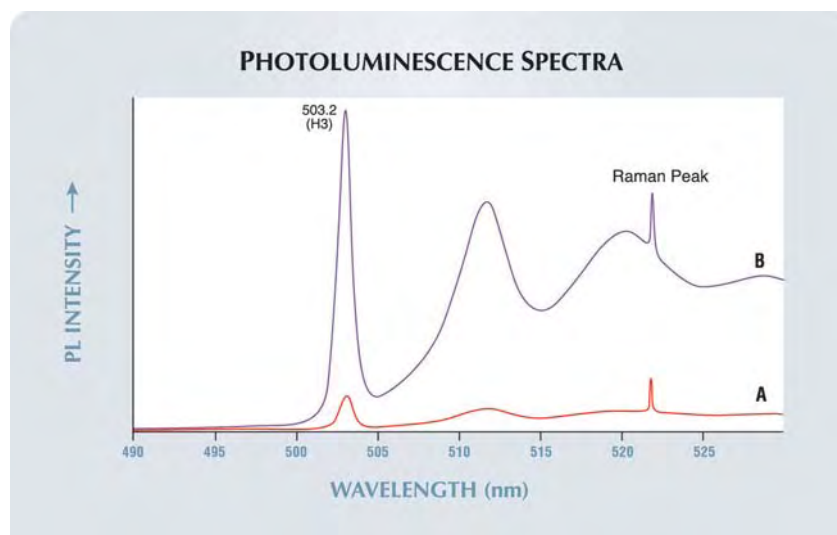
Figure 6. A typical cape diamond (left) shows homogenous blue fluorescence in the DTC DiamondView. In contrast, the 1.03 ct diamond on the right displayed blue and greenish yellow luminescence zoning. The greenish yellow fluorescence is caused by the H3 defect.

6, right). A strong greenish yellow reaction was seen in some narrow parallel bands that extended across almost half the table facet, while most of the remainder of the stone showed typical blue luminescence. Of the more than 100 cape diamonds examined face-up in the laboratory with the DiamondView, this is the only one that has ever shown such heterogeneous luminescence.

To confirm our belief that the strong greenish yellow fluorescence in

these bands was caused by localized high concentrations of the H3 defect, we took PL spectra with a Raman microspectrometer (using 488 nm laser excitation) in both the blue and greenish yellow fluorescing areas of the stone. As seen in figure 7, the blue area showed only a very weak H3 peak, whereas the isolated greenish yellow area showed a very strong H3. Note that in an irradiated yellow diamond, the H3 absorption would have been observed across the entire stone.

Figure 7. These PL spectra of the unusual cape diamond in figure 5 clearly illustrate the difference in intensity of H3 emission between a blue fluorescing area (marked A on figure 6, spectrum A here) and an area showing a greenish yellow fluorescence (B on figure 6, spectrum B here).



These results confirm that natural cape diamonds can have localized regions with high concentrations of the H3 defect. Because it was not homogenous throughout the stone, the H3 center in this cape diamond would have gone undetected with standard testing methods. Random PL analyses would not have revealed it. Likewise, standard short-wave UV lamps do not have enough intensity to excite the H3 defect, and therefore would not have shown the greenish yellow zoning. Discovery of this rare cape diamond indicates that the occurrence of H3 in a (natural-color) type Ia cape diamond could be more common than we had believed. We continue to gather useful information about the distribution of defects in diamond using the DTC DiamondView.

Paul Johnson and Kyaw Soe Moe

Irradiated and Fracture-Filled Diamond

Recently, the East Coast laboratory received a bluish green 1.22 ct round brilliant cut diamond for a colored diamond grading report. Preliminary visual inspection of the stone raised questions about the origin of its color, which appeared quite similar to that seen in artificially irradiated

diamonds. Indeed, magnification revealed a bluish green color zone that followed the faceting outline—a common side effect of laboratory irradiation—at the culet (figure 8). This zonation, along with features in the visible spectrum observed with a desk-model spectroscope, confirmed that the color of this stone was the result of artificial irradiation.

However, microscopic examination revealed signs of additional treatment. A number of large fractures displayed the flash-effect colors typically associated with fracture filling to improve apparent clarity (figure 9). Closer inspection revealed both the flash-effect colors and, within the fractures, the flow structures that are commonly seen in a glass-like filler (again, see figure 8). An X-radiograph provided final proof of clarity enhancement (the filling material absorbs more X-rays than the surrounding diamond).

Although it is not uncommon for us to see treated diamonds, it is rare to see two such treatments in one stone. From the brown grain lines that were still visible and the large fractures, one could speculate that this round brilliant was a heavily included brown diamond before treatment. Since fracture filling is a non-stable treatment, it is laboratory policy not to provide any grading

information on diamonds enhanced in this fashion.

Thomas Gelb

A Coated “NIGHT GLOWING PEARL”

“Night glowing pearls” are legendary jewels in Chinese and south Asian cultures, and were a symbol of supernatural power and wealth in Imperial China. One such “pearl” is said to have been placed in the mouth of Dowager Empress Cixi, the last empress of the Qing Dynasty, after her death. These jewels have always been greatly sought after, and in recent years they have fetched high prices in the Chinese jewelry market. However, they have remained mysterious due to their scarcity, which has hampered thorough documentation of their nature. According to historical Chinese literature, as quoted in Joseph Needham’s *Science and Civilization in China* (Cambridge University Press, Cambridge, UK, 1954), they are not actually pearls; rather, they are spheres of a mineral or rock of various colors that exhibit phosphorescence at night (i.e., “glow in the dark”). Ancient Chinese imperial courts acquired these spheres from Persia or Ceylon. Today, they are believed to be composed of fluorite or calcite with rare-earth elements that act as phosphorescent agents (A. S. Marfunin, *Spectroscopy, Luminescence and Radiation Centers in Minerals*, Springer-Verlag, Berlin, 1979; Y. R. Huang, “The glowing stones,” *Jewelry World*, No. 2, 2004, pp. 112–115 [in Chinese]).

Recently, a semitranslucent to opaque mottled green-and-gray sphere (figure 10) was submitted to the East Coast laboratory for identification. Due to its size (63 mm in diameter) and weight (366 g), we could not measure its specific gravity using the hydrostatic method; however, it is possible to estimate the S.G. of a spherical object from its mass and diameter. Using this method, we calculated the S.G. to be approximately 2.80. Spot R.I. measurements varied

Figure 8. This 1.22 ct round brilliant diamond displays an obvious color zone at the culet, which is a typical side effect of artificial irradiation. Also visible are flow structures from extensive fracture filling. Magnified 30×.

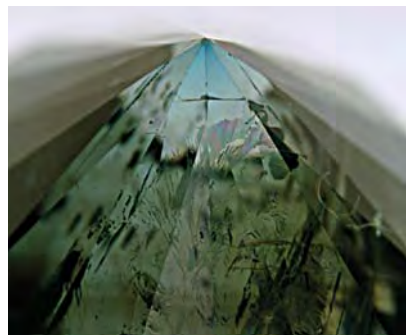
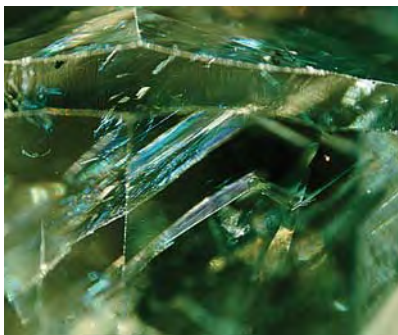


Figure 9. Closer examination of the diamond in figure 8 shows the numerous flash-effect colors associated with fracture filling to improve apparent clarity. Magnified 45×.



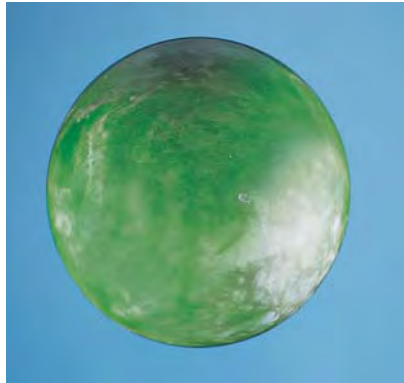


Figure 10. This mottled green-and-gray sphere (63 mm in diameter) proved to be a talc-serpentine rock with a phosphorescent coating.

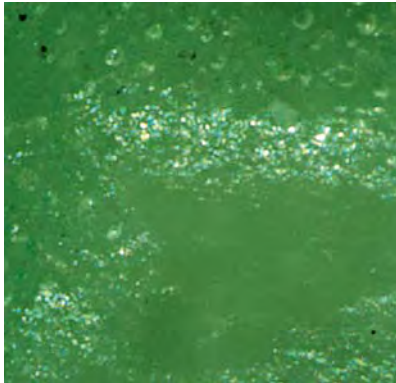


Figure 11. Magnification revealed numerous gas bubbles on the surface of the talc-serpentine sphere. No bubbles are apparent in the rectangular area in the lower right corner, where there was no coating. Magnified 112 \times .

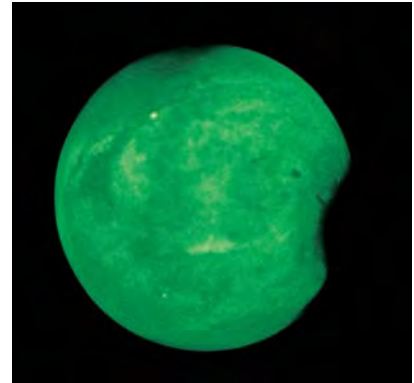


Figure 12. After exposure to ultraviolet radiation, the sphere in figure 10 shows exceptional phosphorescence. This phosphorescence lasted longer than 15 minutes following exposure to both long- and short-wave UV. The areas showing less or no phosphorescence correspond to the areas that appeared gray under normal lighting conditions.

from 1.56 in the green areas to as high as 1.60 in a gray area.

Magnification with a standard gemological microscope revealed numerous small round gas bubbles, some of which broke the surface (figure 11). These were observed across the sphere, with the exception of one gray area. The sphere fluoresced very strong green-yellow to long-wave UV radiation and strong green to short-wave UV. The most impressive gemological property was the strong green-yellow phosphorescence to both long- and short-wave UV, which lasted longer than 15 minutes. However, both the fluorescence and the phosphorescence were unevenly distributed, as the gray areas showed less or none of either reaction (compare figures 10 and 12), and the area without any bubbles was inert. Even more unusual was the fact that when the sphere was subjected to a strong fiber-optic light source, the phosphorescence was visible even in regular office lighting. Due to the strength and duration of the phosphorescence, we suspected this sphere would probably be considered a legendary “night glowing pearl.”

Because of the many gas bubbles, our first impression was that the sphere was likely a mineral or rock that had some sort of coating, with the gray areas—from their higher R.I. and

weaker phosphorescence—representing spots where the coating was thin or nonexistent. Thus, with the client’s permission, we analyzed a green area and a gray area with Raman spectroscopy both at and beneath the surface by digging two very small, shallow (approximately 0.5 mm deep) craters. The spectra obtained at the bottom of the craters clearly differed from those taken on the surface, even in the gray area, but neither set of spectra provided a conclusive identification. We subsequently performed energy-dispersive X-ray fluorescence (EDXRF) analysis of another green area and the gray area without bubbles, and found that the green area contained a major amount of Sr, as well as significant amounts of Al, Ba, S, Zn, Fe, and Ca, and minute quantities of Eu and Dy. In comparison, the gray area contained Mg, Al, Si, Ca, Fe, and Ni.

We also performed X-ray diffraction analysis on small quantities of powder scraped from the bottom of the previously mentioned craters and from the surface. For both craters, the former pattern matched that of a talc-serpentine mixture (Mg, Al silicates), whereas the pattern from the surface matched that of a mixture of SrAl₂O₄ and SrAl₄O₇ (generally known as

strontium aluminates).

Based on this evidence, we concluded that the sphere was a talc-serpentine rock covered unevenly with a coating that contains an Eu- and Dy-doped SrAl₂O₄-SrAl₄O₇ mixture. This manufactured coating has several modern uses as a long-lasting phosphorescent pigment. Its phosphorescence has been documented to last for many hours and, in some cases, even days (T. Katsumata et al., “Characteristics of strontium aluminate crystals used for long-duration phosphors,” *Journal of the American Ceramic Society*, Vol. 81, No. 2, 1998, pp. 413–416; K. R. S. Preethi et al., “SrAl₄O₇:Eu²⁺ nanocrystals: Synthesis and fluorescence properties,” *Journal of Physics D*, Vol. 37, No. 19, 2004, pp. 2664–2669).

Andy Shen, Wendi M. Mayerson,
and Dino DeGhionno

QUARTZ Covellite in Quartz

We recently had the opportunity to examine four oval buff-top modified



Figure 13. Covellite inclusions are responsible for the “hot pink” schiller in these two samples of smoky and near-colorless quartz (18.81 and 18.00 ct).

brilliant cut samples of a material that was being represented as “pink fire quartz.” The stones (8.07–18.81 ct) were transparent to semitransparent and near-colorless to light brown; most had numerous inclusions (see, e.g., figure 13). At first there did not seem to be anything unusual about these stones, which were readily identified as quartz based on standard

gemological testing, but closer examination revealed a flash of pink to purple from some viewing angles. The flash was directional and at times very bright, resembling the schiller sometimes seen in corundum when light reflects off oriented rutile inclusions.

We had not witnessed such an effect in quartz before, and at first glance we thought it might have been

Figure 14. With magnification and darkfield illumination, these covellite inclusions appeared as transparent to semitransparent grayish green hexagonal platelets in the host quartz. Magnified 33 \times .

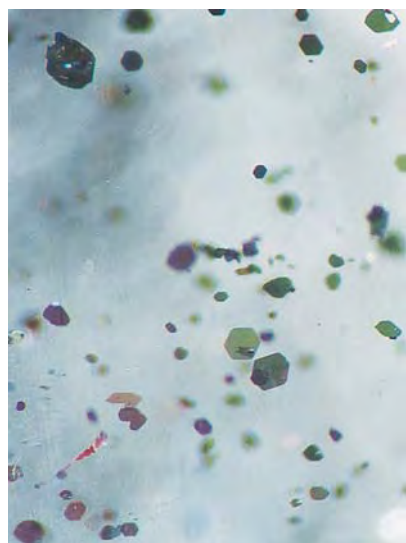
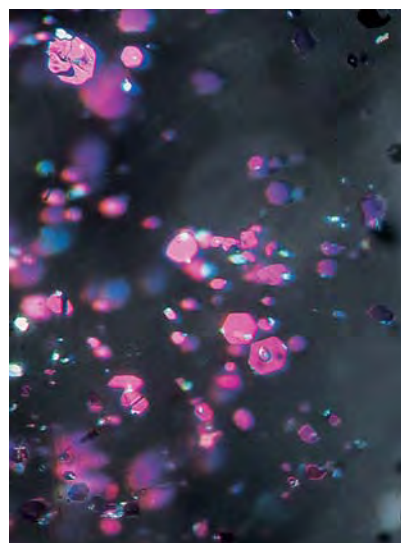


Figure 15. When viewed with reflected light, the platelets seen in figure 14 appeared bright pink due to unusually strong iridescence, a property well documented in covellite.



produced by some form of treatment. However, the inclusions creating this schiller could be seen with the unaided eye as dark specks throughout the stones. With magnification and dark-field illumination, these inclusions proved to be very thin transparent to semitransparent grayish green hexagonal platelets oriented in parallel planes (figure 14). The pink/purple schiller was iridescence off the flat surfaces of these platelets when they were viewed in reflected light (figure 15). These inclusions were so thin that they almost disappeared when viewed at 90° from the flat surface.

Raman analysis identified a couple of these platelets as the copper sulfide covellite (CuS), which is typically opaque with a mottled dark blue color, metallic luster, and strong pink-to-purple iridescence. Covellite usually forms as hexagonal platelets, and can appear green in transmitted light when the platelets are thin enough (M. Fleischer et al., *Microscopic Determination of the Nonopaque Minerals*, U.S. Geological Survey Bulletin 1627, 1984, p. 62). It is occasionally seen cut into cabochons, but we were unfamiliar with it as an inclusion. Dino Deghionno, manager of West Coast Identification Services, attempted to confirm this identification using powder X-ray diffraction analysis, but the inclusions were too small to provide sufficient material for analysis. However, EDXRF chemical analysis of the quartz samples by research associate Sam Muhlmeister did reveal copper. Based on the Raman analysis, presence of Cu, and appearance of the inclusions, we concluded that there was a high probability they were indeed covellite. Our literature search did not uncover a reference to covellite as an inclusion in quartz, but the two minerals are known to occur together.

This material reportedly was from Brazil’s Minas Gerais region. The stones contained additional inclusions typical of quartz: “fingerprints,” two-phase inclusions, and elongated, angular orangy red crystals that Raman analysis identified as hematite.

Elizabeth P. Quinn and SFM

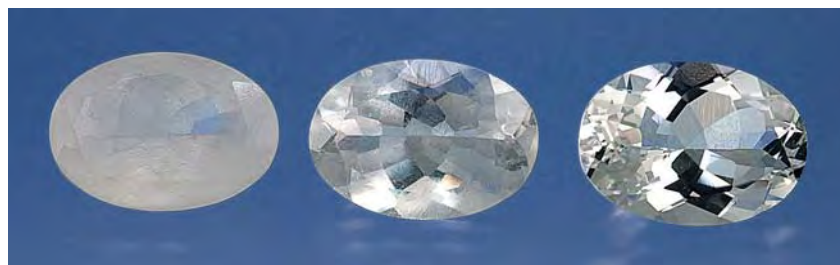


Figure 16. These three faceted samples of rock crystal (5.20–5.40 ct) show varying degrees of an unusual surface texture. The stone on the right has the texture only on the girdle.

Rock Crystal Quartz with Unusual Surface Texture

Recently, the East Coast laboratory received for identification three transparent to semitransparent near-colorless oval modified brilliants ranging from 5.20 to 5.40 ct. Standard gemological testing on all three stones revealed properties consistent with rock crystal quartz. What caught this author's attention was an unusual surface texture seen on all three stones in varying degrees (figure 16).

Figure 17. The unusual surface texture—numerous small, very shallow, irregular grooves and channels—almost completely covered the stone on the far left in figure 16. Magnified 112 \times .



The first stone was almost completely covered with numerous small, very shallow, irregular grooves and channels (figure 17). Although different in structure, this overall pattern was reminiscent of the "crazed layer" seen on stones with a Lechleitner synthetic emerald overgrowth (see Winter 1992 Lab Notes, pp. 263–264), which aroused suspicion. The texture was seen in random patches on the second stone, although in some places it appeared as thin crystalline layers on the surface (figure 18), very different from the first stone. Synthetic

Figure 18. In addition to areas of channels and grooves, the middle stone in figure 16 also showed thin, uneven crystalline layers on its surface. These layers are transparent (left) but slightly rough, and therefore scatter light and have a white appearance when viewed at certain angles (right). Magnified 20 \times (left), 15 \times (right).



overgrowths normally display some sort of disturbance at or near the point of interface with the substrate; frequently, this disturbance appears as a plane of inclusions. However, no interface was detected on any of these stones. The third stone had only remnants of the unusual surface texture on its girdle, which suggested that it might have been repolished.

No differences in properties were detected between the areas of unusual texture and the polished areas with either standard gemological or spectroscopic (EDXRF and Fourier-transform infrared) testing; nor were any differences in properties detected among the three stones. A discussion with the client revealed that these stones were part of a larger parcel that had been purchased as topaz and then sent to be treated by a "diffusion" process. These three were rejected by the treater because they were quartz and were returned to the client in this condition.

This new information gave us much-needed insight. The textured surface was not an overgrowth, but

rather the result of dissolution or etching. Whether or not this treatment of topaz (which uses cobalt or a cobalt oxide) is actually “diffusion” or merely a durable surface treatment has not been established (see S. F. McClure, “Identification challenges of the new millennium,” Fall 1999 *Gems & Gemology*, pp. 86–87). In either case, it was first seen at the Tucson gem shows in 1998 (Summer 1998 Gem News, pp. 143–144) and is a patented process (R. Pollak, *Method for Enhancing the Color of Minerals Useful as Gemstones*, U.S. Patent 5,888,918, filed April 25, 1997; issued March 30, 1999) that is currently being marketed under the trademark PHD.

The patent mentions that during preparation for treatment, the stones may be soaked in a series of acid and solvent baths. Although the patent also covers the treatment as it applies to quartz, it specifically states that “[c]are should be taken in selecting the temperature to which stones are heated, as quartz tends to develop surface damage when subjected to excessive temperatures.” Even more interesting in relation to the three stones in question, the patent goes on to mention, “[i]n the event surface damage does occur, the treated stones can be repolished, producing a smooth colored finished product.” According to the patent, cobalt typically produces a light to dark pink coloration with quartz.

Since these three stones were colorless, it is likely the surface dissolution/etching, and hence their identity as quartz rather than topaz, was discovered during the preparation process, and they never underwent the cobalt treatment.

Wendi M. Mayerson

SPHENE Cabochon with an Unusual Natural Surface

Sphene, or titanite, a monoclinic calcium titanium silicate, is a relatively uncommon gem mineral primarily known for its strong dispersion, or “fire.” This colorful property is best displayed when material of suitable



Figure 19. This 8.49 ct sphene was cut as a cabochon to showcase the interesting natural surface that was used as the base.

quality is fashioned as a round brilliant or similar faceting style, so virtually all transparent gem-quality sphene is faceted. Therefore, it was interesting to examine an 8.49 ct transparent yellowish green pear-shaped sphene cabochon that had been cut from a facetable crystal purchased in Governador Valadares, Minas Gerais, Brazil. Leon M. Agee sent the 17.64 × 14.04 × 3.73 mm partially polished cabochon to the West Coast laboratory for gemological examination.

As can be seen in figure 19, this cabochon showed virtually no dispersion, which at first glance seemed to be a waste of this gem material’s potential. However, Mr Agee informed us that the stone was not cut to display this sphene’s dispersion, but rather to highlight and magnify an interesting natural crystal surface, which was left unpolished and used as the base of the cabochon.

With the dome serving as a magnifying lens, not only did the convoluted contours and depressions on the base stand out, but sphene’s characteristic strong double refraction could also be seen. With low-power magnification, it was evident that the base of the cabochon was decorated with an intricate random arrangement of partial mineral casts with a micaceous habit (figure 20).

From observation of this microfeature, it appeared that the sphene was at one time either superficially dusted with numerous twisted worm-like columns or stacks of a mica- or chlo-

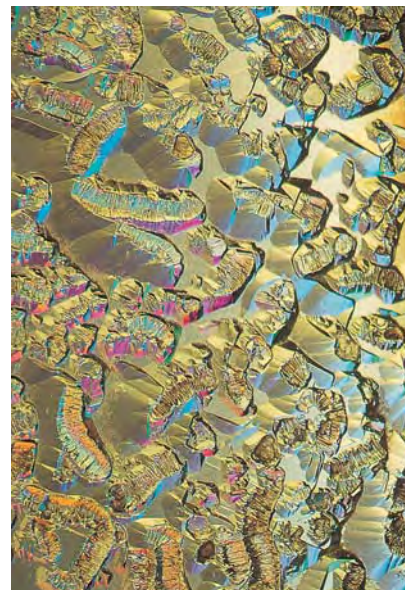


Figure 20. With 5× magnification and a combination of polarized and fiber-optic lighting, the base of the sphene cabochon in figure 19 revealed an intricate random arrangement of what appear to be casts of a mineral with a micaceous habit.

rite-group mineral, or it grew up against such minerals. Then, as the sphene continued to grow, the micaceous minerals became embedded in its surface, leaving their characteristic visual impressions. However, growth must have ceased before they could be completely enclosed as inclusions. As a result, only partial casts of the micaceous mineral(s) were left behind.

To complete the examination of this gem, we identified the cabochon itself as sphene using classical gemological testing techniques.

John I. Koivula and Maha Tannous

PHOTO CREDITS

Wuyi Wang—1 and 5; Jessica Arditi—3; Paul Johnson—6; Thomas Gelb—8 and 9; Maha Tannous—10, 12, 13, and 19; Wendi Mayerson—11, 17, and 18; Shane F. McClure—14 and 15; Elizabeth Schrader—16; John I. Koivula—20.



EDITOR

Brendan M. Laurs (blaurs@gia.edu)

CONTRIBUTING EDITORS

Emmanuel Fritsch, *IMN, University of Nantes, France* (fritsch@cnsr-immn.fr)

Henry A. Hänni, *SSEF, Basel, Switzerland* (gemlab@ssef.ch)

Kenneth V. G. Scarratt, *GIA, Bangkok, Thailand* (kscarratt@aol.com)

James E. Shigley, *GIA Research, Carlsbad, California* (jshigley@gia.edu)

Christopher P. Smith, *GIA Gem Laboratory, New York* (chris.smith@gia.edu)

Tucson

2005

This year's gem and mineral shows in Tucson, Arizona, featured new finds from a number of previously known localities. Many of these discoveries were made in African countries—but there were also several important finds made in the U.S. Although no major new localities came to light at this year's show, there were plenty of unusual pieces to entertain and inspire. An example of these curiosities is the carved bicolored beryl rose from Brazil in figure 1. Additional items are described in greater

detail below, with more included in the upcoming Summer 2005 GNI section. *G&G* thanks our many friends who shared material with us this year.

COLORED STONES AND ORGANIC MATERIALS

AGTA Design Center features lapidary art. At the new Spectrum of Design center at the AGTA show, jewelry artist Paula Crevoshay of Albuquerque, New Mexico, displayed a collection of jewels containing gem carvings from some of North America's most prominent lapidary artists (see, e.g., figure 2). As she has done previously (see S. E. Thompson, "Voices of the Earth: Transcending the traditional in lapidary arts," Winter 2001 *Gems & Gemology*, pp. 310–317), Ms. Crevoshay enlisted lapidary artists such as Larry Woods, Sherris Cottier Shank, Glenn Lehrer, Lawrence Stoller, Larry Winn, Thomas McPhee, and Arthur Lee Anderson to carve pieces that were used to create one-of-a-kind jewels. This collection, called "Elements," is intended to evoke the four classic elements: air, earth, fire, and water.

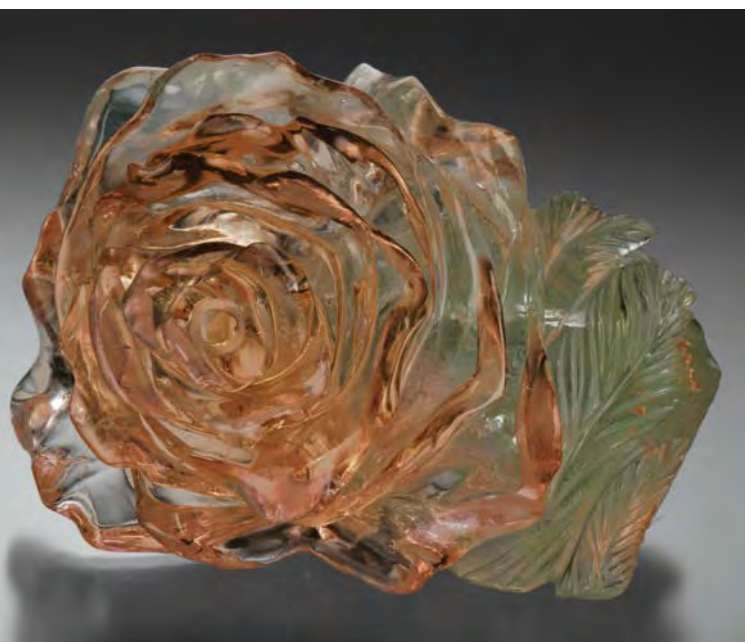


Figure 1. This 8.5-cm-long beryl from Brazil is carved into a rose that shows a clever use of the color zoning, with pinkish orange concentrated in the petals and yellowish green in the leaves. The piece came from the Coronel Murta mine in Minas Gerais, and was carved by "Docinho" of Governador Valadares, Brazil. Courtesy of Bernardo Felner, *Brazrio International, Los Angeles*; photo © Robert Weldon/Professional Jeweler.



Figure 2. These pieces are from Paula Crevoshay's "Elements" collection. From left are "Ether," a brooch featuring a 53.80 ct carved opal with zircon; "Spring Waterfall," incorporating a 6.15 ct carved opal with zircon, demantoid, aquamarine, moonstone, and diamond; "Sky," a gold and diamond ring showcasing a 9.54 ct tanzanite carving; and "Ocean Dream," a brooch featuring a 199.62 ct chrysocolla octopus with a moonstone "eye" and diamond and zircon accents. The chrysocolla in "Ocean Dream" was fashioned by Glenn Lehrer; the other carvings are by Sherris Cottier Shank. Courtesy of Paula Crevoshay; photo © Harold and Erica Van Pelt.

One of the most notable pieces is "Green Dream," a diamond, tourmaline, and tsavorite necklace featuring a 217 ct peridot carving by Larry Woods (see the cover of this issue). According to Mr. Woods, the central stone was carved from a 69 gram Pakistani peridot crystal, incorporating the abstract organic style he uses for most of his work.

Editor's note: The initials at the end of each item identify the editor or contributing editor who provided it. Full names and affiliations are given for other contributors. Shane F. McClure and Dr. Mary L. Johnson of the GIA Gem Trade Laboratory in Carlsbad are thanked for their internal review of the Gem News International section.

Interested contributors should send information and illustrations to Brendan Laurs at blaurs@gia.edu (e-mail), 760-603-4595 (fax), or GIA, 5345 Armada Drive, Carlsbad, CA 92008. Original photos will be returned after consideration or publication.

GEMS & GEMOLOGY, Vol. 41, No. 1, pp. 52-73
© 2005 Gemological Institute of America

Two other pieces contain memorable, though very different, opal carvings by Sherris Cottier Shank (again, see figure 2). "Spring Waterfall" features a 6.15 ct crystal opal from Lightning Ridge, Australia. The difficulty in working with this material, according to Ms. Shank, is that the intense play-of-color requires great care in planning a design, so that the final carving works with the color patterns instead of against them. The other jewel, "Ether," also features a crystal opal; however, this larger (53.80 ct) stone, though near-colorless at first glance, displays elegant textures and tones brought out by precise carving of the back of the piece.

"Elements" will be the focus of a future museum exhibit intended to showcase the growth of gem carving as an art form in North America.

Thomas W. Overton (toverton@gia.edu)
GIA, Carlsbad

Amethyst from Georgia. At the Arizona Mineral & Fossil Show (Clarion Hotel) and the Tucson Gem & Mineral Society show (Tucson Convention Center), Terry Ledford



Figure 3. Fine amethyst crystals and faceting rough were recently mined in Georgia. The doubly terminated crystal shown here is 6.4 cm tall, and the Portuguese cut (faceted by Mike Watkins) weighs 19.95 ct. Courtesy of Mountain Gems & Minerals; photo © Jeff Scovil.

of Mountain Gems & Minerals, Little Switzerland, North Carolina, had some newly mined amethyst from Wilks County, Georgia. The mine is located between the communities of Rayle and Tignall, in an area known as Jackson's Crossroads, about 150 km east of Atlanta. Amethyst has been produced from surface workings in this area since the mid-1980s.

The current property owner, Rodney Moore, began mining in August 2004. After the initial work yielded some high-quality amethyst, Mr. Moore began working the subsurface deposits with a trackhoe, starting in late October. The following month, he formed a partnership with Mr. Ledford to market the rough and cut material. Their excavations have exposed a series of pockets to a depth of 6 m in the weathered granitic host rock. The largest pockets measured 60–80 cm long and 25–30 cm wide, and contained crystals of amethyst that were “floating” within clay. So far, more than 100 kg of amethyst crystal specimens and fragments have been produced, from which several stones were faceted. The largest stones cut so far weigh 19.95 (figure 3), 36.22, and 48.55 ct.

The cut material typically displays a deep purple color in incandescent light, and Mr. Ledford indicated that a

noticeable color shift (more blue) is seen in daylight. According to gem cutter Mike Watkins of Hiddenite, North Carolina, the orientation of the rough is critical to attaining the maximum color shift in the faceted material.

In early March 2005, Mr. Ledford indicated that further mining has resulted in additional amethyst production. The site is open to public mineral collecting on a fee-dig basis (see www.dixieuhedrals.net/jxr).

BML

Amethyst and citrine from northwestern Namibia. At the Arizona Pueblo Inn Gem & Mineral Show, Hannes Kleynhans (Kristall Galerie, Swakopmund, Namibia) showed this contributor some amethyst and citrine from the Sarusas mine in northwestern Namibia. Bill Barker (Barker & Co., Scottsdale, Arizona) also had Sarusas citrine at the AGTA show. Mr. Kleynhans, who is mining the deposit, has enlisted Mr. Barker to market both the amethyst and citrine cut stones in the future.

The deposit is located in the Namib Desert, within a remote area of Skeleton Coast Park. According to Mr. Kleynhans, quartz was mined there on a small scale from the late 1960s to the mid-1980s, and all the production went to Germany. In 2004, after completing a three-year permitting procedure to mine in this environmentally sensitive area, he started reworking the deposit with mechanized equipment. The requirements of the permit stipulate that no permanent structures or roads may be built in the area, and all pits must be reclaimed.

Figure 4. Mining for amethyst geodes at the Sarusas mine in northwestern Namibia employs pneumatic drills to make holes in hard areas of the basalt, which are then filled with an expansion compound to help fracture the rock. Courtesy of Kristall Galerie.



According to Mr. Kleynhans, the deposit hosts geodes of amethyst (and, rarely, pale citrine) in vugs within basalt. An excavator is used to dig shallow open pits, and the miners also drill in the more solid areas of the basalt (figure 4) and fill the holes with an expansion compound. After this compound is moistened with seawater, it expands and fractures the surrounding rock.

During the latter part of 2004, about 1,500 kg of rough was produced. So far, less than 1% of the rough has been facetable, with the cut stones weighing between 2 and 20 ct. The color of the amethyst ranges from light to dark purple, and the citrine is typically orangy yellow to deep orange (figure 5). The commercially available citrine is produced by heating the amethyst up to 600°C, with the deeper orange colors corresponding to a deeper purple color in the original amethyst.

BML

Aquamarine from Mt. Antero, Colorado. A recent discovery of spectacular aquamarine crystals from the historic Mt. Antero locality in Colorado was displayed for the first time at the Tucson Gem & Mineral Society show. The gem-quality aquamarines were associated with smoky quartz and feldspar, and the specimens were exhibited together with some faceted aquamarines from the same pocket.

Mt. Antero is located 27 km northwest of Salida in the Sawatch Range, Chaffee County, central Colorado; the area has fascinated mineral collectors for over a century (see, e.g., M. I. Jacobson, *Antero Aquamarines: Minerals from the Mt. Antero–White Mountain Region, Chaffee County, Colorado*, L. R. Ream Publishing, Coeur d'Alene, Idaho, 1993). According to Stephen Brancato, who discovered and mined the aquamarines in July 2004, they were found in a

Figure 5. Amethyst and citrine (here, approximately 4.5 ct each) from the Sarusas mine show a wide range in color. Courtesy of Barker and Co.; photo by Maha Tannous.

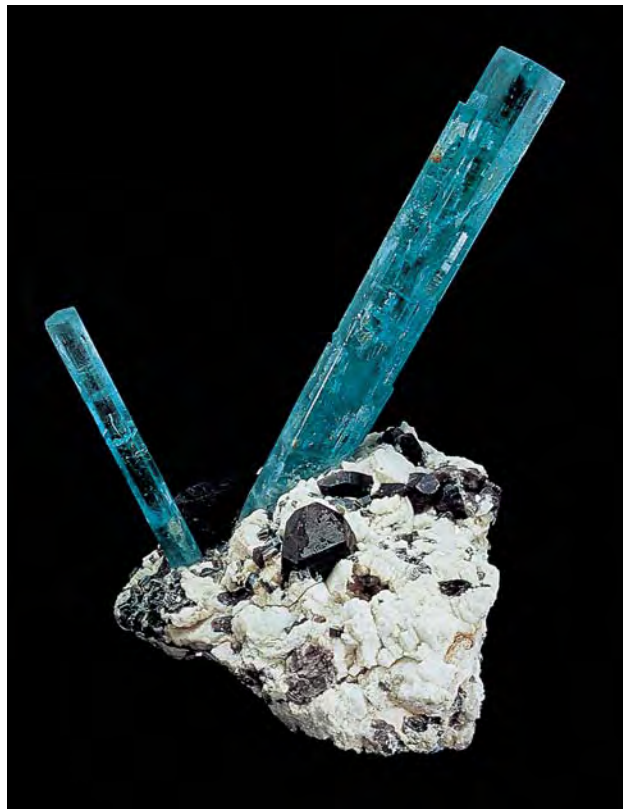


Figure 6. Reportedly the best matrix aquamarine crystals ever found in North America were recovered in July 2004 at Mt. Antero, Colorado. The larger aquamarine crystal in this repaired specimen measures 16.5 cm tall. Courtesy of The Collector's Edge; photo © Jeff Scovil.

miarolitic cavity (called "Diane's Pocket") on the Claire Mary Ellen #1 claim, at an elevation of about 12,500 feet (3,810 m). This discovery considerably overshadows previous finds at Mt. Antero, possibly yielding the finest matrix aquamarine crystals from North America.

So far, five stones (ranging from 2 to 4 ct) have been cut from aquamarine fragments in the pocket. According to Bryan Lees (The Collector's Edge, Golden, Colorado), there is sufficient gem rough to cut several dozen stones, possibly up to 20 ct. As such, this discovery could yield Colorado's largest faceted aquamarine; the weight of the current record holder is 18.95 ct (see J. A. Murphy and P. J. Modreski, "A tour of Colorado gemstone localities," *Rocks & Minerals*, Vol. 77, No. 4, 2002, pp. 218–238). The faceted aquamarines are being marketed by Paul Cory (Iteco Inc., Powell, Ohio), while the mineral specimens are sold through Mr. Lees. About six high-quality matrix aquamarines were produced, with the longest crystal measuring 16.5 cm (figure 6). All of the specimens required simple repairs to reattach crystals that had been broken from the matrix by natural forces. In addition to these specimens, the pocket yielded dozens of well-formed loose aquamarine crystals.

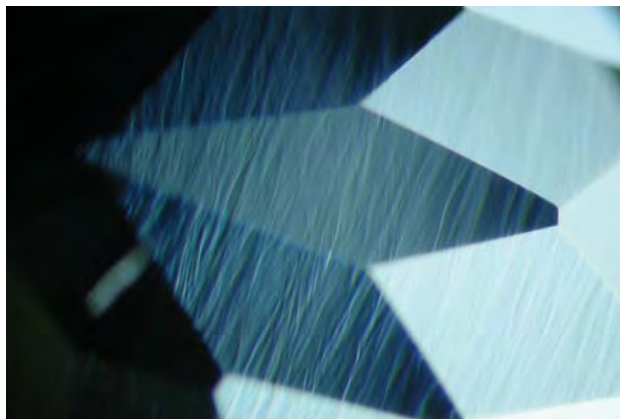
BML



Figure 7. This aquamarine from Nigeria (0.40–2.91 ct) shows a saturated blue color. Courtesy of Fine Gems International; photo © Harold and Erica Van Pelt.

Saturated blue aquamarine from Nigeria. At the AGTA show, Robert Kane (Fine Gems International, Helena, Montana) had some aquamarine from northern Nigeria that was notable for its saturated blue color. According to Mr. Kane, the intensely colored rough was purchased as natural-color aquamarine, and the material was not subsequently subjected to any treatment. The stones were cut from a 103 gram parcel of rough, with pieces weighing

Figure 8. An unusual wavy growth zoning was seen in the Nigerian aquamarine. Photo by Maha Tannous; magnified 40×.



0.5–3 grams. A total of 107 carats were faceted, ranging from approximately 0.25 to 3 ct (see, e.g., figure 7).

In January 2005, Mr. Kane loaned 17 of the better-quality faceted samples to GIA for examination. A 2.91 ct emerald cut was examined in detail for a GIA Gem Laboratory identification report, and the following properties were recorded: color—blue; pleochroism—strong, dark blue and light blue-green (visible even to the unaided eye when viewed face-up); R.I.—1.582–1.589; birefringence—0.007; S.G.—2.76; and fluorescence—inert to long- and short-wave UV radiation. The desk-model spectroscope showed a standard aquamarine absorption spectrum (caused by iron) that ruled out a Maxixe-type color origin. Magnification revealed growth tubes, pinpoints, white mineral inclusions (identified as a carbonate by Raman analysis), and an unusual growth zoning (figure 8) with wavy and planar features that were reminiscent of some hydrothermal synthetic beryls. EDXRF spectroscopy revealed major amounts of Al and Si, and traces of K, Sc, Mn, Fe, Zn, Ga, Rb, and Cs. This chemical composition, as well as the inclusion characteristics, proved a natural origin for this aquamarine.

The R.I., birefringence, and S.G. values are in the high end of the range reported for aquamarine (see, e.g., R. Webster, *Gems*, 5th ed., revised by P. G. Read, Butterworth-Heinemann, Oxford, England, 1994, pp. 124–125). While these properties (and the color) are consistent with beryl containing small amounts of iron, they are substantially lower than those documented recently in dark blue beryl from Canada that contained high amounts of iron (see Winter 2003 Gem News International, pp. 327–329).

BML

Carved chalcedony chain. At the Arizona Pueblo Inn Gem & Mineral Show, Steve Ulatowski (New Era Gems, Grass Valley, California) showed this contributor a chain that had been carved in China from a single piece of Brazilian chalcedony (figure 9). According to Mr. Ulatowski, only two such chains (22 and 43 cm long) were successfully carved in early 2002, from about a dozen attempts by the carvers. Although this style of carving also is seen in jadeite, the brittle nature of chalcedony makes the chains particularly challenging to execute. In addition, relatively large pieces of unfractured material were needed to carve the chalcedony chains.

BML

New emerald deposit in Xinjiang, China. At the AGTA show, one of us (DB) had a few rough and cut samples of emerald from a new deposit in China. From recent conversations with miners and mineral dealers in northern Pakistan who have visited the deposit or purchased rough near it, this contributor learned that it is located in the Taxkorgan region in western Xinjiang Province, near the village of Dabdar, which is approximately 120 km (or a two-hour drive) from the Khunjerab Pass. At 15,800 feet (4,816 m), this pass lies on the border between northern



Figure 9. This delicate chain (88.68 ct) was carved from a single piece of chalcedony in China. The chain is 43 cm long, and the thickness of the chalcedony in each link is approximately 2 mm. Courtesy of New Era Gems; photo by Don Mengason.

Pakistan and China. Visiting the emerald area is reportedly not straightforward, requiring a special travel permit from a government office in Kashgar (6–8 hours by road from the Khunjerab Pass). After backtracking to the mine area, Dabdar village is then about 2.5–3 km from the main Kashgar road.

This contributor first learned of the Chinese emerald discovery while in northern Pakistan in November 2003, but he saw only poor-quality rough at that time. He obtained additional samples during a return visit to Pakistan in June 2004, including a matrix specimen containing a small bright green emerald crystal, as well as a few cut emeralds; three of these were subsequently examined at GIA for this report (see below). He also was offered attractive faceted examples, each about 2 ct, by a Pakistani dealer who had knowledge of a very few cut stones up to ~5 ct. News about the deposit became more widespread in Pakistan by October–November of last year, when the specimen in figure 10 was purchased from a dealer who had also taken photographs of the mine; these revealed a large pit made with bulldozers and other earth-moving equipment. According to this dealer, the price of rough material at the mine had escalated considerably.

Examination of the three faceted emeralds (0.29–0.46 ct; again, see figure 10) by one of us (EPQ) showed the following properties: color—bluish green, with moderate dichroism in yellowish green and bluish green; diaphaneity—transparent; R.I.— $n_o=1.588$ – 1.589 and $n_c=1.580$ – 1.581 ; birefringence 0.007–0.008; S.G.—2.69–2.74; Chelsea filter reaction—weak red; and fluorescence—inert to both long- and short-wave UV radiation. Absorption lines in the red end of the spectrum (due to chromium)

were visible with the desk-model spectroscope. Microscopic examination revealed “fingerprints,” fractures, two- and three-phase inclusions (some of which were jagged in appearance resembling those in Colombian emeralds), and fine growth lines parallel to the c-axis (observed perpendicular to the optic axis) that had an almost “Venetian blind” appearance. Testing with a thermal reaction tester caused some of the fractures to “sweat,” and air bubbles in certain fractures were seen to contract, indicating the presence of a filling substance. One of the stones contained low-relief crystals that were identified by Raman analysis as plagioclase.

EDXRF chemical analysis of all three samples by one of us (SM) revealed the expected Al and Si as major components, and K, Sc, V, Cr, Fe, and Ga as trace elements. The UV-Vis spectra showed typical emerald absorption features. Although Fe was detected by EDXRF, the absorption spectra indicated that this element did not have a significant influence on their color, which was due to Cr.

Dudley Blauwet
Dudley Blauwet Gems
Louisville, Colorado

Elizabeth P. Quinn and Sam Muhlmeister
GIA Gem Laboratory, Carlsbad

Figure 10. These rough and cut emeralds are from a new deposit in western Xinjiang Province, China. The crystal is 1.3 cm long, and the faceted emeralds weigh 0.29–0.46 ct. Courtesy of Dudley Blauwet Gems; photo © Jeff Scovil.





Figure 11. Renewed mining of a historic lode deposit in Mariposa County, California, is producing gold-in-quartz for jewelry uses, as well as polished art objects and specimens. The sphere measures 3.8 cm in diameter. Courtesy of Mineral Search Inc.; photo © Jeff Scovil.

Gold-in-quartz from Mariposa County, California. At the Clarion Hotel, Doug Wallace (Mineral Search Inc., Dallas, Texas) had specimens, art objects, cabochons, and finished jewelry featuring gold-in-quartz from a historic lode deposit in Mariposa County, central California (figure 11). The material was mined by his partner, Bill Forrest (Fresno, California), from the former Badger and No. 5 mines, located near the town of Hornitos. In 2004, they purchased the property—consisting of nine claims on 150 acres—from Ed Coogan (Turlock, California), who had used metal detectors to work the surface deposits intermittently since the late 1980s. According to Mr. Wallace, the Badger mine was first worked in the 1850s, when it reportedly produced \$80,000 worth of gold from trenches and shallow tunnels. During this time, the miners collected only pieces showing visible gold on the surface. As a result, reworking of the Badger dump material has yielded abundant gold, through the use of metal detectors or by simply breaking open pieces of quartz. Substantial amounts also were produced from the No. 5 mine, beginning in 1910. The original miners processed all of the vein material they recovered for gold, so the tailings do not contain any high-grade ore. Nevertheless, there is a considerable amount of loose vein material within soil downslope of the No. 5 deposit. Both mines are located on a lode

known as the Prescott vein. This quartz vein system, which ranges up to nearly 10 m wide, forms prominent traceable outcrops in the mining area.

According to Mr. Wallace, most of the material they have recovered comes from the Badger mine, and is therefore marketed as Badger Gold. Mr. Forrest works the area using a backhoe, to a depth of 6 m, by excavating portions of the vein that were not mined by the historic operations. In addition, he has achieved considerable production from the dump material by digging down more than 50 cm, which is the detection limit of the metal detectors used previously on the property. Mr. Wallace indicated that they have recovered an average of 25 pounds (12 kg) of gold-bearing quartz each month, starting in July 2004. The production is first soaked in oxalic acid to remove iron staining, and then classified as specimen-grade material or pieces that are suitable for polishing. The specimens are characterized by relatively large clots of gold that are mechanically exposed (rather than etching the quartz using hydrofluoric acid). The polish-grade material is formed into spheres, eggs, and cabochons (ranging up to 25 mm) that are mounted into fine jewelry (again, see figure 11).

In addition to this new production from Mariposa County, other commercial sources of jewelry-quality gold-in-quartz also were available in Tucson. These included material from Australia that was sold through Kabana Inc., Albuquerque, New Mexico (GJX show), and Gold Nugget Exports Australia, Gold Square, Victoria (Arizona Mineral

Figure 12. Iolite from the Santa Barbara mine, Rio Grande do Norte, Brazil, is mined from shallow open pits and trenches. Courtesy of Paraíba Inc.





Figure 13. The iolite is associated with quartz; the dark brown areas are the host rock adjacent to the quartz veins. Courtesy of Paraiba Inc.

& Fossil Show, InnSuites Hotel). The latter dealer also was marketing jewelry-quality rough material that was recovered from the highly productive Sixteen to One mine in Sierra County, California, by Orocal Natural Gold (Oroville, California). Also of note in Tucson was a new manufactured gold-in-quartz product (see report on p. 63).

BML

Iolite from northeastern Brazil. During the AGTA show, David Sherman (Paraiba Inc., Reno, Nevada) showed GNI editor Brendan Laurs some newly mined iolite from Rio Grande do Norte State. The stones were produced shortly before the 2005 Tucson gem show, from a locality near Parelhas that is now called the Santa Barbara mine (figure 12). According to Mr. Sherman, the deposit was originally discovered about 15 years ago, when about 1,000 kg of rough iolite of various grades was produced. The area was later reworked for a brief period 4–5 years ago, yielding 3–4 kg of material per month.

Mr. Sherman stated that the iolite forms in pods within narrow quartz veins (figure 13). Since January 2005, mining by his partner, Horst Munch (T.O.E. Mineração Ltda., Parelhas), has uncovered small iolite pods approximately every half meter from shallow open pits. A crew of 3–4 miners uses a portable compressor and pneumatic drill to make holes (about 2 m deep) that are loaded with dynamite. After blasting, wheelbarrows and hand tools are used to process the blasted material and recover the iolite. Production has averaged about 10 kg/month of rough that will cut clean stones up to 5 ct. Typically they are somewhat smaller (figure 14), because much of the rough is fractured.

BML

Kyanite widely available. At the G&LW Holiday Inn/Holidome show, numerous dealers were offering kyanite beads. The beads ranged from transparent deep blue rondelles and briolettes to unpolished translucent blue and grayish green elongated blades. The majority of the strands consisted of polished semitransparent to



Figure 14. These iolites (0.98–1.60 ct) were cut from recent Santa Barbara mine material. Courtesy of Paraiba Inc.; photo by Maha Tannous.

translucent beads, in various shapes and sizes, that were color-zoned in lighter and darker blues (figure 15). The dealers reported that the kyanite originated from Brazil, Tanzania, or Sri Lanka.

Although not new, mineral specimens of kyanite from Brazil were available in abundance through several dealers at the various satellite shows. Fine decorator pieces consisted of clusters of kyanite blades (with small amounts of interstitial matrix) that ranged up to about 20 cm long. Such specimens were seen at the Inn Suites and Clarion hotels, with Vasconcelos Ltda. and Geometa Ltda. (both of Governador Valadares, Minas Gerais, Brazil). According to Carlos Vasconcelos, the kyanite is mined from 3–4 small deposits in Minas Gerais; the largest kyanite blade seen by him measured 50 cm long. The most common colors are bluish gray to blue to deep blue. Although some gem-quality material is mined, it is quite difficult to cut.

Nevertheless, large quantities of faceted kyanite were available from Nepal. At the AGTA show, Anil Dholakia (Anil B. Dholakia Inc., Franklin, North Carolina) had approximately 20,000 carats of moderate-to-dark blue

Figure 15. This strand of color-zoned beads (each approximately 11.0 × 7.5 mm) consists of polished kyanite that is reportedly from Brazil. Photo by Maha Tannous.



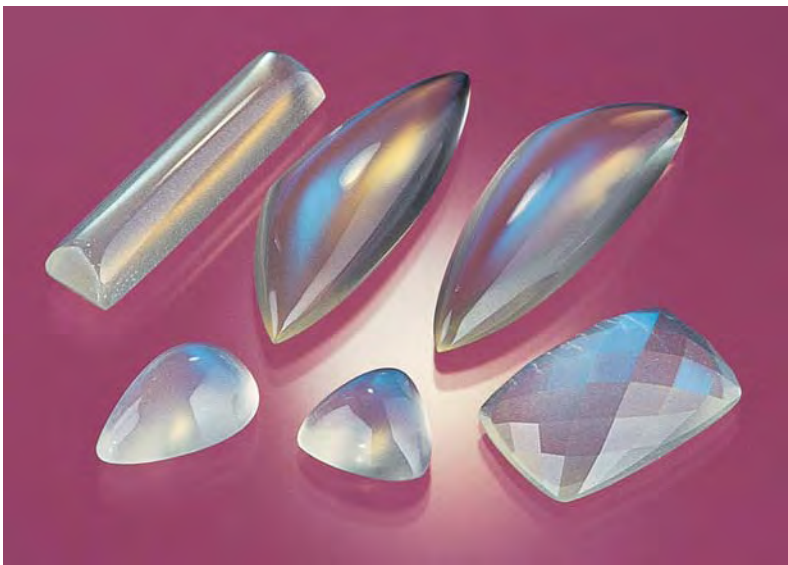


Figure 16. These albitic “moonstones” from Tanzania (5.44 to 19.88 ct) display strong blue adularescence. Courtesy of Pearl Gem Co.; photo by Maha Tannous.

transparent Nepalese kyanite in calibrated sizes ranging from 6×4 mm to 10×8 mm. Some of the stones were already mounted in bracelets and earrings. While transparent kyanite from Nepal has been known for several years (see Spring 1999 Gem News, pp. 51–52 and Spring 2002 Gem News International, pp. 96–97), the abundance of attractive calibrated material is expected to make this little-known gemstone more popular in finished jewelry.

BML and Elizabeth P. Quinn

Albitic “moonstone” from the Morogoro region, Tanzania.

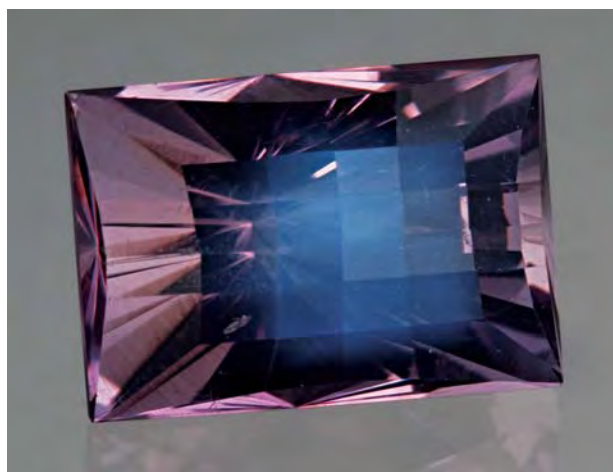
Among the many interesting items seen at the 2005 Tucson gem show was some Tanzanian “moonstone” that showed relatively high clarity and strong blue adularescence. This material was first brought to our attention in August 2004 by Hussain Rezayee (Pearl Gem Co., Beverly Hills, California), who indicated that the mining area is located near the town of Kilosa, about 80 km west of Morogoro in east-central Tanzania. The deposits have been known for almost 15 years, but until fairly recently they only produced low-grade material. Since mid-2003, further mining (by hand methods) has yielded some high-quality rough in relatively large sizes. He estimated that a few hundred kilograms have been produced, with about 10% being cuttable.

Mr. Rezayee loaned six samples to GIA for examination, consisting of five cabochons and one cushion mixed cut, ranging from 5.44 to 19.88 ct (figure 16). Gemological testing of three stones by one of us (EPQ) yielded the following properties: color—very light gray to very light yellow, with strong blue adularescence; diaphaneity—transparent to semitransparent; R.I.—1.530–1.540 from the faceted stone (birefringence 0.010), and 1.54 spot readings on the two cabochons tested; S.G.—2.64; Chelsea filter reaction—none; fluores-

cence—inert to long-wave UV radiation and a weak red reaction to short-wave; and no absorption lines were visible with the desk-model spectroscope. Microscopic examination revealed that all three samples contained numerous needles and platelets as well as cleavage fractures. Polysynthetic twinning was visible between crossed polarizers when the samples were viewed along their edge (i.e., perpendicular to the direction that showed adularescence).

The term *moonstone* is most commonly used to designate orthoclase feldspar that shows adularescence. However, the R.I., birefringence, and S.G. values of the Tanzanian samples were significantly higher than those reported for gem orthoclase (1.520–1.525, 0.005, and 2.56–2.59, respectively; see R. Webster, *Gems*, 5th ed., revised by P. G. Read, Butterworth-Heinemann, Oxford, England, 1994, p. 208). Rather, the Tanzanian feldspar has properties that are consistent with albitic feldspar (see W. A. Deer et al., *Rock-forming Minerals, Vol. 4A—Framework Silicates: Feldspars*, 2nd ed., The Geological Society, London, 2001, pp. 626–908). A comparison of the R.I. and S.G. values to the charts provided by Deer et al. also shows the Na-rich nature of the plagioclase. This agrees with the composition of the six samples that was determined by one of us (SM) using EDXRF spectroscopy. One set of analytical parameters was used to detect major elements and light trace elements in all samples. In addition, one sample was run under two additional conditions to detect heavier elements. All the samples contained major amounts of Al, Si, and Na, and traces of Ca and K. In addition, Fe was detected in five of the samples, and Sr and Ba were also detected in the one sample run under multiple conditions.

Figure 17. The adularescence shown by this 1.83 ct pink doublet is created by a cap of transparent Tanzanian “moonstone” that was affixed to a light-colored amethyst base. Courtesy of New Era Gems; photo by Maha Tannous.



Albitic plagioclase with the appearance of moonstone is most commonly known from Ontario and Quebec, Canada (Webster, 1994). This feldspar consists of albite-oligoclase (with an anorthite content of An_1 - An_{17} , called *peristerite*) that have unmixed into submicroscopic lamellae. When these lamellae are on the scale of the wavelength of visible light, an iridescent optical phenomenon is seen when the feldspar is viewed in a direction that is perpendicular to the lamellar planes. Although this mechanism is probably responsible for the adularescence in the Tanzanian plagioclase, further work would be necessary to confirm this.

Because the orientation is critical for displaying adularescence, and the rough is commonly fractured in the same direction as the lamellae, large polished stones are rare. Nevertheless, according to Dimitris Mantheakis (Ruvu Gemstone Mining Ltd., Dar es Salaam, Tanzania), cut Tanzanian “moonstones” can attain weights up to 300 ct.

The transparency shown by some of the Tanzanian material may lend it to some rather unconventional uses, as illustrated by the doublet in figure 17, which was shown to one of us (BML) at the Arizona Pueblo Inn Gem & Mineral Show by Steve Ulatowski of New Era Gems. The feldspar top was placed over a light-colored amethyst base to give the appearance of a pink gem showing adularescence.

Elizabeth P. Quinn, Sam Muhlmeister, and BML

A faceted pezzottaite from Afghanistan. So far, gem-quality pezzottaite is known from only one mine in Madagascar, which appears to be exhausted (B. M. Laurs et al., “Pezzottaite from Ambatovita, Madagascar: A new gem mineral,” *Winter 2003 Gems & Gemology*, pp. 284–301). In 2004, one of us (BML) received some samples that were represented as pezzottaite from Afghanistan, which is the second-known source of this rare mineral (see H. A. Hänni and M. S. Krzemnicki, “Caesium-rich morganite from Afghanistan and Madagascar,” *Journal of Gemmology*, Vol. 28, No. 7, 2003, pp. 417–429). The specific locality was reported to Hänni and Krzemnicki as the Deva mine, Paroon Valley, in Nuristan, Afghanistan. The Afghan samples were supplied by E. “Buzz” Gray (Missoula, Montana), Herb Obodda (H. Obodda, Short Hills, New Jersey), and Haleem Khan (Hindukush Malala Gems & Minerals, Peshawar, Pakistan). Since we did not know of any prior reports of faceted pezzottaite from Afghanistan, we were surprised to see that one of the samples we received from Mr. Gray in May 2004 was a 1.11 ct cut stone (figure 18).

Mr. Gray obtained the gem rough in late 2002 from a Pakistani dealer who represented them as being from Afghanistan. He faceted five stones that ranged from 1 to 6 ct; all were heavily included. Gemological properties were obtained by one of us (EPQ) on the 1.11 ct octagonal modified brilliant, which was subsequently donated to GIA by Mr. Gray. The R.I, birefringence, and S.G. values are shown in table 1, and other properties were as follows: color—purple-pink (with no color zoning), showing moderate dichroism in pink-orange and pink-purple; diaphane-



Figure 18. This 1.11 ct pezzottaite is reportedly from Afghanistan. GIA Collection no. 31418; photo by Maha Tannous.

ity—transparent to semitransparent; fluorescence—a very weak violet to long-wave UV, and a weak banded white to short-wave. With a desk-model spectroscope, the stone showed a band at 500 nm and a weaker band at 570 nm. Microscopic examination revealed a network of feathers and smaller internal fractures throughout the stone, giving it an almost “quench crackled” appearance; stringers of particles; and both angular and straight growth lines. Evidence of clarity enhancement was seen when the stone was exposed to a thermal reaction tester.

Chemical analyses of this 1.11 ct stone by electron microprobe (seven spot analyses) confirmed its identity as pezzottaite, with 10.18 to 12.56 wt.% Cs_2O (table 1). This is somewhat more cesium than was documented by Hänni and Krzemnicki in the sample of Afghan pezzottaite they analyzed (up to 10.05 wt.%); in addition, our analyses showed less Si and slightly more Al (again, see table 1). Compared to pezzottaite from Madagascar (11.23–18.23 wt.% Cs_2O , as reported by Laurs et al.), the Cs content of the Afghan pezzottaite was typically lower. The Afghan samples also showed slightly more Na, and less Rb, than the Madagascar material.

The R.I. and birefringence of the 1.11 ct stone are very close to those reported for the Afghan pezzottaite studied by Hänni and Krzemnicki (again, see table 1). However, the S.G. reported by those authors is significantly lower than the value we obtained. As documented by Hänni and Krzemnicki, the faceted Afghan pezzottaite we examined had a slightly lighter pink color, and significantly lower R.I. and S.G. values, than pezzottaite from Madagascar.

Interestingly, electron-microprobe analysis of another Afghan pezzottaite sample (from Mr. Obodda) yielded a broad range of cesium contents. A traverse across a 27×11 mm slab that was cut from a crystal specimen yielded

TABLE 1. Physical and chemical properties of a 1.11 ct faceted pezzottaite from Afghanistan, as compared to published values for another Afghan pezzottaite and samples from Madagascar.

Property	Afghanistan		Afghanistan	Madagascar
	Reference	This study	Hänni and Kzernicki (2003)	Laurs et al. (2003)
R.I.				
n_o		1.605	1.606	1.615–1.619
n_e		1.598	1.598	1.607–1.610
Birefringence		0.007	0.008	0.008–0.009
S.G.		2.97	2.91	3.09–3.14
Chemical composition ^a	Lowest Cs	Highest Cs	Representative analysis of one sample	Average of 49 analyses of 11 samples
Oxide (wt.%)				
SiO ₂	56.75	56.51	61.32	56.77
Al ₂ O ₃	16.79	16.52	15.72	15.99
Sc ₂ O ₃	0.01	0.00	nd	0.03
BeO (calc)	8.97	8.71	8.13	8.14
MnO	0.03	0.08	0.02	0.11
CaO	nd	nd	0.98	nd
Li ₂ O	1.76	1.88	1.35 ^b	2.16 ^c
Na ₂ O	1.33	1.01	1.15	0.41
K ₂ O	0.06	0.07	0.03	0.11
Rb ₂ O	0.14	0.25	0.14	0.85
Cs ₂ O	10.18	12.56	9.70	13.55
Total	96.04	97.61	98.54 ^d	98.12
Ions per 18 oxygens, anhydrous basis				
Si	5.943	5.956	6.000	6.030
Al	0.057	0.044	0.000	0.000
Sum tet.	6.000	6.000	6.000	6.030
Be	2.258	2.204	1.190	2.077
Li	0.741	0.796	0.532	0.923
Sum Be+Li	2.999	3.000	1.722	3.000
Al	2.015	2.008	1.813	2.000
Sc	0.001	0.000	nd	0.002
Ca	nd	nd	0.103	nd
Mn	0.003	0.007	0.001	0.010
Sum oct.	2.021	2.018	1.917	2.012
Na	0.270	0.206	0.218	0.085
K	0.008	0.009	0.004	0.015
Rb	0.010	0.017	0.009	0.058
Cs	0.455	0.564	0.405	0.617
Sum channel	0.743	0.796	0.636	0.775

^a All analyses by electron microprobe, unless otherwise noted. The low analytical totals are likely due to water being omitted from the analyses. For the Afghan pezzottaite analyzed for this study, Li was calculated to allow for charge balance, by setting it equal to the sum of the alkalis in the channel sites (Na+K+Rb+Cs). Be was calculated as 3-Li. The following elements were below the detection limit (shown in wt.%): MgO (0.01), TiO₂ (0.002), FeO (0.02), CaO (0.07). In addition, the following were checked for (scanned), but not detected: Cr₂O₃ (0.03), Bi₂O₃ (0.03), V₂O₅ (0.03), PbO (0.01), ZnO (0.08), BaO (0.03), Cl (0.04), F (0.05). Abbreviation: nd = not detected.

^b Li was calculated.

^c Li was assumed, based on an ICP (inductively coupled plasma) analysis of another sample of Madagascar pezzottaite (see Laurs et al., 2003).

^d Includes 0.02 wt.% iron, reported as Fe₂O₃.

3.58–12.95 wt.% Cs₂O. This indicates the presence of both cesian beryl and pezzottaite in the same sample, and demonstrates the need to perform advanced testing (ideally quantitative chemical analysis and crystal structure refinement to confirm rhombohedral structure) to confi-

dently identify pezzottaite in such material.

BML and Elizabeth P. Quinn

William B. (Skip) Simmons and Alexander U. Falster
University of New Orleans, Louisiana

Tanzanite marketing initiatives. TanzaniteOne (Johannesburg, South Africa), the world's largest producer of tanzanite, has instituted a De Beers-like sales and marketing system to create market stability, build demand, and address consumer confidence issues. At a February 3 news conference in Tucson, Michael Nunn, CEO of TanzaniteOne, explained that the company would channel its rough sales through six primary sightholders. These firms would receive six sights yearly, with a three-year guarantee of supply. The firms chosen as sightholders will have to meet several criteria, including a tanzanite-focused business, excellent distribution in primary consumer markets, financial strength, and a long-term marketing strategy.

According to Mr. Nunn, TanzaniteOne supplies just under 50% of all tanzanite on the market. It acquired the tanzanite assets of AFGEM in December 2003, and plans to institutionalize AFGEM's grading system for polished stones. The system divides tanzanite into two color categories: blue-violet and violet-blue, with grades ranging from pale to "vivid exceptional." The clarity grades range from internally flawless to heavily included. Mr. Nunn said that lack of a standard grading system has led to a situation where there is a skewed price differentiation between highest and lowest qualities, with the upper end being underpriced by half, and the lower being considerably overpriced.

The company has also helped foster the Tanzanite Foundation, an organization that issues certificates of origin, which provide assurance that all tanzanite mined and sold by participating companies is done so responsibly and ethically. The foundation is also developing marketing programs to support tanzanite sales in major consumer markets. TanzaniteOne has contributed \$3 million to the foundation thus far. The sightholders, and other miners belonging to the foundation, will contribute 10% of their revenues toward marketing; the goal is to raise \$5-6 million a year. The foundation also intends to provide assistance to other operators through its Small Mine Assistance Program, and channel development funds back to local communities near the mining area.

*Russell Shor (rshor@gia.edu)
GIA, Carlsbad*

SYNTHETICS AND SIMULANTS

Manufactured gold/silver-in-quartz. At the Tucson Electric Park Gem & Mineral show, James Taylor (Eureka Gems LLC, Fountain Hills, Arizona) had some slabs and cabochons of quartz containing "veins" of gold or silver that were manufactured by a new process in a partnership with Onnik Arakelian, Todd Allen, and Gnel Gevorkyan. Several varieties were available, using gold alloys in 14K or 20K, as well as fine silver. According to Mr. Taylor, smoky quartz from Brazil is used to make "Grizzly Gold" and "Grizzly Silver," whereas rock crystal from Arizona, or milky quartz from Nova Scotia, is employed in the



Figure 19. A new process is being used to introduce gold and silver into smoky, milky, and colorless quartz for jewelry use. The elongate piece on the bottom measures 52 x 30 mm. Courtesy of Eureka Gems LLC; photo © Jeff Scovil.

"Glacier Gold" and "Silver Lightning" lines (figure 19). The materials is sold in slabs that are at least 2.5mm thick, and as finished cabochons. Opticon is used to stabilize the thin slabs and cabochons.

At the time of the Tucson show, 15 kg of each variety was being produced each month. At press time, Mr. Taylor anticipated that the production would increase to 50 kg/month by April-May 2005. The material is produced in Mesa, Arizona, using a proprietary, patent-pending process developed by Mr. Gevorkyan. He reported that the gold or silver is mobilized into fractures within the host quartz under heat and pressure; if necessary, the quartz is fractured before the metal is introduced. Mr. Taylor also had some display samples of Australian black jade containing gold that were manufactured by the same process. He expects this product to become commercially available in time for the 2006 Tucson gem shows. In addition to the gold and silver alloys mentioned above, he indicated that white gold and a platinum alloy (with silver) could be used in the process.

The manufactured products can usually be separated from natural gold-in-quartz by the typical fracture-aligned or spiderweb-like texture of the gold, which is distinct from the blebs and irregular pods of gold that occur in natural quartz (see GNI entry on p. 58). However, Mr. Taylor indicated that some of the manufactured gold-in-quartz looks so natural that it cannot be

separated by visual means. In that case, chemical analysis of the metal alloy could be used to identify it. Distinguishing the manufactured silver-in-quartz from natural material (which is quite rare in jewelry quality) is straightforward, due to the distinctive texture and the use of fine silver in this product.

BML

GNI Regular Features

DIAMONDS

10.53 ct gem-quality diamond from Saskatchewan, Canada. Kensington Resources Ltd., of Victoria, British Columbia, reported that it recently recovered a 10.53 ct gem-quality diamond crystal (figure 20) from a core sample of kimberlite at its Fort à la Corne Diamond Project in central Saskatchewan (see B. A. Kjarsgaard and A. A. Levinson, "Diamonds in Canada," Fall 2002 *Gems & Gemology*, pp. 208–238, for more information about diamond exploration in this area). The diamond was one of several recovered from core samples drilled in 2004. These diamonds (which also included a 1.32 ct crystal) were sampled from a depth interval of 118–130 m. A 140.34 tonne core sample from another drill hole yielded 135 macrodiamonds (generally defined as larger than 0.5–1.0 mm) weighing a total of 15.45 carats; the largest diamond was 0.46 ct, and 16 others weighed more than 0.25 ct. A 10.23 ct diamond was recovered from this property in 2002.

Figure 20. This 10.53 ct diamond was recently recovered from a drill core at the Fort à la Corne Diamond Project in Saskatchewan, Canada. Courtesy of Kensington Resources.



The Fort à la Corne Diamond Project is a joint venture between Kensington, De Beers Canada Inc., Cameco Corp., and UEM Inc.

Russell Shor

INCLUSIONS IN GEMS

Spiral in aquamarine. Dudley Blauwet of Dudley Blauwet Gems in Louisville, Colorado, provided us with an interesting Pakistani aquamarine crystal from Nyet, Braldu Valley, Baltistan. As shown in figure 21, the transparent, singly terminated gem-quality crystal weighed 117.64 ct and measured $53.4 \times 19.3 \times 11.3$ mm. The most intriguing feature of this aquamarine was an eye-visible decorated dislocation pattern in the form of a centrally located growth spiral extending the entire length of the crystal.

With low magnification, when viewed through the side in any one of several different directions perpendicular to the length, the spiral pattern looked very much like a feather or a partial fish skeleton (figure 22). The crystal's overall clarity made a dramatic showcase for the intricate growth spiral. This feature is actually a visual form of growth disturbance propagated through the host crystal along a screw dislocation that develops from a source such as a small solid inclusion or structural defect, often at or near the base of a crystal during the earliest stages of growth. Growth spirals also have been observed in other beryls, such as natural and synthetic emerald (see *Photoatlas of Inclusions in Gemstones*, pp. 82 and 473).

John I. Koivula (JohnKoivula@hotmail.com)

AGTA Gemological Testing Center
New York and Carlsbad, California

Maha Tannous
GIA Gem Laboratory, Carlsbad

"Bamboo" moonstone. An 81.59 ct freeform orthoclase feldspar from Mogok, Myanmar, was provided to these contributors for examination by Mark Smith of Thai Lanka Trading Ltd., Bangkok, because of its obvious eye-visible inclusions. The identification as orthoclase was confirmed through standard gemological testing. As shown in figure 23, this $38.2 \times 27.3 \times 12.3$ mm polished feldspar not only showed adularescence, as would a moonstone, but also contained



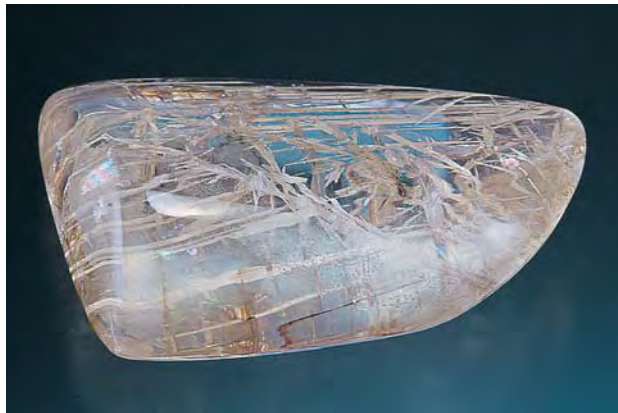
Figure 21. Weighing 117.64 ct and measuring 53.4 mm long, this aquamarine crystal from Pakistan hosts a striking eye-visible spiral dislocation pattern. Courtesy of Dudley Blauwet; photo by Maha Tannous.



Figure 22. When viewed through the side of the aquamarine crystal, the spiral pattern is reminiscent of a feather or fish skeleton. Photomicrograph by John I. Koivula; magnified 10x.

several etch tubes of varying thickness that appeared to be oriented along twin planes. The light brown color of these tubes appeared to be due to an epigenetic filling material.

Figure 23. This 81.59 ct orthoclase feldspar (moonstone) from Mogok, Myanmar, contains obvious etch tubes filled with a light brown material. Courtesy of Mark Smith; photo by Maha Tannous.



Some of these rough-edged, "dirt-filled" tubes were in near-parallel formation, and with low magnification they resembled stalks of dried bamboo (figure 24). The "nodes" apparent on these "stalks" were created by intersecting cleavage cracks. Interestingly, the epigenetic fillings in some of the tubes fluoresced moderate yellow to long-wave UV radiation. This is the first moonstone with such inclusions that we have seen.

John I. Koivula and Maha Tannous

Pezzottaite in quartz. Pezzottaite, a Cs,Li-rich member of the beryl group that is known from Madagascar and Afghanistan, has been described in detail in recent articles (see, e.g., F. C. Hawthorne et al., "Pezzottaite, Cs(Be₂Li)Al₂Si₆O₁₈, a spectacular new beryl-group mineral from the Sakavalana pegmatite, Fianarantsoa Province,

Figure 24. Where they are aligned in near-parallel formation, the etch tubes in the moonstone resemble stalks of dried bamboo. Photomicrograph by John I. Koivula; magnified 5x.

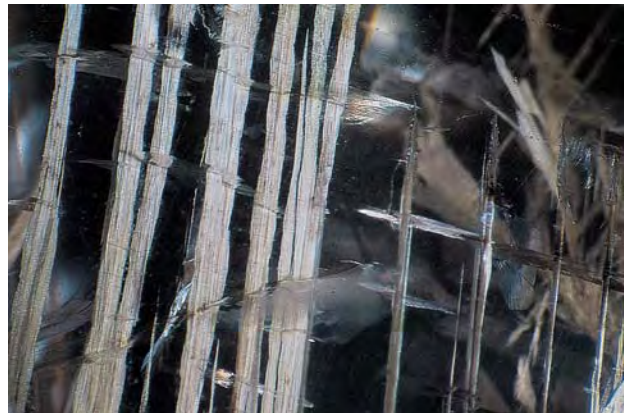




Figure 25. The 5.0-mm-long color-zoned pezzottaite in this 4.39 ct rock crystal from the Sakavalana pegmatite in Madagascar is the first pezzottaite reported as an inclusion. Photo by Maha Tannous.

Madagascar, *Mineralogical Record*, Vol. 35, No. 5, 2004, pp. 369–378, and references cited in the Afghanistan pezzottaite entry on p. 61). Although these articles discuss pegmatite minerals (e.g., quartz and tourmaline) found in association with pezzottaite, as well as inclusions with pezzottaite as the host, pezzottaite has not yet been reported as an inclusion in another mineral.

During a visit to the Sakavalana pegmatite in July 2003, *Gems & Gemology* editor Brendan Laurs acquired several representative specimens from the deposit. One sample was a broken piece of rock crystal that appeared to contain a pinkish inclusion. The quartz was given to Leon M. Agee of Agee Lapidary, Deer Park, Washington, who faceted a 4.39 ct cushion-shaped step cut (figure 25) that revealed an approximately 5.0-mm-long light pink six-sided doubly terminated crystal that was thought to be pezzottaite.

Microscopic examination showed that the inclusion was color zoned down its length. Stronger pink was obvious at both ends, and the pink zone tapered inward from both ends toward the center like an hourglass. The quartz host had several cracks near and around the inclusion, and numerous tiny primary fluid inclusions also were present. Polarized light revealed the birefringent nature of the inclusion and the fact that it had a weak pleochroism from pink to orange pink. The pink color was most obvious down the inclusion's length.

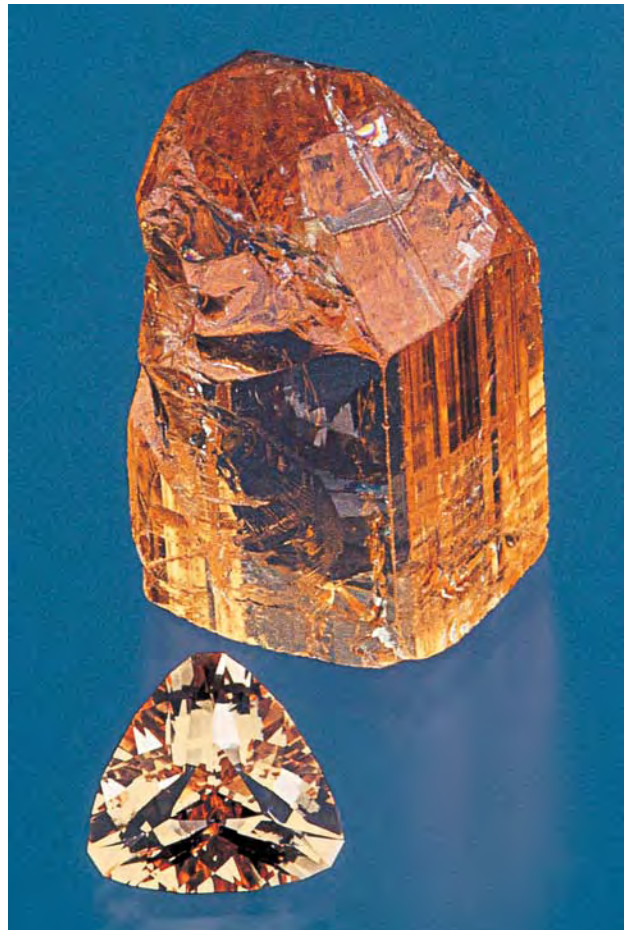
Raman analysis indicated that the inclusion was of the beryl group, and comparison with aquamarine, morganite, red beryl, and pezzottaite standards confirmed that the Raman pattern obtained from this inclusion was that of pezzottaite. To our knowledge, this is the first report of pezzottaite as an inclusion in another mineral, in this instance rock crystal quartz.

John I. Koivula and Maha Tannous

TREATMENTS

Treated-color topaz from Pakistan. Since late 2002, this contributor has been receiving periodic reports that treated-color orange topaz was being sold in the mineral market of Peshawar, Pakistan. Most of this information has been supplied by Farooq Hashmi of Intimate Gems, Jamaica, New York. Mr. Hashmi, who regularly visits the Peshawar market, reported that the starting material was pale-colored topaz from the Katlang area of Pakistan's North West Frontier Province (see E. Gübelin et al., "Pink topaz from

Figure 26. The orange color of this topaz from the Katlang area of Pakistan is probably due to an irradiation process. Although the color of some of the treated topaz is reportedly stable to sunlight, it fades on exposure to heat. The color of the 2.88 ct triangular brilliant, which was originally the same as the crystal (2.5 cm tall), faded due to heat from the cutting wheel. The stone was faceted for GIA's examination by Scott Fenstermacher of Grand Rapids, Michigan. Both samples are courtesy of Farooq Hashmi; photo by Maha Tannous.



Pakistan," Fall 1986 *Gems & Gemology*, pp. 140–151). Mines in this area are famous for producing fine pink topaz, although near-colorless and pale-colored topaz is much more commonly recovered.

Mr. Hashmi reported that the topaz has been treated both as loose crystals and matrix specimens, possibly by an irradiation process. The color ranges from light to dark orange or pinkish orange. According to Syed Iftikhar Hussain (Syed Trading Co., Peshawar), the treated topaz first appeared in the local market in late 2001, sometimes available as relatively large, clean crystals. However, dealers soon discovered that the material commonly faded after a few days' exposure to sunlight. Nevertheless, some of the treated-orange topaz appears to be stable to sunlight; samples obtained by Mr. Hashmi have retained their color after exposure to sunlight for over one month. The color is sensitive to heat, however, as discovered when one of the samples was cut on a diamond lap. As shown in figure 26, the stone faded appreciably during the cutting process. Clearly, when faceting such material, gem cutters should—as much as possible—avoid heating the stones (e.g., by using a water-cooled lap with oxide abrasives).

While information on the precise treatment process has not been revealed, it is interesting to note that experiments by Gübelin et al. (1986) succeeded in creating orange-brown topaz from pale-colored Katlang material through heating and subsequent irradiation. They reported that the treated color was heat-sensitive, and speculated that it would also fade on exposure to sunlight. According to K. Nassau (*Gemstone Enhancement*, 2nd ed., Butterworth-Heinemann, Oxford, England, 1994, pp. 187–193), the coloration of yellow-to-orange-to-brown topaz may be created through relatively low doses of radiation, which forms color centers that may or may not be stable to light. These coloration and stability characteristics are consistent with the orange coloration in the treated-orange topaz from Pakistan. Unfortunately, the only way to determine the sensitivity of such material to light is to perform a direct fade test.

BML

CONFERENCE REPORTS

International Geological Congress. The 32nd IGC took place in Florence, Italy, August 20–28, 2004. Held every four years, this large earth science conference featured over 300 scientific sessions, with more than 6,100 delegates registered from 141 countries. Presentations on gems were submitted to a special session on gem materials, but also were heard in a variety of other sessions. Conference abstracts can be searched on-line according to author name or keyword at www.32igc.info/igc32/search. This report highlights selected presentations that provided new information or innovative approaches to gem materials.

Diamonds were featured in presentations covering their origin, characteristics, and exploration. Some of this



Figure 27. The 61 ct Tiger Eye is the largest documented hydrogen-rich diamond. It is faceted precisely enough to stand on its culet. Photo by Franck Notari.

information was previously given at the 2003 International Kimberlite Conference held in Canada (and reviewed in the Fall 2003 Gem News International section, pp. 245–248), and will not be repeated here. **Dr. I. Swinititsky** of Moscow State University, Russia, and colleagues used geographic information system (GIS) computer technology to show that the world's highly diamondiferous areas coincide with regional lineaments (particularly at lineament intersections). **Mikhail Krutoyarskiy**, a geologic consultant from Chicago, determined that diamondiferous kimberlites and lamproites formed during only five of the more than 15 epochs of alkaline magmatism in the earth's history, and that higher diamond reserves were correlated to younger epochs.

The coloration of brown and black diamonds was classified into four categories each by **Dr. E. Fritsch** of the University of Nantes, France, and colleagues. Brown diamonds include those with brown graining and associated near-infrared absorptions called the "amber center," certain "H-rich" (see, e.g., figure 27) and CO₂-rich diamonds, and extremely N-rich type Ib diamonds. Black diamonds may consist of polycrystalline material (carbonado) with a variety of dark inclusions, or of monocrystalline material that is colored by abundant inclusions (typically graphite), scattering, or other causes (e.g., very dark yellow to green coloration).

Cathodoluminescence (CL) in conjunction with scanning electron microscopy was used by **Dr. Monica**

Mendelssohn and coauthors from the University College London to reveal growth features, platelets, plastic deformation, slip planes, and brecciation/regrowth textures in gem diamonds, which help characterize the natural material. **Dr. Maxim Viktorov** and colleagues from Moscow State University, Russia, documented a decrease in the red CL of irradiated synthetic diamonds as compared to those that were not treated.

Numerous presentations covered Russian diamond deposits. **Dr. Nikolay Gorev** of the Yakutian Geological Enterprise of Exploration, Research & Development CNI-GRI, Alrosa Co. Ltd., Mirny, Sakha, Russia, showed that kimberlites of the Yakutian diamond province are localized within structural channels (grabens) that range up to 20–40 km long and 1–4 km wide. **Dr. Nikolay Zintchouk** and coauthors, also from the Yakutian Geological Enterprise, studied the morphology of diamonds from Yakutia. In general these diamonds were octahedral to rhombic dodecahedral, although specific differences were found in diamonds from various economically important pipes. In a separate presentation, these authors reported on the morphology of diamonds from placers in this region, which can be broadly divided into two ages: late Paleozoic (octahedral to rhombic dodecahedral) and Upper Triassic (dodecahedral, rounded, and cuboid). **Andrey Ukhanov** of the Vernadsky Institute of Geochemistry and Analytical Chemistry, Russian Academy of Sciences, Moscow, and colleagues found a wide range of carbon isotope values in diamonds from primary and alluvial deposits in Yakutia. They were able to trace some alluvial diamonds back to known kimberlite pipes, whereas others (with isotopically light signatures) could not be correlated to any known primary source. **Dr. Zdislav Spetsius** and coauthor from the Institute of Diamond Industry, Alrosa Co. Ltd., Mirny, studied the mineral inclusions in diamonds from the Botoubinskaya pipe (Nakyn District), and determined that unlike diamonds from other pipes in Yakutia, these showed mainly eclogitic paragenesis (e.g., garnet, clinopyroxene, and pyrrhotite). **Dr. Victor Garanin** of Moscow State University and colleagues had several presentations on diamond indicator minerals from Russian kimberlites. For example, they measured the perovskite fraction of the microcrystalline oxides in kimberlite groundmass and correlated <5% perovskite with high diamond grade, and 30% perovskite with low-grade to non-diamondiferous pipes.

Margarita Dobrynina and colleagues of the Ecology Institute of Northern Region, Russian Academy of Sciences, proposed that kimberlites of the Arkhangelsk diamond province in western Russia are localized in areas where fractures are concentrated in the basement rocks, as imaged by airborne magnetic surveys. **Dr. Nikolai Golovin** of the joint stock company “Arkhangelskgeoldobycha” and colleagues documented systematic differences in the morphology and spectroscopic characteristics of diamonds from the two main deposits of the Arkhangelsk diamond

province (M.V. Lomonosov and V. Grib mines). They also found that diamonds from this province generally contain relatively high amounts of structural hydrogen and low nitrogen (of low aggregation state) compared to other diamonds worldwide, as revealed by infrared spectroscopy.

Dr. Tatiana Posukhova of Moscow State University and coauthors studied diamond morphology and associated mineral assemblages from placer deposits in western and central Africa (Bafit and Chikapa) and found no correlation with those from the Koidu kimberlite pipe in Sierra Leone, which indicates that they come from a different primary source. **Dr. Geraldo Sgarbi** and coauthors from the Federal University of Minas Gerais (UFMG), Brazil, suggested that Quaternary diamond placers of western Minas Gerais are derived from Upper Cretaceous conglomerates of the Bauru Group. They proposed that the large diamonds in these deposits may have come from kimberlites that were weathered into laterites in this area.

Colored stones were featured in a wide variety of presentations, covering databases, analytical techniques, and gems from pegmatites or particular localities. **Dr. Islamia Kovalenko** and colleagues from the Russian Research Institute for the Synthesis of Materials (VNIISIMS), Alexandrov, presented a comprehensive gem locality map of Russia that included approximately 150 deposits, the largest of which consist of amethyst, “chrysolite,” tourmaline, jadeite, lazurite, and nephrite. **Dr. Jean-Pierre Milesi** of Bureau de Recherches Géologiques et Minières (BRGM), Orleans, France, and coauthors developed an innovative map using GIS that correlated gem localities of East Africa and Madagascar with the underlying geology; the deposits were classified according to their geologic origin (magmatic, metamorphic, metasomatic, hydrothermal, and volcanic-related).

Dr. Don Marshall of Relion Industries, Bedford, Massachusetts, described a technique for the macrophotography of cathodoluminescence of gem and mineral specimens that uses a CL instrument mounted on a custom stand, rather than a microscope, allowing for CL photos of areas up to 4–5 cm in diameter. **Dr. Olga Yakushina** of the All-Russian Research Institute of Geological, Geophysical, and Geochemical Systems, Moscow, used X-ray computed microtopography to nondestructively image the internal structure of pearls (natural and cultured) and corals at room temperature. **Gioacchino Tempesta** and colleagues from the Università degli Studi di Bari, Italy, demonstrated how faceted samples (up to 4 mm thick) of synthetic moissanite could be identified using X-ray topography, by imaging their distinctive structural defects.

Dr. Igor Peretyazhko of the Vinogradov Institute of Geochemistry, Irkutsk, Russia, and colleagues proposed that rare-element assemblages near gem-bearing pockets in granitic pegmatites crystallized from melt-like gels that represent the transition between a silicate melt and an aqueous fluid. **Dr. Antônio Carlos Pedrosa-Soares** and a colleague from UFMG classified the geologic affiliation,

age, and gem production of the famous Brazilian pegmatite districts of Conselheiro Pena (two-mica granites, 585–565 My), São José da Safira and Araçuaí (two-mica granites, 530–500 My), and Padre Paraíso and Pedra Azul (biotite granite and charnockite, 520–500 My). **Dr. Olugbenga Okunlola** of the University of Ibadan, Nigeria, differentiated seven Precambrian granitic pegmatite belts in Nigeria; the geochemically most-evolved pegmatites (according to Ta mineralization) are located in the Kabba-Isanlu, Lema-Share, and Kushaka–Birnin Gwari belts. **This contributor** and colleagues proposed that gem-quality pezzottaite formed at the Sakavalana pegmatite in Madagascar via Cs remobilization by late-stage hydrothermal fluids.

Dr. Gaston Giuliani of the Centre de Recherches Pétrographiques et Géochimiques (CRPG), Nancy, France, and coauthors presented preliminary oxygen isotope data on gem corundum from several world sources, which show potential for differentiating the geographic origin of stones from some localities (e.g., rubies from Mogok vs. Mong Hsu, Myanmar). **Dr. Daniel Ohnenstetter** of CRPG and colleagues proposed that marble-hosted ruby deposits in central and southeast Asia formed during the uplift of the Himalayas from the metamorphism of impure carbonate rocks containing layers of organic and evaporitic material. **Dr. Frederick (Lin) Sutherland** of the Australian Museum, Sydney, and colleagues explored the geologic origin of gem corundum from basalt-related deposits in eastern Australia, southeast Asia, eastern China, and eastern Russia, and found that they consist mainly of magmatic sapphires with subordinate metamorphic sapphire and/or ruby suites and minor metasomatic sapphires. **Dr. Khin Zaw** of the University of Tasmania, Australia, and coauthors performed PIXE and Raman analyses of fluid and melt inclusions in gem corundum from eastern Australia, and found that Tasmanian sapphires crystallized from a magmatic source, whereas Barrington corundums have a metamorphic signature with an igneous component. **Andrea Cade** of the University of British Columbia (UBC), Canada, and coauthors showed that the recently discovered sapphire deposits on Baffin Island, Nunavut, Canada, are hosted by the Lake Harbor marble unit and share similarities in their origin with marble-hosted sapphires from central and southeast Asia.

Dr. Ricardo Castroviejo of the Polytechnic University of Madrid, Spain, and colleagues reported that emerald deposits of the central Ural Mountains in Russia are hosted by metasomatized ultramafic rocks, and the emeralds formed under conditions of repeated tectonic activity at 350–400°C and 1.5–2 kbar. **Dr. Mohammad Arif** and coauthor from the University of Peshawar, Pakistan, indicated that emeralds of northwest Pakistan's Swat Valley formed due to carbonate alteration of previously serpentinized ultramafic rocks by CO₂-bearing fluids released from the metamorphism of adjacent Indian-plate sedimentary rocks. **Heather Neufeld** of UBC and colleagues suggested

that emerald crystallization at Regal Ridge in Canada's Yukon Territory may have been triggered by the destabilization of hydrothermal fluids as a result of mixing, albitization (to release Ca), tourmaline crystallization, and/or a change in host-rock permeability. Ms. Neufeld also reported (in the absence of poster author Dr. Lee Groat of UBC and coauthors) that pale green beryl at the Lened Property in the Northwest Territories, Canada, contains up to 0.5 wt.% V₂O₃ and 0.04 wt.% Cr₂O₃, and formed at 250–550°C and <3.7 kbar. The composition of these green vanadian beryls is similar to those from Gandao, Pakistan.

Dr. Peter Ermolov of the Academy of Sciences of Kazakhstan in Karaganda reported that jadeite-omphacite of the Itmurundy mélange in central Kazakhstan formed via a metasomatic interaction between the host serpentinite and its tectonic inclusions. **He Mingyue** of the China University of Geosciences, Beijing, indicated that "Hetian jade" (nephrite) from the western Kunlun Mountains of Xinjiang Province consists mainly of tremolite that formed in two stages by the metasomatic replacement of marble. **Dr. Douglas Nichol** of Newtra Geotechnical Group, Wrexham, United Kingdom, reported that the main nephrite jade deposits in Europe are located in Poland, Switzerland, and Italy, while smaller deposits are found in Finland, Germany, and Scotland.

Bertha Oliva Aguilar-Reyes of the University of Nantes, France, and colleagues studied the "crazing" of fire opal from Mexico and other localities, and proved that the whitening of these opals is due to water loss. Comparisons between whitened and uncrazed areas generally revealed about 10% water loss (although from 6% to 95% water loss was documented in one sample). **Dr. Xiaoyan Yu** and coauthors from the China University of Geosciences, Beijing, studied play-of-color opal by transmission electron microscopy and determined that there are two types of water present: molecular water (H₂O) attached to the surface of silica spheres, and minor amounts of hydroxyl (OH) found between the silica spheres.

Dr. Corina Ionescu and colleagues from Babes-Bolyai University, Cluj-Napoca, Romania, distinguished three compositional groups of Cenozoic fossil resins from five specimens: 1—Romanian amber, 2—Polish (Baltic), Dominican, and German (Bitterfeld) amber, and 3—"krantzite" (a soft amber-like resin) from Königsau, Germany.

Dr. Margherita Superchi of CISGEM, Milan Chamber of Commerce, Italy, and colleagues documented the properties of faceted musgravite and taaffeite (now each classified by the International Mineralogical Association as polytypes of magnesiothaumhaite), and documented inclusions consisting of quartz, apatite, calcite, augite, and scapolite. **Valentin Prokopets** of Kiev Geological College, Ukraine, described the Kukhilal spinel deposit of the southwestern Pamir Mountains in Tajikistan, where the spinel is associated with forsterite in magnesite marbles.

BML

World Diamond Conference, Perth, Australia. Approximately 180 people attended this event, which was held in conjunction with the Australian Diamond Conference on November 22–23, 2004. The format consisted of 28 presentations and a concluding panel session. There were five presenters from outside the country. **James Picton**, diamond analyst of W. H. Ireland, London, emphasized (as he did at the 2003 Australian Diamond Conference) that by 2012 there will be a US\$3–3.5 billion shortfall in the supply of rough, and thus the price will rise. This has greatly encouraged both major and junior diamond exploration companies to increase their exploration efforts, and has added to the general feeling of optimism in the diamond exploration industry. **Dr. Craig Smith** of De Beers Geoscience Centre, Johannesburg, South Africa, emphasized the importance of “good science” (i.e., geology, volcanology, and lithology) in the study of kimberlites and their diamond potential. De Beers’s diamond laboratories in Johannesburg and Kimberley are available to assist joint-venture partners with improving target selection and diamond recovery. **Norman Lock** of RSG Global, Johannesburg, discussed the difficulty of applying standard guidelines to the calculation of reserves for alluvial diamond deposits. These deposits are notoriously inconsistent in their extent, thickness of gravel, and diamond content, so a bankable feasibility study based on such calculations is not realistic. Therefore, either the rules for alluvial deposits must be changed or capital can only be raised from private subscribers, not from a bank or by prospectus from the money market. **Carl Pearson**, diamond industry observer, London, said that synthetic diamonds will have little effect on the retail diamond market, as bridal jewelry must contain natural diamonds; however, custom and fashion jewelry may be affected a bit more. **David Duval**, of Duval Mincom, Vancouver, gave an overview of the current diamond exploration scene in Canada and remarked that it is much easier for Canadian companies to raise venture capital than it is for Australian ones.

Most of the conference speakers were locally based and reported on the results of their respective companies. **Miles Kennedy** of Kimberley Diamond Co., Perth, presented the latest news from their mine at Ellendale. Last year’s production included about 60,000 carats of good-quality yellow diamonds worth US\$200–250/ct. Use of the large-diameter Bauer drill has given much better results in outlining reliable reserves than the smaller drills used previously. Reserves have increased up to 60 million carats from the original 9 million; the overall grade is 6 carats/100 tonnes (cpht). Mr. Kennedy claimed the company can break even with open-pit mining down to 3 cpht. Kimberley has paid off its Aus\$23.5 million debt to Rio Tinto and is confident of having a profitable 10-year mine life.

Dr. Kevin Wills of Flinders Diamonds, Norwood, South Australia, announced the discovery of three kimberlites next to the Barossa Valley (famous for its viniculture) in

South Australia. However, so far they are not diamondiferous. **Charles Mostert** of Crown Diamonds, Perth, discussed the incorporation of four separate South African fissure mines (Star, Messina, Helam, and DanCarl) into one company. These old mines, which date from the late 1930s (Helam and Star) to late 1950s (Messina and DanCarl) explore kimberlite dikes down to 500–700 m. Collectively, they are expected to produce up to 200,000 carats annually as of 2006. **Don Best** of Elkedra Diamonds, Perth, reviewed this company’s entry into the Brazilian alluvial diamond mining scene with the takeover of the Chapada deposit in Mato Grosso State. The previous Chapada Diamonds company failed twice to raise sufficient capital on the AIM market (of the London Stock Exchange), but Elkedra succeeded in raising Aus\$12 million in September 2004. The value of the alluvial diamonds at Chapada is very high, at more than US\$400/ct.

Mike Woodborne of the newly floated company Bonaparte Diamonds, Perth, maintained that there is a chance of a viable deposit offshore in the Bonaparte Gulf along the north coast of Western Australia, despite previous failed attempts in the 1980s and early 1990s. **Tom Reddcliffe** of Striker Resources said that this company only recently gained access to the dormant Merlin mine, after more than a year of legal wrangling with Rio Tinto. Striker believes that the small kimberlite pipes on the property join up at shallow depth, and that this increased volume of ore may form a viable deposit. Drilling is underway to prove this theory. In addition, since no crusher was used in previous mining operations, the grade may be higher than first thought due to the presence of diamonds in oversized “waste.”

For this contributor, the most significant talk was by **Carl Simich** of Namakwa Diamonds, Perth, who told the gathering that despite new South African regulations and the requirement of 51% equity being held by Black Economic Empowerment groups, they managed to acquire all the necessary permits and have started mining in coastal Namaqualand. This shows that a new diamond mining project proposed by a foreign company on property with state-owned mineral rights and in an environmentally sensitive area can actually get off the ground. This gives hope to many new ventures promoted by diamond juniors from Australia and Canada. **Dr. Neil Allen** of Ka Pty. Ltd., Melbourne, showed a new magnetic separator, the Rotomag, which uses the property that some minerals are not only magnetic but are also rotated in a magnetic field. Combining these two properties, the new machine provides a better recovery of the kimberlite indicator minerals ilmenite, chromite, and pyrope. Other speakers gave updates on their projects, but no significant new discoveries or developments were announced. Overall the mood was guardedly optimistic.

*A. J. A. “Bram” Janse (archonexpl@iinet.net.au)
Archon Exploration Pty. Ltd.
Perth, Western Australia*

MISCELLANEOUS

Burmese faceted rubies and the U.S. import ban. A recent ruling by the U.S. Customs Service has held that ruby rough from Myanmar (Burma) that has been faceted in other countries does *not* come under the import ban of the Burmese Freedom and Democracy Act of 2003 (see U.S. Customs Ruling HQ 563127, Dec. 15, 2004; <http://rulings.customs.gov/detail.asp?ru=563127>).

Under long-standing U.S. law defining "country of origin" for customs regulations, the origin of a manufactured product differs from the origin of its raw materials if the materials have undergone a "substantial transformation" in another country (see Code of Federal Regulations title 19, section 134.1[b]). A material has undergone a substantial transformation if processing and/or other modifications have created a different product having a distinctive character or use. For example, the Customs Service has historically defined a polished diamond's country of origin as the location where the polishing took place, not the country where the diamond was mined (see, e.g., U.S. Customs Ruling J80098, Jan. 15, 2003; <http://rulings.customs.gov/detail.asp?ru=J80098>).

In a petition by Tiffany & Co. (New York) late last year, the Customs Service was asked to determine if the heat treating, pre-forming, faceting, and polishing that ruby rough undergoes is sufficient to qualify as a substantial transformation. The ruling held that, indeed, as a result of these manufacturing processes carried out in other countries, "[t]he finished stones are no longer considered products of Burma." Thus, they are not prohibited from import under the Burmese Freedom and Democracy Act.

The ruling was specifically limited to faceted rubies and excluded cabochon or other stones with no facets. However, in light of this and an earlier ruling that reached the same conclusion (see U.S. Customs Ruling K85866, May 14, 2004; <http://rulings.customs.gov/detail.asp?ru=k85866>), it seems likely that the Customs Service could rule that other gem materials from Myanmar that are polished elsewhere also fall outside the import ban.

Tiffany & Co. has recently stated, however, that it will not import any gems of Burmese origin, despite this ruling.

Thomas W. Overton

ANNOUNCEMENTS

Gem-A field trip to Brazil. The Gemmological Association of Great Britain is planning a tour of Minas Gerais State, Brazil, August 15–29, 2005. The trip will include visits to cutting centers and gem mines. E-mail doug@gem-a.info or visit www.gem-a.info/membership/fieldTrips.htm.

Exhibits

Native American jewelry at AMNH. "From Totems to Turquoise: Native North America Jewelry Arts of the Northwest and Southwest," an exhibition of more than

500 pieces of contemporary and historic Native American jewelry, is being held at the American Museum of Natural History in New York City until July 10, 2005. Visit www.amnh.org/exhibitions/totems or call (212) 769-5100.

Pearls at the Milwaukee Public Museum. "Pearls: A Natural History," a traveling exhibition tracing the natural and cultural history of pearls that was organized by the American Museum of Natural History (New York) in collaboration with the Field Museum (Chicago), will be on display at the Milwaukee Public Museum, Milwaukee, Wisconsin, until June 26, 2005. The many exhibits include pearl formation and culturing, as well as historical pearl jewelry that once belonged to Great Britain's Queen Victoria and Marie Antoinette of France. Visit www.mpm.edu/Pearls/Pearlsmain2.htm.

Gems at the Hungarian Natural History Museum. "Wondrous Gemstones," an exhibition of gems from the Spanish Programa Royal Collections, will be on display at the Hungarian Natural History Museum in Budapest until July 3, 2005. The collection includes notable pieces such as a 1,490 ct rutilated kunzite from Minas Gerais, Brazil, and a 455 ct heart-shaped emerald, in addition to over 150,000 carats of other gems. Visit www.dragako.nhmu.hu.

Cameos at the Met. "Cameo Appearances," a display of more than 160 examples of the art of gem carving from Greco-Roman antiquity to the 19th century, will be on display until October 30, 2005, at the Metropolitan Museum of Art in New York City. Among the pieces featured will be works by the neoclassical Italian masters Benedetto Pistrucchi, Giuseppe Girometti (figure 28), and Luigi Saulini. A variety of educational programs will be offered in conjunction with the exhibition. Also on display at the Met (through January 2006) is "The Bishop Jades," a selection of fine Chinese and Mughal Indian jades from the collection of Heber R. Bishop that was donated to the museum in 1902. Visit www.metmuseum.org or call (212) 535-7710.

Conferences

GemmoBasel 2005. The first open gemological conference in Switzerland will be presented by the SSEF Swiss Gemmological Institute at the University of Basel, April 29–May 2. Among the events scheduled is a field trip to a Swiss manufacturer of synthetic corundum and cubic zirconia. Visit www.gemmobasel2005.org or e-mail gemplab@ssef.ch.

Kimberlites at UBC. A two-day introductory course on Canadian kimberlite geology will be presented by the Mineral Deposit Research Unit of the University of British Columbia in Vancouver, May 5–6, 2005. Both classroom



Figure 28. This cameo brooch, Priam Supplicating Achilles for the Body of Hector, was carved from sardonyx by Italian master Giuseppe Girometti (1779–1851) in the early 19th century. Courtesy of the Metropolitan Museum of Art, The Milton Weil Collection, 1940.

lectures and laboratory practical work are included. Visit www.mdru.ubc.ca/home/courses/sc42.phpall, e-mail mdru@eos.ubc.ca, or call 604-822-6136.

ICNDST-10 in Japan. The 10th International Conference of New Diamond Science and Technology will be held at the National Institute of Advanced Industrial Science and Technology Conference Hall in Tsukuba, Japan, May 11–14, 2005. Among the topics covered will be HPHT synthesis and processing and the growth of CVD synthetic diamond. Visit www2.convention.co.jp/ICNDST-10 or e-mail icndst-10@convention.co.jp.

Diamonds at GAC-MAC. The 2005 joint meeting of the Geological Association of Canada and the Mineralogical Association of Canada will take place May 15–18, 2005, in Halifax, Nova Scotia. "From Cratons to Carats: A Symposium to Honour the Career of Herwart Helmstaedt" will feature presentations on geotectonic controls on diamond exploration. Visit www.halifax2005.ca or e-mail hfx2005@gov.ns.ca.

Bead Expo in Miami. The 2005 International Bead Expo will be held in Miami, Florida, May 18–22. Over 60 workshops and educational lectures on bead jewelry design and manufacture are scheduled. Visit www.beadexpo.com or e-mail info@beadexpo.com.

Goldschmidt geochemistry conference. The 15th Annual Goldschmidt Conference will take place May

20–25, 2005, in Moscow, Idaho. The meeting will include a session on the geochemistry of gem deposits, as well as numerous presentations on advanced analytical techniques. E-mail gold2005@uidaho.edu or visit www.uidaho.edu/gold2005.

Elba 2005. Crystallization processes in granitic pegmatites will be addressed at the Elba 2005 International Meeting, May 23–29, 2005, on the island of Elba, Italy. Both educational seminars and field trips to local granitic pegmatites are planned. Visit www.elba-pegmatites.org.

Corundum treatment seminar. A seminar on corundum treatments will be presented by Ted Themelis at the Italian Gemmological College on May 29, 2005, in Milan, Italy. The subjects will include heat treatment (with and without beryllium) of rubies and sapphires; lead-glass-filled rubies; and new heat-treatment processes for star rubies. A presentation on gems from Mogok, Myanmar, also will be given. Visit www.themelis.com.

JCK Show–Las Vegas. Held at the Sands Expo and Convention Center and the Venetian Hotel on June 2–7, 2005, this gem and jewelry trade show will also host a comprehensive educational program beginning June 2. Scheduled seminars will cover industry trends, diamond sales and marketing strategies, legal issues for retailers and manufacturers, and developments in gemology. The AGTA will also be offering seminars focusing on color and fashion on June 2 at the AGTA Pavilion. To register, call 800-257-3626 or 203-840-5684, or visit <http://jckvegas2005.expoplanner.com>.

Maine Pegmatite Workshop. The Fourth Annual Maine Pegmatite Workshop will take place June 4–10, 2005, in Poland, Maine. This one-week seminar will focus on the mineralization and origin of granitic pegmatites of the world, and will include daily field trips to numerous quarries in Maine. Also featured will be a one-day field trip to the famous Palermo pegmatite in North Groton, New Hampshire and visits to several gem and mineral displays in Maine. E-mail Raymond Sprague at rasprague@mac.com or visit <http://homepage.mac.com/rasprague/PegShop>.

Gem inclusions at ECROFI. The 18th Biennial Meeting of European Current Research on Fluid Inclusions will take place July 6–9, 2005, in Siena, Italy. The event will include a two-day short course on fluid inclusions in gems. Visit www.unisi.it/eventi/ECROFIXVIII or e-mail ecrofixviii@unisi.it.

Jewelry Camp 2005. The 26th Annual Antique & Period Jewelry and Gemstone Conference will be held July 15–20, 2005, at Hofstra University, Hempstead, New York. The program emphasizes hands-on jewelry examination techniques, methods of construction, understand-

ing materials used throughout history, and the constantly changing marketplace. Visit www.jewelrystcamp.org, call 212-535-2479, or e-mail registrations@jewelrystcamp.org.

Afghanistan Gem Tour. Gary Bowersox will be leading another tour of Afghan gem mining areas during the second half of August 2005. Visits to the mines for Jegdalek rubies and Panjshir emeralds are planned, in addition to a tour of Kabul and meetings with local dignitaries. Visit www.gems-afghan.com/guidetours.htm or e-mail mrgary77@aol.com.

Raman Spectroscopy in Art and Archeology. The 3rd International Conference on the Application of Raman Spectroscopy in Art and Archeology will be held August 31-September 3, 2005, in Paris, France. Among the planned topics are development of Raman instrumentation for the nondestructive analysis of art, approaches in

dealing with Raman imaging, and the investigation of gemstones. Visit www.ladir.cnrs.fr/ArtRaman2005 or e-mail artraman2005@glvt-cnrs.fr.

Diamond 2005. Scientific and technological aspects of natural and synthetic diamond (as well as related materials) will be discussed at the 16th European Conference on Diamond, Diamond-like Materials, Carbon Nanotubes & Nitrides, September 11-16, 2005, in Toulouse, France. Visit www.diamond-conference.com

Agate symposium at CSM. On September 10-11, 2005, a symposium on agate and cryptocrystalline quartz will take place at the Colorado School of Mines in Golden, Colorado, in connection with the Denver Gem and Mineral Show on September 16-18. Field trips to Colorado mineral localities are planned for September 12-13. Call 303-202-4766 or e-mail pmodeski@usgs.gov.

Mark your calendar for the

GIA Gemological Research Conference August 26-27, 2006

To explore the most recent technical developments in gemology, GIA will host a Gemological Research Conference in conjunction with the 4th International Gemological Symposium in San Diego, California.

Invited lectures, submitted oral presentations, and a poster session will explore a diverse range of contemporary topics including the geology of gem deposits, new gem occurrences, characterization techniques, treatments, synthetics, and general gemology. Also scheduled is a one-day pre-conference field trip to the world-famous Pala pegmatite district in San Diego County.

Abstracts should be submitted to gemconference@gia.edu (for oral presentations) or ddirlam@gia.edu (for poster presentations). The abstract deadline for all submissions is March 1, 2006. Abstracts of conference presentations will be published in a special proceedings volume.

For further information,
contact the organizing
committee at
gemconference@gia.edu
or visit
www.gia.edu/gemsandgemology

Mark your calendar today!

Challenge 2005

Gems & Gemology Challenge 2005 Gems & Gemology Challenge 2005 Gems & Gemology Challenge 2005 Gems & Gemology Challenge 2005 Gems & Gemology Challenge 2005

The following 25 questions are based on information from the four 2004 issues of *Gems & Gemology*. Refer to the feature articles and “Notes and New Techniques” in those issues to find the **single best answer** for each question; then mark your choice on the response card provided in this issue. (Sorry, no photocopies or facsimiles will be accepted; contact the Subscriptions Department—dortiz@gia.edu—if you wish to purchase additional copies of this issue.) Mail the card so that we receive it no later than Monday, August 1, 2005. Please include your name and address. All entries will be acknowledged with a letter and an answer key **after the due date**.

Score 75% or better, and you will receive a GIA Continuing Education Certificate. If you are a member of the GIA Alumni Association, you will earn 10 Carat Points toward GIA’s Alumni Circle of Achievement. (Be sure to include your GIA Alumni membership number on your answer card and submit your Carat card for credit.) Earn a perfect score, and your name also will be listed in the Fall 2005 issue of *Gems & Gemology*. Good luck!

- The FTC Guides for the jewelry industry require disclosure of
 - any treatment to a gem material.
 - any treatment to a gem material that substantially affects its value.
 - only those treatments that are impermanent or create special care requirements.
 - only those treatments that are not generally accepted in the trade.
- The cultured pearls produced by Perlas del Mar de Cortez in Mexico are grown in ____ oysters.
 - Pinctada margaritifera*
 - Pinctada mazatlanica*
 - Pinctada maxima*
 - Pteria sterna*
- The seven major components that yield an overall cut grade in the GIA diamond cut grading system are: brightness, fire, scintillation, weight ratio, ____, polish, and symmetry.
 - crown angle
 - durability
 - optical symmetry
 - sparkle
- Since 1994, extraordinary amounts of fine, large gem peridot have been discovered in the Sapat Valley of
 - Pakistan.
 - Vietnam.
 - Tanzania.
 - Myanmar.
- The practical use of X-ray topographs to fingerprint diamonds has historically been limited because
 - faceted diamonds cannot be diffracted by this technique.
 - high-clarity diamonds with few inclusions do not create usable topographs.
 - too much exposure to X-rays can damage a diamond.
 - many individual topographs are necessary to characterize a single diamond.
- The presence of the 3543 cm^{-1} infrared absorption band in amethyst is
 - proof of synthetic origin.
 - proof of natural origin.
 - indicative of possible synthetic origin.
 - meaningless.
- One disadvantage of laser-induced breakdown spectroscopy (LIBS) in detecting Be-diffused sapphire is that it
 - is not affordable for most commercial gemological laboratories.
 - is slightly destructive.
 - cannot detect beryllium in very low concentrations.
 - requires elaborate preparation of the sample.
- Which of the following is *not* a common identifying characteristic of HPHT-grown synthetic diamonds?
 - Metallic inclusions
 - Color zoning
 - Diamond type
 - Cuboctahedral crystal shape
- Colorless as-grown (high-purity) CVD synthetic diamonds have been created by
 - the addition of nitrogen to the growth chamber.
 - the removal of all impurities other than hydrogen from the growth chamber.
 - the addition of diborane to the growth chamber.
 - different temperature and

- pressure conditions than for colored CVD synthetics.
10. A small percentage of amethyst from the Four Peaks mine displays red overtones and/or a deep reddish purple bodycolor that is known in the trade as ____ quality.
- “Siberian”
 - “Brazilian”
 - “Arizonan”
 - “Bolivian”
11. A customer shopping for an emerald ring says he only wants a natural, untreated emerald. The sales associate replies that her store sells only natural stones. The owner—who knows the associate misunderstood the request—overhears this, but is in the middle of another transaction and does not intervene before the customer buys a resin-filled emerald. The owner
- is guilty of fraud.
 - has engaged in a deceptive trade practice under the FTC Guides for the jewelry industry.
 - both A and B
 - is not liable for his employee's good-faith mistake.
12. Almost all the faceted synthetic diamonds from Chatham Created Gems that were examined by GIA scientists showed ____, which is a strong indication of synthetic origin.
- a photoluminescence (PL) feature at 589 nm
 - eye-visible metallic inclusions
 - an infrared (IR) absorption line at 1344 cm^{-1}
 - distinctive color zoning related to growth sectors
13. When laser-induced breakdown spectroscopy (LIBS) is used to analyze a faceted stone, the best part to test is its
- crown.
 - pavilion.
 - girdle.
 - table.
14. ____ of brown nitrogen-doped CVD synthetic diamonds can produce colorless or near-colorless material.
- HPHT annealing
 - Fracture filling
 - Irradiation
 - No known treatment
15. For observation of overall diamond cut appearance, the GIA “common viewing environment” combines daylight-equivalent ____ lamps with spot lighting from light-emitting diodes (LEDs).
- halogen
 - incandescent
 - metal halide
 - fluorescent
16. Pearl farming has been conducted in the Gulf of California, Mexico, since the early 1900s, although it is only since ____ that full-round dark cultured pearls from this area have become commercially available.
- 1936
 - 1966
 - 1996
 - 2000
17. The 3543 cm^{-1} infrared absorption band is present in the majority of synthetic amethyst seen in the jewelry trade because
- the vast majority of synthetic amethyst is grown on seed crystals cut parallel to the *z* crystallographic sector.
 - the vast majority of synthetic amethyst is grown on seed crystals cut parallel to the *r* crystallographic sector.
 - synthetic amethyst cannot be grown on seeds cut parallel to *r* crystallographic sectors.
 - it is induced by post-growth irradiation treatment.
18. To provide the best protection, a well-crafted disclosure policy should
- be in writing.
 - be part of any employee training program.
 - be carefully reviewed for legal compliance well before any problems arise.
 - all of the above
19. GIA's research into diamond proportions has established that top-grade diamond cuts can have crown angles ranging from approximately 32.0° to
- 36.0° .
 - 37.0° .
 - 38.0° .
 - 39.0° .
20. The process of grinding a piece of rough into the approximate shape of the finished colored stone is known as
- cobbling.
 - preforming.
 - girdling.
 - bruting.
21. The pink synthetic diamonds from Chatham Created Gems do not display the ____ that is common in natural pink diamonds.
- magnetism
 - purplish color component
 - 637 nm line in their visible absorption spectra
 - strong strain visible in cross-polarized light
22. The dense accumulations of ____ inclusions in some Four Peaks amethyst prove that it is natural.
- rutile
 - apatite
 - hematite
 - flurite
23. A square or ____-shaped fluorescence pattern is commonly seen in HPHT synthetic diamonds.
- triangle
 - cross
 - rod
 - crescent
24. X-ray topography can “fingerprint” a faceted diamond by imaging
- structural characteristics such as crystal lattice defects.
 - patterns created by luminescence to X-rays.
 - trace-element concentrations such as nitrogen and boron.
 - isotopic ratios of inclusions.
25. High-purity CVD synthetic diamonds have few identification features other than ____ in the De Beers DiamondView.
- an orange to orangy red reaction with striations
 - a green to blue-green reaction with striations
 - the absence of mosaic or slip-related patterns of blue dislocation luminescence
 - a blue-green reaction with features relating to surface morphology

EDITORS

Susan B. Johnson
Jana E. Miyahira-Smith
Stuart Overlin

Understanding Jewellery, 3rd Edition

By David Bennett and Daniela Mascetti, 426 pp., illus., publ. by Antique Collector's Club, Woodbridge, England, 2003. US\$89.50*

True to its name, *Understanding Jewellery* provides the reader with a strong grasp of jewelry history in Europe and the United States from the late 18th century to the present day. This excellent reference text shows how social and economic factors influenced the way jewelry was designed and worn through the decades from the French Revolution to the start of the new millennium. Instantly popular at the time of its first publication in 1989, *Understanding Jewellery* has been reprinted twice and undergone two revisions. The first revision, in 1994, added a chapter on jewelry from 1960 to 1980; the current revision brings the text up to the present day with a chapter on 1980–2000.

The authors have unique qualifications that give them the authority to write about jewelry history in Europe. With 32 years at Sotheby's for David Bennett and 24 years for Daniela Mascetti, they have a lofty vantage point from which to observe trends in the evolution of jewelry design. During their tenure, they have been in a prime position to see superlative examples from every era, giving them real insight into the subtleties of the subject.

Unlike most books on jewelry history, *Understanding Jewellery* opens with a section on gemology that provides descriptions of the various gems encountered in jewelry, some simple

tests that will aid in their identification, and the basics of instrumentation. This section includes appendices on the refraction of light and the refractometer, the Mohs hardness scale, pastes (glass imitations) and composite stones, and (new to this edition) gemstone enhancement. The last summarizes the types of treatments that might be encountered in diamond, corundum, and emerald, and suggests that when in doubt, the gem in question should be submitted to an independent laboratory for analysis.

The remainder of the book consists of 10 chapters, each of which covers an approximately 20-year segment (except Chapter 1, which also includes the late 18th century). Each chapter begins with an historical overview that describes how changes in society impacted the use of gems, metals, and stylistic elements in the jewelry manufactured during the period. This overview is followed by individual sections that give greater detail on specific types of jewelry, such as tiaras and combs, parures (groups of matching pieces), earrings, necklaces, pendants, brooches, bracelets, and rings.

The chapters are lavishly illustrated with beautiful examples of exquisite jewels, all of which have passed through Sotheby's auction house in the last two decades. The layout of the book is better in this latest manifestation, as many more of the illustrations are closer to the text that describes them. Another plus is the addition of numerous dazzling new photos, particularly in the Gemstones section of Chapter 9, and in the new chapter that follows, which covers the period 1980–2000. Unfortunately, however,

several photographs have been re-mastered with the intent of making them sharper. While this is an improvement in some cases, in others it has the effect of making the pieces appear flat and unnatural. Sadly, in comparison with previous editions, many of these digitally enhanced images have lost some of the richness of the gems, the warmth of the gold, and nuances in the details. Other changes include an updated bibliography to reflect the addition of the new chapter, and the deletion of approximate auction values, a section featured in previous editions.

The newly added Chapter 10 describes how the social and professional roles for women changed at the end of the 20th century, and how this influenced jewelry design. The authors describe the 1980s as a "decade of greed and excess," which was followed by a decade largely of recession and restraint. In their descriptions of how jewelry reflected these traits, Bennett and Mascetti do a wonderful job of profiling an era that is still in progress, or at least not far behind us. In this reviewer's estimation, if one could afford just one book on the subject, *Understanding Jewellery* would be a prime choice for any aspiring jewelry historian.

ELISE B. MISIOROWSKI
Gemological Institute of America
Carlsbad, California

**This book is available for purchase through the GIA Bookstore, 5345 Armada Drive, Carlsbad, CA 92008. Telephone: (800) 421-8161; outside the U.S. (760) 603-4200. Fax: (760) 603-4266. E-mail: myorder@gia.edu*

Collecting Fluorescent Minerals

By Stuart Schneider, 192 pp., illus., publ. by Schiffer Publishing Ltd., Atglen, PA, 2004. US\$29.95*

In this fascinating work, Stuart Schneider introduces readers to the amazing beauty of fluorescent rocks and minerals. A photographic *tour de force*, it will likely inspire more people to pay attention to minerals that “glow in the dark” under ultraviolet light (actually, on exposure to UV radiation, but “under ultraviolet light”—a common misnomer—is used throughout the book).

For the most part, this book is a catalogue of color photos comparing mineral specimens as they appear in ordinary daylight and when exposed to short- and/or long-wave UV. Of its 192 pages, fully 156 are devoted entirely to such juxtaposed photos, with only 22 pages of text. After briefly covering the basics of what fluorescence is, how to get started building a collection, and the equipment needed, most of the remaining text focuses on three of the world's most prolific collecting areas for fluorescent minerals: Franklin, New Jersey; Mont St. Hilaire, Quebec; and Ilimaussaq, Greenland.

The best feature of the book is the photographs of fluorescent minerals. The author has done a superb job of compiling this exhaustive collection of photos, which are enhanced by the high-quality printing and paper. An interesting component of the photo captions is the guide to the monetary value. Given the volatility of specimen prices, few authors would be brave enough to attempt such a guide, but Schneider does a reasonably good job of providing novices with a rough idea of what they will have to spend to purchase a particular fluorescent mineral if they aren't inclined to go mucking about in mines and quarries themselves.

The weakest area, unfortunately, is the geological and mineralogical

information, where there are a number of errors. To cite just one example, of the six “radioactive minerals that fluoresce” listed on page 31, only one (autunite) is actually fluorescent. The text would have benefited from proofreading by someone more familiar with mineral species.

The intended audience for this book is people with a collector instinct. It will undoubtedly achieve its objective and induce more of those who thrive on building collections to acquire fluorescent rocks. Most gemologists are already familiar with the uses of fluorescence in gem identification (a subject not covered in the book), although they might be interested in the use of fluorescent minerals as gemstones. The book contains several pages with photos of fluorescent cabochons. Many of these, however, are “collector's gems” only. They could not be considered “wearable,” given that they are not particularly attractive in daylight and fluoresce only when exposed to short-wave UV radiation, which is not advised for any length of time.

ALFREDO PETROV
Peekskill, New York

OTHER BOOKS RECEIVED

50-Year History of the Tucson Show.

By Bob Jones, 183 pp., illus., publ. by *The Mineralogical Record*, Tucson, AZ, 2004, US\$20.00. This special supplement to *The Mineralogical Record* offers a nostalgic look at the history of the Tucson Gem and Mineral Show, the most important annual event for the mineral collecting community. Reconstructed from personal scrapbooks and unofficial archives, the book features highlights from every TGMS, beginning with the inaugural event: a two-day show held at an elementary school in March 1955. The descriptions are complemented by enjoyable photos

of the memorable specimens and personalities through the years.

STUART OVERLIN

The Grandmasters of Mineral Photography.

136 pp., illus., publ. by *Mineralogical Almanac*, Moscow, 2004, US\$45.00. This book, a special issue of the Russian publication *Mineralogical Almanac*, features 14 of the world's most talented gem and mineral photographers, including Nelly Bariand, Olaf Medenbach, Jeffrey Scovil, Harold and Erica Van Pelt, and Wendell Wilson. Each artist has chosen nine gorgeous photographs for this book; these are accompanied by biographical sketches and a brief overview of their techniques.

SO

Tone Vigeland: Jewellery + Sculpture

Movements in Silver. By Cecilie Malm Brundtland, 182 pp., illus., publ. by *Arnoldsche Art Publishers*, Stuttgart, 2004 [in German and English], US\$75.00. Influential Norwegian jeweler Tone Vigeland (born 1938) has been creating modernist masterpieces in silver, gold, steel, and lead for nearly 50 years. This artist monograph documents Vigeland's career and captures her finest silver jewelry and sculpture with 160 dramatic photos.

SO

The Tourmaline: A Monograph.

By Friedrich Benesch and Bernard Wöhrmann, 234 pp., illus., publ. by *Verlag Urachhaus*, Stuttgart, Germany, 2003, US\$150.00. The first English version of this oversized book (41 × 31 cm) follows three German editions. The text includes a historical review of tourmaline, a section on crystallography and chemical composition, and an extensive bibliography. The book is lavishly illustrated, with 380 large color photos and illustrations that encompass tourmaline's incredible variety.

SO

Gemological ABSTRACTS

2005

EDITOR

A. A. Levinson
University of Calgary
Calgary, Alberta, Canada

REVIEW BOARD

Christopher M. Breeding
GIA Gem Laboratory, Carlsbad

Jo Ellen Cole
Vista, California

Michelle Walden Fink
GIA Gem Laboratory, Carlsbad

Eric Fritz
GIA Gem Laboratory, Carlsbad

R. A. Howie
Royal Holloway, University of London

Alethea Inns
GIA Gem Laboratory, Carlsbad

David M. Kondo
GIA Gem Laboratory, New York

Taijin Lu
GIA Research, Carlsbad

Wendi M. Mayerson
GIA Gem Laboratory, New York

Kyaw Soe Moe
GIA Gem Laboratory, New York

Keith A. Mychaluk
Calgary, Alberta, Canada

Joshua Sheby
GIA Gem Laboratory, New York

James E. Shigley
GIA Research, Carlsbad

Boris M. Shmakin
Russian Academy of Sciences, Irkutsk, Russia

Russell Shor
GIA, Carlsbad

Maha Tannous
GIA Gem Laboratory, Carlsbad

Rolf Tatje
Duisburg University, Germany

Christina Taylor
Boulder, Colorado

Sharon Wakefield
Northwest Gem Lab, Boise, Idaho

COLORED STONES AND ORGANIC MATERIALS

The origin of precious opal—A new model. B. Deveson, *Australian Gemmologist*, Vol. 22, No. 2, 2004, pp. 50–58.

A new model is proposed for the formation of opal showing play-of-color, as well as patch (common opal). According to this new model, the essential requirements for opal formation are: (1) artesian “mound” springs with alkaline, silica-rich waters; (2) a mechanism for changing the physicochemical features of this water so that suitable silica spheres are precipitated in linear chains; and (3) the occurrence of suitable voids lined with clay—which acts as a semipermeable membrane to concentrate and purify the silica solution by ultrafiltration and dialysis.

Active and extinct artesian mound springs are found in general proximity to several sedimentary rock-hosted opal fields in New South Wales, South Australia, and Queensland. In the Great Artesian Basin, the natural springs lie on a NE-trending line over 300 km long, subparallel to the Lightning Ridge opal fields. The lepispheres in play-of-color opal are very uniform in size (apparently within 2–3% of the mean size), indicating a batch process rather than a continuous one. The mixing of the high-pH spring water with cool, slightly acidic groundwater that has low total dissolved salts would decrease the pH, lower the temperature, and lower the ionic strength of the spring water; all three processes facilitate the formation of silica spheres. Montmorillonite (clay) can act as a semipermeable membrane and assist in the pressurization of the fluids for ultrafiltration.

RAH

This section is designed to provide as complete a record as practical of the recent literature on gems and gemology. Articles are selected for abstracting solely at the discretion of the section editor and his reviewers, and space limitations may require that we include only those articles that we feel will be of greatest interest to our readership.

Requests for reprints of articles abstracted must be addressed to the author or publisher of the original material.

The reviewer of each article is identified by his or her initials at the end of each abstract. Guest reviewers are identified by their full names. Opinions expressed in an abstract belong to the abstracter and in no way reflect the position of Gems & Gemology or GIA.

© 2005 Gemological Institute of America

Preliminary studies on rainbow-pearl of penguin wing oyster *Pteria penguin*. Y. Mao, F. Liang, S. Fu, X. Yu, F. Ye, and C. Deng, *Chinese Journal of Zoology*, Vol. 39, No. 1, 2004, pp. 100–102 [in Chinese with English abstract].

Although there are nearly 40 species of pearl oysters worldwide that can produce saltwater cultured pearls, ~99.9% of the production comes from just three species: *Pinctada fucata martensii*, *P. margaritifera*, and *P. maxima*. Currently, the winged oyster *Pteria penguin* is used solely for the commercial production of mabe or half-round cultured blister pearls. However, research in Guangxi, China, showed that spherical cultured pearls with a rainbow color ("rainbow pearls") can be produced from *P. penguin*.

The research involved 144 winged oysters that were 2.5 years old (11.0–14.2 cm in longest dimension); these were housed in cages suspended at 3 m depth. The oysters were nucleated with beads (5.1 mm in diameter) and pieces of mantle tissue (2 × 2 mm). After three months of culturing, the nacre layer was up to 300 µm thick, and after nine months it was up to 890 µm thick. Twelve cultured pearls were produced that ranged from 5.8 to 6.9 mm in diameter with the color, shape, luster, and nacre thickness that met the requirements for cultured pearls in China. Some of them displayed a "rainbow" appearance. At present, because of space limitations in the vicinity of the nucleus, cultured pearls larger than 10 mm cannot be produced in *P. penguin*. TL

Taphonomy of insects in carbonates and amber. X. Martínez-Delclòs, D. E. G. Briggs, and E. Peñalver, *Palaeogeography, Palaeoclimatology, Palaeoecology*, Vol. 203, No. 1–2, 2004, pp. 19–64.

Taphonomy deals with the incorporation of organic remains into sediments or other media (e.g., resins) and the fate of these materials after burial. Such occurrences are uncommon in the case of insects, as compared, for example, to fossil mollusk shells. In this article, the authors present an extensive review of the wide range of major taphonomic processes that control insect preservation in both carbonate rocks (e.g., limestones) and resins (e.g., amber and copal). These processes (both biologic and diagenetic) are restricted in geologic time and geographic distribution, which generates biases in the fossil record in terms of the number, type, and location of insects preserved. The authors suggest that taphonomic studies are an essential prerequisite to the reconstruction of fossil insect assemblages, to the interpretation of the sedimentary and environmental conditions where insects lived and died, and to the investigation of the role of insects in ancient ecosystems. JES

Traditional pearl and chank diving technique in Gulf of Mannar: A historical and ethnographic study. N. Athiyaman and K. Rajan, *Indian Journal of History of Science*, Vol. 39, No. 2, 2004, pp. 205–226.

Using traditional methods, divers have retrieved pearls and

chank (*Turbinella pyrum*, also known as "Indian conch") shells from the Gulf of Mannar, on the southeast coast of India, for several millennia. At present there is no pearl fishery along this coast, but chank shell is still harvested. Historically, the pearl oyster beds were located at a depth of 4–12 fathoms (7–22 m), and the best period for pearl diving was between March and mid-May. Before the season began, divers would survey potential sites to determine the best locations. Early reports indicate that hundreds (even thousands) of boats were used for pearl fishing each season, some accommodating as many as 60–90 divers. Thousands of divers participated in the pearl harvest. Chank shell recovery was accomplished by similar methods but with fewer people.

The harvested oysters would be left in a pit to decay for one month before the pearls were extracted. A 16th century account states that, after washing, the pearls would be sorted into four grades, according to size and quality, that were directed to specific markets: *Aia* of Portugal, or round goods, which were purchased by Portuguese merchants; *Aia* of Bengal, or off-round; and *Aia* of Canara, which were inferior to the previous two. The lowest grade of pearls, *Aia* of Cambaia, was sold in the local countryside. RS

DIAMONDS

Characterization of carbonado used as a gem. K. de Corte, Y. Kerremans, B. Nouwen, and J. van Royen, *Gemmologie: Zeitschrift der Deutschen Gemmologischen Gesellschaft*, Vol. 53, No. 1, 2004, pp. 5–22.

The popularity of colored diamonds and the availability of advanced laser cutting techniques have advanced the use of carbonado as a gem. Carbonado is an opaque polycrystalline diamond material with properties that are quite different from those of "normal" diamonds. This article presents a study of 21 carbonados from the Central African Republic that is augmented with data from the literature, mostly on Brazilian stones.

Morphologically, two categories of carbonado are distinguished. The first has a mostly homogeneous grain size (20–30 µm in diameter), while the second comprises larger crystals (>80 µm in diameter) that are embedded in a fine-grained matrix. Pores among the crystals are filled with a variety of oxide, phosphate, or silicate minerals. Due to its porosity, the density of a carbonado is distinctively lower than that of a pure diamond (3.07–3.45 vs. 3.52 g/cm³). Sr, Pb, Fe, and Y were detected as major elements in the pores by EDXRF. Infrared spectroscopy showed that the diamonds were types Ia or Ib; both types were found in some samples. Raman photoluminescence spectroscopy revealed N-V centers at 638 and 575 nm, as well as the H3 center at 503 nm; all of these defects are caused by exposure to natural radiation.

Carbonados have only been found in alluvial deposits, and their source rock is unknown. They can be quite

large, with stones >1,000 ct reported. Various hypotheses have been offered to explain their origin, ranging from formation in the earth's interior to meteorites, but the matter is still unresolved. *KSM*

Conditions of incipience and growth of diamond crystals.

V. N. Anfilogov, *Proceedings of the Russian Mineralogical Society*, Vol. 133, No. 1, 2004, pp. 110–116 [in Russian with English abstract].

Mechanisms of nucleation and the subsequent growth of natural diamond crystals are discussed. It is postulated that morphological and structural features in the central zones of diamond crystals (i.e., their nuclei) may initially form under extreme physical conditions (e.g., impacts or mechanical deformation) as a metastable, diamond-like modification of the carbon. Alternately, in accordance with the commonly accepted mantle origin of kimberlites, their formation may be due to an interaction between basaltic melts in the mantle and rocks occurring at the base of a craton in the earth's crust. In this case, the kimberlite is viewed not as a hypothetical mixture of a melt and a gaseous phase, but as a fluid from which all the "magmatic" minerals of kimberlite crystallize. There is some evidence that diamond crystals grow while kimberlite pipes are being emplaced. *RAH*

How long can diamonds remain stable in the continental lithosphere?

C. J. O'Neill and L. Moresi, *Earth and Planetary Science Letters*, Vol. 213, No. 1–2, 2003, pp. 43–52.

A question of importance to diamond geologists is: Do Archean ages (>2.5 billion years [By]) obtained for diamonds from many of the world's cratons constrain the thermal state of the Archean continental lithosphere? Recent evidence suggests that the published ages may not represent the ages of the diamonds themselves, but rather may significantly pre-date them. To study this possibility, the authors mathematically modeled the thermal stability of the continental lithosphere in the convecting mantle.

If diamonds have survived in cratonic roots since the Archean, the conditions necessary for their stability must have existed in the Archean continental lithosphere and remained relatively unperturbed for ~3.0 By. In this study, the longevity of the diamond stability field is explored for systems with chemically distinct continental crust and a strongly temperature-dependent mantle viscosity. Such models frequently produce the temperature conditions needed to form diamonds within the Archean lithosphere, but temperature fluctuations experienced within the modeled mantle lithosphere are generally able to destroy these diamonds within 1 By. The models show that the maximum residence time of diamonds in the lithosphere is ~284–852 million years. While this approaches the order of magnitude (of Archean ages) required, extremely fortuitous mantle conditions are required to explain the apparent longevity of Archean diamonds. *RAH*

Mineralogy of diamonds from the Yubileynaya pipe (Yakutia).

N. N. Zinchuk and V. I. Koptil, *Geology of Ore Deposits*, Vol. 46, No. 2, 2004, pp. 135–149.

The Yubileynaya (Jubileynaya) kimberlite pipe in the Daldyn-Alakit diamondiferous district of Yakutia is the largest (59 ha) primary diamond deposit in Russia. It was concealed by an overlying dolerite sill (average thickness of 66 m) that has been stripped away to allow for open-pit mining. This article presents the results of a comprehensive study of the mineralogy and physical properties of ~7,000 diamonds taken from drill core and large tonnage samples. Data are presented on crystal morphology (crystal varieties and habits, twins and intergrowths, etching features), transparency, color, photoluminescence, X-ray luminescence, degree of preservation, mineral composition of solid inclusions, optically active defects, infrared spectroscopy, and carbon isotopic composition.

Many of the diamonds from the Yubileynaya pipe, similar to those of other primary deposits of the Siberian province, are colorless; about 40% have octahedral and transitional forms from octahedral to rhombic dodecahedra. However, variations in crystal morphology according to diamond size are distinctly different from the variations seen at the Mir, Aikhal, and other pipes in the region. Diamonds from this pipe also show strong evidence of natural dissolution (e.g., corrosion features, frosting) compared to diamonds from other Yakutian deposits. The colored diamonds are mainly pale "smoky" brown, pinkish violet, and violet-brown (caused by ductile deformation). Many of the Yubileynaya diamonds appear gray because of numerous graphite inclusions. Most of the diamonds have blue, pinkish violet, and green photoluminescence, with a large number showing yellow-green photoluminescence. These and other data are used to distinguish diamonds from the Yubileynaya pipe from those produced elsewhere in Yakutia. *Paul Johnson*

A new type of synthetic [syngenetic] xenomineral inclusions in diamond.

V. I. Silaev, I. I. Chaikovskii, V. I. Rakin, and V. N. Filippov, *Doklady of the Russian Academy of Sciences, Earth Science Section*, Vol. 394, No. 1, 2004, pp. 53–57.

A new class of syngenetic inclusions composed of Ti-Fe-Si-Zr-Al oxide solid solutions has been found in diamond crystals obtained from placers in the Middle Ural Mountains. The inclusions, which are linearly arranged and probably represent two generations, have been detected in both the marginal and central parts of the diamonds. They are up to 20 μm in size and have a wide range of compositions, as evidenced by the analysis of 17 inclusions. These inclusions are probably suitable for determining conditions of diamond nucleation and growth, because they could be close analogues of mineral phases present in the inferred deep mantle. *RAH*

GEM LOCALITIES

Aventurescent oligoclase feldspar from Oregon, USA. U. Henn, *Journal of Gemmology*, Vol. 29, No. 2, 2004, pp. 72–74.

Basaltic rocks in Oregon have been the source of gem-quality plagioclase feldspars since the 1960s. The most abundant species is labradorite, but bytownite, andesine, and oligoclase have also been recovered. Oligoclase comprises only 1% of the gem material. The gemological properties (e.g., R.I. of 1.535–1.547) and chemical composition (e.g., an anorthite content of An_{12.7}) of the transparent oligoclase “sunstone” are reported along with a description of the euhedral hematite inclusions that are responsible for their aventurescence. Similar transparent sunstones from Norway and colorless oligoclase from Brazil can be differentiated from the Oregon material, as the latter has both lower refractive indices and a lower anorthite content. [Editor's note: Most of the sunstone previously reported from Oregon is labradorite (An₇₀ in composition), with aventurescence attributed to platelets of native copper (C. L. Johnston et al., Winter 1991 *Gems & Gemology*, pp. 220–233).] WMM

Amethyst in the Thunder Bay region, Ontario. M. I. Garland, *Canadian Gemmologist*, Vol. 25, No. 2, 2004, pp. 44–57.

The Thunder Bay amethyst area (~125 km long and ~40 km wide) in Ontario extends along the northern shore of Lake Superior from Thunder Bay to Lake Nipigon. The amethyst is related to the hydrothermal system that formed the Thunder Bay silver and the Dorion lead-zinc-barite veins. There is a spatial relationship between these veins and an Archean and Proterozoic unconformity (containing 2.7 and 2.0 billion-year-old rocks, respectively), suggesting that the unconformity provided a conduit for silica-rich solutions. Areas with good amethyst potential are recognized by development of quartz-rich breccia zones along recurrent faults. The amethyst has a variety of occurrences, such as in vugs and zoned veins, with colors ranging from the palest violet to almost black. Facetable amethyst is produced at several operating mines.

Although amethyst was used by native people, “modern” mining began in the 1860s; interest waned in the early 1900s with the appearance of abundant, inexpensive, good-quality Brazilian material. In the 1950s, there was a resurgence of exploration, resulting in the discovery of several large deposits. In addition to recovering amethyst for sale in their own shops, many Thunder Bay producers (14 are listed in a table) offer fee digging. The amethyst industry is important to the local economy, but it suffers from a lack of consistent marketing and production, as well as competition (particularly from South America). Currently, the economic strength of Thunder Bay amethyst lies in the variety of spectacular specimens, particularly in combination with barite and fluorite. AAL

Conditions of pocket formation in the Oktyabrskaya tourmaline-rich gem pegmatite (the Malkhan field, central Transbaikalia, Russia). I. S. Peretyazhko, V. Y. Zagorsky, S. Z. Smirnov, and M. Y. Mikhailov, *Chemical Geology*, Vol. 210, No. 1–4, 2004, pp. 91–111.

Coexisting melt, fluid-melt, and fluid inclusions in quartz from the Oktyabrskaya gem tourmaline deposit in Russia were studied to elucidate the conditions of pocket formation. At room temperature, fluid-melt inclusions in early pocket quartz and in quartz from the coarse-grained quartz-oligoclase host pegmatite contain crystalline aggregates and an orthoboric-acid fluid. The prevalence of fluid-melt inclusions decreases, and the volume of fluid in the inclusions increases, from the early to the late growth zones in the pocket quartz. No fluid-melt inclusions were found in the late growth zones. Analysis of the fluid inclusions and accompanying fluids suggests that the residual melts of the latest magmatic stage were strongly enriched in H₂O, B, F, and Cs, and contained elevated concentrations of Li, Be, Ta, and Nb. Fluid-melt inclusion microthermometry showed that those melts could have crystallized at 615–550°C. EF

Emerald mineralization in the Kafubu area, Zambia. A. V. Seifert, V. Záček, S. Vrána, V. Pecina, J. Zachariáš, and J. C. Zwaan, *Bulletin of Geosciences*, Vol. 79, No. 1, 2004, pp. 1–40.

This study provides the first quantitative geochemical, petrological, and mineralogical data on major rock types and minerals of the Kafubu emerald area in Zambia. The emerald-bearing phlogopite schists are confined to the contacts of quartz-tourmaline veins (and less commonly, quartz-feldspar pegmatites) with the host chromium-rich metabasites. The veins and pegmatites are the source of Be, and are genetically related to a hidden fertile granite pluton. The formation of the phlogopite schists from the metabasites was also associated with the addition of K, F, Li, and Rb. Data on pegmatite occurrences in active mines and exploration pits and their extrapolation into surrounding areas point to the existence of a single, major pegmatite field that overlaps the extensive horizons of metabasite.

The emeralds range from light to dark green and are often color zoned. They are typically heavily included and moderately fractured. They are dichroic, inert to long- and short-wave UV radiation, and commonly appear green through the Chelsea filter. Fluid inclusion data indicate that the most common interval of quartz veins associated with emerald mineralization was at approximately 350–400°C and 200–400 MPa. EF

Gem corundum deposits in Vietnam. P. V. Long, H. Q. Vinh, V. Garnier, G. Giuliani, D. Ohnenstetter, T. Lhomme, D. Schwarz, A. Fallick, J. Dubessy, and P. T. Trinh, *Journal of Gemmology*, Vol. 29, No. 3, 2004, pp. 129–147.

This paper reviews the main types of gem corundum

deposits in Vietnam, the history of their discovery, and their geologic framework, gemological and mineralogical properties, and inclusions. Beginning in 1983, gem-quality rubies were mined first from marble-hosted deposits near Luc Yen and later from the Yen Bai and Quy Chau mining districts, all of which are in the northern part of the country. Blue, green, and yellow sapphires (associated with basalt) have been mined since 1991 from the Dak Lak, Lam Dong, and Bin Thuan provinces of southern Vietnam. Although corundum is known from amphibolite, gneiss, and metasomatites in Vietnam, these deposits are not currently viable. The physical appearance of these various gem corundums, and the inclusions found within them, are directly related to their respective geologic environments.

Trace-element variations in the corundums underline the diversity of their host rocks. Plots of the ratios $\text{Cr}_2\text{O}_3/\text{Ga}_2\text{O}_3$ versus $\text{Fe}_2\text{O}_3/\text{TiO}_2$ divide the corundums into three main geochemical fields that are discrete and partly overlap. Some rubies, as well as some blue and colorless sapphires, are found in placer deposits and therefore are of unknown geologic origin. Fluid composition signatures, inclusions, and oxygen isotope compositions clearly differentiate Vietnamese corundums of different origins. WMM

Inclusions in Vietnamese Quy Chau ruby and their origin.

P. V. Long, H. Q. Vinh, and N. X. Nghia, *Australian Gemmologist*, Vol. 22, No. 2, 2004, pp. 67–71.

The inclusions found in ruby from Quy Chau, Vietnam, were studied by optical and scanning electron microscopy, as well as Raman spectroscopy. The following were identified: anatase, andalusite, anorthite, apatite, biotite, boehmite, brookite, calcite, corundum, diaspore, dolomite, graphite, margarite, muscovite, phlogopite, pyrite, rutile, zircon, and zoisite. The compositions of both primary and secondary gas-liquid phases, and negative crystals, are also described. The authors suggest that the mixed composition of the inclusions in Quy Chau rubies is suggestive of both metamorphic and metasomatic origins. RAH

Sapphire-blue kyanite from Nepal. U. Henn, *Australian Gemmologist*, Vol. 22, No. 1, 2004, pp. 35–36.

Gem-quality deep blue kyanite, yielding faceted stones up to 12.2 ct, is described from Nepal. Refractive indices were $\alpha = 1.715\text{--}1.718$, $\beta = 1.726\text{--}1.727$, and $\gamma = 1.731\text{--}1.734$ (birefringence = 0.016). S.G. values were 3.67–3.69. The kyanite showed a distinct red luminescence to long-wave UV radiation. Growth tubes were oriented parallel to the c-axis of the kyanite and were accompanied by distinct color zoning. A second type of growth tube (oriented perpendicular to the other tubes) was tapered and partly filled by a doubly refractive mineral. The nonpolarized absorption spectrum showed bands attributable to Fe^{3+} occupying octahedral Al sites. RAH

Spinel from Kayah State (Myanmar). U. T. Hlaing, *Australian Gemmologist*, Vol. 22, No. 2, 2004, pp. 64–66.

Gem-quality pink-to-red spinels were recovered in 2001 from an alluvial deposit between the Pawn Chaung and Salween Rivers, some 40 km south of the township of Hsa-taw, Kayah State, eastern Myanmar. They were likely derived from marbles associated with the Pawn Chaung rock series. Some of these spinels have yielded faceted stones up to 1 ct. Gemological properties were R.I. = 1.713 and S.G. = 3.63, and inclusions were rare. RAH

INSTRUMENTS AND TECHNIQUES

The application of the confocal micro-Raman in the gemstone identification. E. Zu, Y. Duan, and P. Zhang, *Journal of Yunnan University*, Vol. 26, No. 1, 2004, pp. 51–55 [in Chinese with English abstract].

The application of Raman spectroscopy to the nondestructive identification of natural gems, simulants, synthetics, enhancements, and inclusions, with particular emphasis on stones likely to be encountered in Yunnan, China (i.e., jadeite), is described. Several examples are given, the most interesting of which relate to green stone axes that were found in Yunnan. These axes were purportedly made of Burmese jadeite that was produced 3,000–7,000 years ago and subsequently imported into China. However, Raman analysis clearly established that the green material was kyanite. TL

Chemical determination of coloured zoned minerals in “natural stones” by EDS/WDS electron microprobe: An example of dumortierite quartzites. A. Borghi, R. Cossio, L. Fiora, F. Olmi, and G. Vaggelli, *X-Ray Spectrometry*, Vol. 33, No. 1, 2004, pp. 21–27.

Quartzite, a metamorphic rock composed primarily of granular quartz, on rare occasions displays a blue color due to dumortierite impurities. This study of dumortierite within quartzite from Mozambique, Brazil, and Madagascar was undertaken to determine the relationship between the color and chemistry of this mineral. The samples from Mozambique contained two generations of dumortierite crystals, both of which exhibited zoning of color and of Al, Si, Ti, and Sb contents. Areas of stronger blue pleochroism could be correlated with higher Ti contents. These dumortierites also displayed an unusual amount of antimony (up to 5 wt.% Sb_2O_3), but with no correlation to color. The authors suggest that Sb and Ti are accommodated in the Mozambique dumortierite by coupled exchange with Si and Al, respectively. The dumortierite in quartzites from Brazil and Madagascar were less zoned in terms of color and chemistry. JES

LIBS: A spark of inspiration in gemological analytical instrumentation. T. Themelis, *Australian Gemologist*, Vol. 22, No. 4, 2004, pp. 138–145.

The application of laser-induced breakdown spectroscopy (LIBS) to the detection of Be, B, and Li in selected untreated and treated gem corundums was studied using a bench-type apparatus. With this technique, laser pulses fired onto the surface of test specimens generate a plasma that gives rise to distinct spectral emission signatures, which are captured by a spectrograph and processed by a computer. The use of LIBS for detecting Be, Li, B, and other elements in gems is hindered by the substantial instrumental error of ~20%. Also, the specimen undergoes some damage. The author concludes that the use of LIBS in gemology appears limited because the technique is not sufficiently quantitative. Nevertheless, LIBS may be useful for detecting polymers and for analyzing the content of jewelry metal alloys.

RAH

The use of optical coherence tomography for monitoring the subsurface morphologies of archaic jades. M.-L. Yang, C.-W. Lu, I.-J. Hus, and C. C. Yang, *Archaeometry*, Vol. 46, No. 2, 2004, pp. 171–182.

When buried for centuries, the mineralogical structures of jade objects gradually alter, resulting in a whitening of the surface and part of the interior. This provides one of the most important characteristics for identifying authentic archaic jade objects. However, an archaic appearance can also be created by heating or burning jade objects. This study shows how optical coherence tomography (OCT) can be used to nondestructively differentiate between authentic archaic jades and forgeries by imaging their subsurface structures.

The authors used an OCT system that was modified for scanning jade objects to study three archaic samples and two artificially treated jades. Systematic differences were found in the small- vs. large-scale structures that were imaged, as well as in the backscattering intensity measured by the technique. OCT can provide a useful means of authenticating archaic jade objects.

AI

JEWELRY RETAILING

Diamond polisher. J. Kutler, *Institutional Investor*, Vol. 38, No. 11, 2004, pp. 18–21.

A profile is presented of Terry Burman, who helped restore the fortunes of Signet Group. Signet is the world's largest specialty retail jewelry chain, with more than 1,700 stores and 17,000 employees in the U.K and the U.S. operating under several well-known names (e.g., H. Samuel, Kay Jewelers). The company began the 1990s with losses incurred by large debts that were exacerbated by adverse publicity generated by former CEO Gerald Ratner. A successor to Ratner, James McAdam, helped restore the company to profitability. However, in the four years since

Burman took the helm, pre-tax profits have increased 65%, a result of stressing product quality and continuous improvement in all aspects of the business. The company also increased its diamond branding efforts, shifted much of its advertising to television, and worked hard on training programs to instill consumer confidence in the sales staff.

RS

A gem of a resourcing strategy. R. Suff, *IRS Employment Review*, Issue 809, 2004, pp. 46–48.

Signet Group recently launched a new human resources strategy to support its prime business goal of "making its existing space work harder." This entailed attracting and retaining employees capable of taking the business forward.

The company set up a screening program to attract people with a strong work ethic, which entailed updating the company's image in the employment market. It then commissioned a business psychology firm to identify key traits of an "ideal" employee. Communication skills were critically important. The company also devised a number of incentive programs, including ongoing training and career tracking, to retain as many employees as possible.

RS

Displaying jewelry in the best light. A. DeMarco, *JCK*, Vol. 175, No. 4, 2004, pp. 96–100.

This article describes how lighting can be used in retail jewelry stores to help attract customers and boost sales. The best lighting arrangements employ fluorescent lights in jewelry showcases and metal halide or tungsten halogen lights from above. This allows pieces to be lit effectively both in and out of the case. In addition, the temperature of the light source can have an effect on color. Temperatures below 3,000 K produce a warm, reddish appearance. From 3,400–3,500 K, the light is white or neutral. Temperatures greater than 4,600 K produce bluish "cool" colors.

Lighting and associated electrical requirements can be one of the most significant store expenses (about 25%) for retail jewelers, and as such they should be considered an investment. Studies have shown that better-lit displays and cases attract more browsers and promote significantly higher sales. The author notes that hiring lighting professionals often saves money in the long run.

RS

TREATMENTS

The effect of high-temperature treatment on the defect-and-impurity state and color of diamond single crystals (review). N. V. Novikov, A. N. Katrusha, S. A. Ivakhnenko, and O. A. Zanevsky, *Journal of Superhard Materials*, Vol. 25, No. 6, 2003, pp. 1–12.

This article presents a detailed review (as of 2003) of the technology for changing diamond color by high temperature/high pressure annealing (HPHT; also called ther-

mobaric treatment). It discusses changes in atomic-level defects and visible absorption spectra from HPHT treatment of both type I and II natural and synthetic diamonds. The color changes result from the formation or annihilation of color centers often involving nitrogen. The treatment technologies used by several companies (such as General Electric and others) are summarized. Results are presented of experiments carried out by the authors to produce a range of colors in diamonds using a toroid-type high-pressure apparatus at conditions of 1,600–2,100°C and 5.5–6.5 GPa. The potential risk of cracking even high-clarity diamonds during HPHT treatment is also discussed.

JES

If you can't stand the heat, get out of the gem business. G. Roskin. *JCK*, **Part I**. Vol. 175, No. 5, May 2004, pp. 182–188; **Part II**. Vol. 175, No. 6, June 2004, pp. 129–132; **Part III**. Vol. 175, No. 8, August 2004, pp. 90–92.

This three-part report summarizes the history and methods of heat treating colored stones to create a more salable product, as well as the issues raised by these treatments in the retail marketplace. Heat treatment has been practiced for centuries, primarily to improve color, but only recently have detection techniques and equipment evolved to the point that most of them can be identified consistently. Detection of treatment for some gem varieties continues to be very difficult or even impossible. Aquamarine is one example, but the list of gems with unidentifiable color origins is growing, and two of the “big three” colored stones—ruby and sapphire—are in danger of joining that list. Corundum treatment was not recognized until the 1970s; a 1979 lab note in *Gems & Gemology* by Robert Crowningshield, then director of GIA's Gem Trade Laboratory in New York, observed that heat-treating of sapphires is “one of the best kept commercial secrets in the jewelry industry.” [Editor's note: see Spring 1979 *Gems & Gemology*, p. 147.]

Heat treatments of Sri Lankan geuda sapphire and later Burmese (Mong Hsu) ruby helped the industry meet the growing demand for these gemstones by transforming unattractive material into salable gems. The treatment bar was raised in the mid-1980s when the process of creating blue color in sapphire by diffusing titanium was introduced to the market. Detection of this process was easy because the color was confined to the surface. However, detecting heat treatment of certain sapphires was much more difficult because the color could be improved with temperatures as low as 300–400°C (which is insufficient to produce telltale altered inclusions). The latest treatment, beryllium diffusion, is even more difficult to detect.

The report also lists five categories of corundum treatment that affect price and therefore must be disclosed:

unenanced, lightly heated (i.e., Madagascar), heated without flux, heated with flux, and heated with an additive (e.g., beryllium). RS

The use of thermobaric treatment to manipulate the defect-and-impurity state of natural diamond single crystals. A. N. Katrusha, S. A. Ivakhnenko, O. A. Zanevsky, and T. Hainschwang, *Journal of Superhard Materials*, No. 3, 2004, pp. 47–54 [in Russian].

Natural brown type I diamonds were treated under HPHT conditions corresponding to the graphite stability region of the carbon phase diagram (1,750–2,000°C, 44–65 kbar) for 10–30 minutes to evaluate the effects of pressure on the aggregation state of nitrogen and the formation of color centers. Following HPHT treatment, mixed type IaA/B diamonds showed considerable decreases in brown coloration at all experimental pressures. However, those samples treated at the lowest pressure (44 kbar) also developed a yellow color, which was attributed to H3, H4, and N3 absorption centers. It is speculated that enhanced mobility of vacancies was responsible for the formation of these color centers at only lower pressures. Despite conditions that favored graphite stability, no graphitization of diamond surfaces or fractures was observed.

HPHT treatment of a brown type Ib diamond caused near-complete aggregation of nitrogen, resulting in a type IaA/B pinkish yellow diamond. The creation of N3 and H3 centers caused the yellow, and a broad absorption band at 560 nm produced the pink color. Nearly pure type IaB brown diamonds, after exposure to HPHT conditions, gave varying results. It was found that 1.1–4.0 ppm of nitrogen in the form of A-aggregates must be present within the IaB diamonds to produce sufficient N3 and H3 centers to cause a green-yellow color under the treatment conditions used. These experiments with type I diamonds indicate that the results of HPHT treatment are dependent not only on the type and amount of nitrogen present but also on the pressure conditions. CMB

MISCELLANEOUS

Criteria and parameters for gemstones [sic] uniqueness. V. S. Chernavtsev and K. K. Atabaev, *Gemological Bulletin*, No. 9, 2003, pp. 12–17 [in Russian with short English abstract].

The authors studied gem exhibits in museums and at mineral shows worldwide with the objective of quantifying the factors that determine the value of museum-quality colored stones, particularly rough specimens but sometimes cut stones. On the basis of the data collected, they were able to classify the stones into several groups and to value them. They also determined characteristics that make certain specimens “unique” (i.e., those of

exceptional quality, rarity, or other attributes). Such specimens are found not only in museums but also in private collections.

The main criteria that determine the uniqueness of gemstones are: (1) aesthetic appeal, (2) purity (i.e., the number and nature of associated minerals) and perfection, (3) rarity, (4) historical importance, and (5) scientific significance. Based on these criteria, several categories of unique stones were recognized, their parameters tabulated, and valuations applied. Particularly unique samples are extremely difficult to value but, as a generalization, their price depends on size, purity, abundance and location of physical defects, availability of details on their geologic occurrence, and publications (scientific or popular) related to the particular specimen. BMS

Managing the commons: An economic approach to pearl industry regulation. B. Poirine, *Aquaculture Economics & Management*, Vol. 7, No. 3-4, 2003, pp. 179-193.

Unregulated use of tropical lagoons for pearl culture has created problems associated with overexploitation, which has led to declining profits (or losses) for pearl farmers. Various factors cause cultured pearl production to decline and oyster mortality to increase when a critical density is reached. Particular emphasis is placed on the problems facing the Tahitian black cultured pearl industry.

In lagoons owned privately by a single producer, overcrowding is not a problem because profits are maximized far below the critical density. However, in public lagoons, the author proposes that the government should regulate, by auction, the use by a single producer for a specific period of time, with rules to ensure equitable policies toward all producers. Arguments are also made for a global cultured pearl production quota to keep prices from falling due to excess supplies; both Australia and Japan have enacted successful oyster quota policies that have prevented overexploitation and the economic havoc that results from such practices. RS

Not forever: Botswana, conflict diamonds and the Bushmen. I. Taylor and G. Mokhawa, *African Affairs*, Vol. 102, No. 407, 2003, pp. 261-283.

Although Botswana, a peaceful democracy in southern Africa, has not been implicated in the campaigns against conflict diamonds, the policies of its government regarding tribes of Bushmen living in the Central Kalahari Game Reserve have come under fire.

Botswana is the world's largest diamond producer by value, and diamonds are responsible for 87% of its foreign exchange. The country, one of the poorest at independence in 1966, is now in the upper-middle income category (with a per capita Gross Domestic Product of more than \$6,000), though the distribution of wealth remains very unequal. Because the country is so depen-

dent on diamond revenues, its government launched a "Diamonds for Development" campaign to ensure differentiation from other African nations beset by wars that spawned the conflict diamond campaigns. However, a number of nongovernmental organizations (Survival International, in particular) have sought to link the government's policy of removing Bushmen tribes, known as the San, from the Reserve to diamond exploration efforts in that area.

The government cut off services, including water, to the area in January 2002 as part of a policy to resettle the San, claiming the action and the resettlements were to protect wildlife and foster tourism in the area. Survival International drew De Beers—a 50/50 partner in Botswana's diamond mining operations—into the controversy, as De Beers holds an exploration license near the affected area. De Beers has distanced itself from the government's resettlement policy and noted that its exploration area comprises only 20 km² of the Reserve's 55,000 km². Survival International continues to organize protests against De Beers and the Botswana government. RS

Strategies for sustainable development of the small-scale gold and diamond mining industry of Ghana. R. K.

Amankwah and C. Anim-Sackey, *Resources Policy*, Vol. 29, No. 3-4, 2003, pp. 131-138.

Small-scale mining of gold and diamonds has helped create employment and government revenue in Ghana. Since the government instituted reforms in 1989 that legalized such activities, more than 1.5 million ounces of gold and 8 million carats of diamonds have been produced. The Small-Scale Mining Law includes a technical assistance program that has helped with prospecting and development, legalized the purchase of mercury for gold recovery, and established a marketing authority to buy and export gold and diamonds. By the end of 2001, 420 small-scale mining concessions (nine for diamonds) had been licensed. These companies have generated employment for more than 100,000 people.

However, there are still thousands of illegal miners, called *galamsey* in local parlance, who have created problems for the government. First, conflicts have arisen over their encroachment on concessions held by larger mining companies. Some large firms have accommodated the illegal miners by ceding less-economic areas of their concession to them—in exchange for their registering with the government. Second, these illegal miners—and some legal mining enterprises—also cause a great deal of environmental damage. Mercury poisoning is a particular problem in some mining villages.

The government has launched an education program to promote cleaner, safer extraction methods. It also has encouraged the formation of small-scale mining associations to better regulate safe and productive mining practices. RS

Fast Facts about **SYNTHETIC DIAMONDS**

1. While very small, industrial-quality synthetic diamonds were documented in the mid-1950s, the first faceted jewelry-quality synthetic diamonds were unveiled by the General Electric Company (GE) on June 17, 1971. The internal characteristics and ultraviolet fluorescence observed in these early synthetic diamonds are among the key identification features still used today.

2. The GE synthetic diamonds were produced by subjecting carbon in a metallic flux to extremely high temperatures and pressures, a process known as high temperature/high pressure (HPHT) growth. In the early 1970s, it took a week or more to grow a 1 ct gem-quality crystal, at a cost of roughly \$20,000 (equal to about \$90,000 today).

3. Also in the 1970s, the De Beers Diamond Research Laboratory in South Africa began manufacturing gem-quality synthetic diamonds of a size suitable for use in jewelry—then, as now, for research purposes only.

4. In April 1985, Sumitomo Electric Industries of Japan announced the first commercial production of gem-quality synthetic diamonds. These yellow crystals, intended only for high-technology industrial applications, were largely free of inclusions and ranged from 1 to 2 ct in size.

5. In the early 1990s, small quantities of Russian gem-quality synthetic diamonds began to turn up in the jewelry trade. Whereas GE, Sumitomo, and De Beers researchers had used a “belt”-type press (so called because it uses a cylindrical growth chamber) to grow synthetic diamonds, the Russians used a new type of machinery. The “split-sphere” apparatus (also known by the Russian acronym “BARS”) applies high pressure on all sides of the growth chamber rather than just the top and bottom.

6. During the 1980s, a *low*-pressure diamond growth technique called chemical vapor deposition (CVD) saw its

first major industrial use. In contrast to HPHT diamond synthesis, CVD growth takes place at a high temperature but at one-tenth atmospheric pressure.

7. The CVD process, which actually pre-dates HPHT synthesis, involves the high-temperature ionization of a carbon-rich gas, typically methane. Carbon atoms are deposited on the substrate as a film of polycrystalline or single-crystal synthetic diamond. So far only thin layers of CVD-grown synthetic diamond (up to several millimeters in thickness) have been produced by the technique.

8. For decades, CVD-grown synthetic diamond was available only as polycrystalline material with a grayish, granular appearance or as very thin single crystals (too thin to be faceted). This changed in 2003, when Apollo Diamond Inc. announced that it had succeeded in growing brown-to-gray and near-colorless CVD synthetic diamond crystals in sizes suitable for faceting small cut stones.

9. Although the latest generations of CVD synthetic diamonds have few if any distinguishing visual features, they can be positively identified through surface luminescence imaging with instruments such as the Diamond Trading Company’s DiamondView, as well as with additional analytical techniques available in larger gemological laboratories.

10. Most of the faceted synthetic diamonds seen in the gem trade to date have been small (0.30 ct and less). Most have been strongly colored, usually yellow or brownish yellow and occasionally blue. In addition, some pink, red, purple, green, and yellow colors have been produced by post-growth irradiation and/or heat treatment. They exhibit a range of distinctive gemological properties that allow them to be identified by gemologists.

Stuart Overlin
Associate Editor

Source: *Gems & Gemology in Review: Synthetic Diamonds*, a compilation of G&G articles and reports on synthetic diamonds published between 1971 and 2004. Edited by Dr. James E. Shigley; published by the Gemological Institute of America, 2005, 294 pp., illustrated.

Available now: To order, visit the GIA Gem Instruments Bookstore at www.gia.edu, or call 800-421-8161. Outside the U.S. and Canada, call 760-603-4200. E-mail myorder@gia.edu

Price: \$49.95 plus shipping and handling